FUNCTIONAL SIGNIFICANCE OF ANDROGEN RECEPTOR MUTATIONS IN PROSTATE AND BREAST CANCER

by

Mara P. Steinkamp

A dissertation submitted in partial fulfillment
of the requirements for the degree of
Doctor of Philosophy
(Human Genetics)
in The University of Michigan
2009

Doctoral Committee:

Professor Diane M. Robins, Chair
Professor Jeffrey W. Innis
Professor Sofia D. Merajver
Associate Professor Thomas M. Glaser
Associate Professor Elizabeth M. Petty

In memory of my grandfather,

Kendell M. Pease

Acknowledgements

So many people have been instrumental to this work. First and foremost, many thanks to my advisor, Didi Robins, for being supportive enough to allow me to be an independent scientist even if it took much trial and error, and wise enough to know when to provide needed insight. Thanks also to the entire Robins lab past and present. I am especially thankful to Orla O'Mahony for scientific discussion and input. She was always willing to discuss science over coffee. Orla performed the bicalutamide/ flutamide mouse studies. Thanks to Megan Albertelli, who worked with the h/mAR mouse model and was the second pair of hands for the mammary gland transplants. Her veterinary skills were extremely helpful. Thanks also to Michele Brogley, who sequenced the SPORE patient samples and keeps us all in line, and Arno Scheller, who painstakingly optimized transfections in the lab and who knows more about cloning than he will ever be able to tell us. I'm extremely thankful for the work done by Haniya Rehman, a talented masters student, who helped with the immunocytochemistry and transfections and Beth Stairnes, a rotation student, who also helped with transfections.. Thanks to my thesis committee: Jeff Innis, Tom Glaser, Liz Petty, and Sofia Merajver, who were very helpful and provided much needed expertise.

I am indebted to my friends in the department, especially Nicole and Cris for have providing novel perspective and a lot of support, and my friends outside of the department, especially Colleen, Felix, and Chrysta, for making sure that I got out of the

lab once in a while. I would also like to thank all of my housemates who have been my family away from home and have kept me sane over the years.

As we are all products of our experiences, I must give credit to all of my mentors along the way. My parents and grandparents fostered inquisitiveness throughout my childhood. My grandfather used to have the kids digging for dinosaur bones in the backyard, and my parents started me down the path of scientific discovery by showing me how to hybridize daylilies. By third grade I had learned about genetic traits, the difference between diploid and tetraploid plants, and how colchicine treatment can alter ploidy. With beginnings like these, how could I not be driven to study genetics? I also owe thanks to Ms. Pilkington, my high school biology teacher who taught us how to both learn from and respect all organisms. Thanks to my undergraduate advisors, Drs. Liz Adler and Robert Savage, and my mentor at Boston Children's Hospital, Dr. Ellis Neufeld.

My entire family, Mom and Dad, Grandma and Grandpa, Alexis and Sarah, have been very supportive throughout my graduate school experience. My husband, Boris, needs more thanks than I can ever say for his inspiration, encouragement, and refreshingly different scientific perspective.

Table of Contents

List of Figures

List of Tables

Abstract

Hormone-dependent tumors of the prostate and breast are the most commonly diagnosed tumors today. Therapy for metastatic disease directly targets the steroid hormone receptors. Therefore it is critical to understand the role of these receptors in cancer initiation and progression. In prostate cancer, although tumors initially respond to therapy, they eventually relapse, progressing to androgen-independence. However, the androgen receptor (AR) is still active as evidenced by expression of many of its target genes. Gain of function *AR* mutations have been identified in androgen-independent prostate cancer suggesting they are selected by treatment. To confirm mutation selection and evaluate their prevalence, we examined a mouse prostate cancer model, thus avoiding the heterogeneity of human disease initiation and treatment. Sequencing the *Ar* coding region from prostate tumors of mice undergoing different treatments identified numerous mutations, each at low frequency. More abundant mutations localized in functional domains by treatment. Extending this analysis to patient metastases identified additional novel as well as previously reported mutations. Characterization of selected mutant ARs revealed diverse effects on receptor function including differential promoter activation, increased stability, and promiscuous ligand activation. Thus AR exploits multiple mechanisms to evade treatment.

Reduced function *AR* mutations in a few male breast cancer patients, suggest that an active AR protein may be protective against this disease. Characterizing these mutants

functionally revealed differential promoter activation as we saw in prostate cancer. To test further the role of AR in breast cancer, tumor development was assessed in AR-null XY mice. Surprisingly AR-null mice did not develop breast cancer, which proved to be due to the absence of mammary ductal development. Mammary gland transplants suggested that lack of ductal growth in AR-null mice is due both to systemic hormonal imbalances and loss of intrinsic AR effects on mammary gland proliferation.

AR activates a broad range of targets involved in cell proliferation and differentiation. These studies together suggest that mutant ARs may activate a subset of targets that influence disease in both prostate and breast. If identified, future therapies may be able to bypass AR and selectively inhibit these targets.

Chapter 1

Introduction

Endocrine cancers of the prostate and breast have the highest incidence of all cancer types apart from nonmelanoma skin cancers. In the US, one in six men will be diagnosed with prostate cancer in their lifetime and one in eight women with breast cancer in their lifetime. Furthermore, cancer deaths due to prostate and breast cancer are second only to lung cancer in men and women respectively (Jemal et al. 2008). Prostate and breast cancers often arise later in life in part due to cumulative exposure to sex hormones. Prostate cancer is initially responsive to androgens while many breast cancers are responsive to estrogens. Because they mediate cellular responses to hormones, the androgen receptor (AR) and estrogen receptor (ER) are also implicated in tumorigenesis. In this thesis, I examine the role of steroid receptors in hormone-dependent cancer, specifically, how somatic *AR* mutations suggest diverse mechanisms by which AR drives androgen-independent prostate cancer progression and how germline *AR* mutations identified in male breast cancer reveal a surprising role for AR in mammary gland development

AR structure and function

Androgens are required for the development and maintenance of male reproductive tissues such as the prostate. Androgens trigger changes in cell proliferation

and differentiation by binding to and activating the specific receptor, AR, which in turn regulates the transcription of numerous target genes involved in proliferation, survival and differentiation (Dehm et al. 2006). The *AR* gene consists of eight exons that encode a 110 kDa protein. *AR* is located on the X chromosome (Xq12), which means that males are hemizygous for a gene that plays a key role in male development and reproductive tissue maintenance (Gelmann 2002).

AR is a member of the nuclear receptor superfamily of transcription factors, which share conserved modular functional domains: an amino-terminal transactivation domain (NTD), DNA binding domain (DBD), and ligand-binding domain (LBD) (Evans 1988) (Figure 1.1A). The NTD is the least conserved domain in the nuclear receptor superfamily. Although fairly unstructured, AR's NTD is extremely important for AR function serving as a scaffold for the binding of coregulators (coactivators and corepressors). The bulk of the NTD is taken up by two overlapping interaction surfaces or activation functions (AFs), AF-1 and AF-5, which affect AR activity independent of ligand binding (Jenster et al. 1995). The highly conserved DBD is comprised of two zinc fingers that make sequence-specific contacts with DNA. The first zinc finger contacts the major groove and is responsible for binding site recognition, while the second zinc finger stabilizes the DBD and is part of the dimerization interface (Luisi et al. 1991; Freedman 1992). A hinge region, beyond the DBD, contains a nuclear transport signal as well as ubiquitination and phosphorylation sites (Zhou et al. 1995; Tanner et al. 2004; Haelens et al. 2007). The LBD consists of 12 alpha helices arranged to form a ligand binding pocket where androgens bind with high affinity (Moras et al. 1998). The LBD also has a nuclear export signal important for AR nuclear/cytoplasmic shuttling (Saporita et al. 2003).

In the absence of hormone, AR resides in the cytoplasm complexed to heat shock proteins 90 (Hsp90) and 70 (Hsp70). Hsp90 stabilizes AR in a conformation that allows high affinity ligand binding (Fang et al. 1996). Upon ligand binding to the LBD, a conformational change releases AR from the heat shock protein complex (Krongrad et al. 1991) and the repositioning of LBD helices 12 and 3 creates a ligand-dependent coregulator binding surface, AF-2 (Moras et al. 1998; Matias et al. 2000). AR is then translocated into the nucleus where it binds as a homodimer to hormone response elements (HREs), located in the promoters of target genes (Figure 1.1B). AR, glucocorticoid receptor (GR), progesterone receptor (PR) and mineralocorticoid receptor (MR) all bind a similar consensus HRE consisting of inverted repeats of a 5'TGTTCT 3' half site separated by a 3 base pair spacer (Matias et al. 2000). AR initiates transcription of androgen-responsive target genes by recruiting coactivators with histone acetyltransferase activity that alter chromatin structure allowing recruitment of the general transcriptional machinery (Shang et al. 2002).

AR's N/C interaction

The AF-2 of most nuclear receptors interact with LXXLL motifs of p160 coactivators (Estebanez-Perpina et al. 2005). Although AR's AF-2 interaction site is capable of interacting with these typical motifs, it preferentially binds F/WXXLF domains (He et al. 2000; Hur et al. 2004). Two such motifs, ^{23}FQNLF^{27} and ^{435}WHTLF^{439}, are located in AR's own N-terminus (Figure 1.1A) and compete for binding to AF-2 in the presence of ligand (He et al. 2000). Binding of either coactivators or AR's N-terminus to AF-2 stabilizes the receptor (Chang et al. 2002), however, the

intramolecular amino-carboxy interaction is important for AR activity, since mutations that abolish this interaction lead to androgen insensitivity (Thompson et al. 2001; He et al. 2006; Toumazou et al. 2007). The N/C interaction may occur between domains within the same AR or between domains on adjacent ARs (Figure 1.1B). Because AR's AF-2 is preferentially bound by the N-terminal motifs, much of the coactivator interaction in AR is shifted to AF-1 in the NTD (He et al. 2004). Interestingly, certain complex promoters, such as those of the prostate specific antigen (PSA) and probasin genes, are more dependent on the N/C interaction than others such as the mouse sex limited protein (Slp) and mouse mammary tumor virus (MMTV) genes (Scheller et al. 1998; He et al. 2002). Thus promoter context might influence AR structure, favoring coregulator binding at one activation surface or another.

While the FXXLF increases AR activity, the WXXLF motif represses transactivation perhaps by competing with FXXLF. The presence of both motifs highlights the tight regulation of receptor activity. The FQNLF may play a further role in AR stability since it has been shown to modulate degradation (Chandra et al. 2008). Binding of FQNLF to AF-2 may further stabilize AR by hiding this proteasome targeting signal.

AR binds two distinct types of response elements

All steroid receptors except ER bind the same consensus HRE consisting of an inverted repeat of the 5' TGTTCT 3' half site separated by a 3 nucleotide spacer (Truss et al. 1993). How each receptor elicits a specific cellular response is not fully understood. Some of AR's specific effects can be attributed to its ability to bind direct repeats as well

as the canonical inverted repeats (Claessens et al. 2001) (Figure 1.1B). Use of chimeric receptors with domains from GR and AR demonstrate that the ability to transactivate on these AR-specific response elements is conferred by AR's DBD (Schoenmakers et al. 2000). AR-specific residues in the second zinc finger of the DBD and its C-terminal extension are necessary for binding to direct repeats and appear to stabilize the AR dimer (Shaffer et al. 2004). Creation of a knockin allele of *Ar* in mice, where the second zinc finger and C-terminal extension of AR is replaced with the homologous region of GR, the specificity-affecting AR knockin (SPARKI), provides the means to distinguish between gene targets that are primarily controlled by AR-specific response elements and those that can be activated solely by general response elements *in vivo* (Schauwaers et al. 2007). SPARKI mice are fully viable, but males have reduced fertility and smaller reproductive organs suggesting that AR-specific elements impact, but are not essential for, male function.

Target gene promoters, in addition to carrying multiple androgen response elements, also have binding sites for numerous other transcription factors that can affect transactivation. The Robins lab has done extensive work characterizing the androgen-responsive mouse sex-limited protein (Slp) promoter and has demonstrated the context dependence of AR-specific transactivation including interactions between multiple AR dimers, coactivators, and other transcription factors (reviewed in (Robins 2004)). The Slp promoter contains one unpaired half site and two repeats, one of which is a general, inverted repeat (HRE3) and the other a selective, direct repeat (HRE2) (Figure 1.2). Although AR binding to tandem repeats of HRE2 only weakly activates a reporter, a fragment of the complex promoter containing both elements (C'Δ9) can be activated by

AR but not GR (Scheller et al. 1996), indicating that HRE2 is more important in conjunction with HRE3 (Robins 2004). AR also cooperates with the general transcription factor Oct-1 and AML3/CBFα1 bound to the Slp promoter (Ning et al. 1999; Gonzalez et al. 2001) in a manner requisite for maximal and androgen-specific transactivation.

Polymorphic repeats and AR function

The AR NTD has two polyamino acid tracts, a glutamine tract and a glycine tract, that are variable in the population. Length of both tracts has been shown to modulate AR activity *in vitro* (Chamberlain et al. 1994; Brockschmidt et al. 2007). Increased polyglutamine tract length reduces interaction of p160 coactivators with the NTD (Irvine et al. 2000). Expansion of the CAG repeat beyond 40 repeats leads to spinal and bulbar muscular atrophy or Kennedy's disease in hemizygous males or lionized females (La Spada et al. 1991). Due to its effect on activity, the polyglutamine tract could affect prostate cancer risk and some epidemiological studies have found an association with short CAG repeats and prostate cancer risk, but others have not (Buchanan et al. 2001). Somatic contraction of the CAG repeat has been found in prostate cancer, suggesting selection of more active ARs during disease progression (Schoenberg et al. 1994; Alvarado et al. 2005). Furthermore, variation in Q-tract length alters disease progression in a mouse model of prostate cancer with shorter alleles promoting earlier disease, but longer survival (Albertelli et al. 2008).

Post-translational modifications of AR

Androgen receptor activity is also sensitive to protein modifications that can either enhance or inhibit transactivation. AR is acetylated and phosphorylated on a variety of sites. This acetylation/phosphorylation code can modulate AR activity by affecting cofactor interaction, AR stability, and degradation (Wang et al. 1999; Gioeli et al. 2002). The phosphorylation state of AR depends on ligand binding, cytoplasmic versus nuclear localization, and interactions with signal transduction pathways (Kesler et al. 2007). Numerous factors including AKT, which lies downstream of the Her2/*neu* growth factor pathway, mitogen-activated protein kinase (MAPK) and Src can phosphorylate AR on different serine and tyrosine residues (Yeh et al. 1999; Wen et al. 2000; Kraus et al. 2006). p300 acetylates AR on a KXKK motif in the hinge region and increases ligand-dependent transactivation by enhancing binding of coactivators (Popov et al. 2007). Mutations in AR that mimic the acetylated state (AR-K631Q or AR-K631T) exhibit increased proliferation when expressed in a xenograft model (Fu et al. 2003). Mutation of the three lysines of the acetylation motif particularly affects AR activation of a selective ARE of the *Rhox5* promoter (Faus et al. 2007).

Unliganded AR is a substrate for ubiquitination and subsequently is quickly degraded by the proteasome (Jaworski 2006; Chandra et al. 2008). Multiple E3 ubiquitin ligases have been implicated in AR degradation including the C-terminal Hsp-interacting protein (CHIP), Mdm2, and PMEPA1 (Lin et al. 2002; He et al. 2004; Rees et al. 2006; Li et al. 2008). AR activation and degradation are linked in a regulatory loop in which phosphorylation by AKT triggers AR ubiquitination and proteosomal degradation (Lin et al. 2002). The proteasome also plays a role in nuclear translocation of AR (Lin et al.

2002). AR is also sumoylated on two lysine residues in the NTD, K388 and K521, which reduces AR activity (Poukka et al. 2000).

Loss of function *AR* mutations and androgen insensitivity

Because *AR* is located on the X chromosome, males are hemizygous and thus germline mutations are often phenotypically obvious. Mutations have been identified in all domains of the AR protein and are associated with a number of diseases (Gottlieb et al. 2004). For instance, loss of function mutations result in partial to complete androgen insensitivity syndromes (PAIS and CAIS, respectively) with varying phenotypes ranging in severity from male infertility (Zuccarello et al. 2008) to sterile XY females (Batch et al. 1992; Feldman 1992; Yong et al. 1998). Many of these mutations are missense mutations in conserved residues where one change severely alters AR structure/function. Analysis of these mutations has provided insight into the specific residues involved in aspects of AR function including DNA and ligand binding affinity and specificity and N/C interaction (Bevan et al. 1996; Langley et al. 1998; Katsumata et al. 2008).

The AR and prostate cancer

All prostate cancers are initially androgen responsive and express AR throughout most stages of disease progression, highlighting the importance of AR in promoting proliferation and limiting apoptosis (Feldman et al. 2001). Interestingly, overexpression of wild type AR does not cause tumorigenesis in a mouse model (Han et al. 2005), and few *AR* mutations have been identified in untreated primary tumors (Newmark et al. 1992; Evans et al. 1996), indicating that while androgen is important for tumor growth it

is not likely the initiator of tumorigenesis.

Normal prostate consists of epithelial and stromal compartments both of which express AR. Interestingly, AR promotes proliferation in the stroma while promoting cell differentiation in the epithelia. Selective knockout of the epithelial *Ar* causes epithelial hyperproliferation (Wu et al. 2007), but AR is expressed in the majority of prostate cancers (Isaacs et al. 1992), indicating that switching from a differentiation to a pro-proliferation/anti-apoptosis program causes oncogenic transformation.

The recent discovery of androgen-responsive gene fusions in prostate cancer has shed light on how AR-dependent prostate cancer may arise (Tomlins et al. 2005). Genomic rearrangments fusing a 5' androgen-responsive regulatory region (usually the prostate-specific TMPRSS2 promoter) to the coding region of an oncogene (most commonly an E26 transformation-specific (Ets) family member) have been found in early neoplastic lesions as well as over 50% of all prostate cancers examined, suggesting that this alteration is an early genetic change (Kumar-Sinha et al. 2008). Expression of this fusion gene *in vitro* and *in vivo* makes cells invasive but does not alter proliferation or cause overt cancer in mice (Tomlins et al. 2007), suggesting that the TMPRSS2-Ets fusion does not initiate hyperproliferation but instead facilitates progression from prostatic intraepithelial neoplasia (PIN) to cancer (Kumar-Sinha et al. 2008).

Prostate cancer treatment and therapy resistance

Historically, early treatment of prostate cancer focused on removal of hormone synthesis through surgical or chemical castration (Huggins et al. 1941). Later it was discovered that combining castration with specific antiandrogens that inhibit AR was more effective then castration alone (Labrie et al. 1983). Antiandrogens, such as

flutamide, bicalutamide, and nilutamide, are synthetic non-steroidal ligands that bind within the ligand binding pocket and competitively inhibit AR activity by disrupting formation of AF-2. This combined androgen blockade remains the standard treatment for metastatic prostate cancer. While tumors are initially responsive to therapy and regress, resistant cells will inevitably emerge and metastasize. It was originally thought that therapy resistant tumors have lost AR expression and no longer require a functional AR pathway to proliferate. However, the AR, and many other androgen-responsive targets, are still expressed in these resistant tumors suggesting that mechanisms of resistance involve alternative activation of the AR pathway under castrate conditions (Culig et al. 1998).

Numerous mechanisms have been proposed for AR activation given no or low hormone levels. Amplification of the *AR* gene has been found in over a third of all recurring prostate cancers (Linja et al. 2004; Haapala et al. 2007). Amplification can increase AR activity either by facilitating a stronger response to low levels of hormone, or by altering AR interaction with antiandrogens or other growth factor pathways. At high levels of receptor, AR interacts with ß-catenin, leading to activation of both AR and Wnt targets (Schweizer et al. 2008) and antiandrogens are converted from antagonists to weak agonists through increased recruitment of coactivators (Culig et al. 1999; Haapala et al. 2007). Increased AR expression is sufficient to transform prostate cancer cells from androgen-responsive to therapy-resistant in xenograft models (Hara et al. 2003; Chen et al. 2004).

Increased coactivator expression and downregulation of AR corepressors can promote growth in the absence of *AR* amplification by allowing more efficient

transactivation by AR under low androgen conditions. For instance, higher protein levels of two AR coactivators, steroid receptor coactivator 1 (SRC-1) and transcriptional intermediary factor 2 (TIF2), correlate with more aggressive and androgen-independent prostate tumors (Gregory et al. 2001; Balk 2002; Agoulnik et al. 2005).

Altered regulation of AR localization can also increase AR activity. Recently a cytoplasmic cochaperone of AR, small glutamine–rich tetratricopeptide repeat containing protein α (αSGT), was found to be down regulated in metastatic prostate cancer (Buchanan et al. 2007). αSGT binds to the hinge region of AR and limits ligand-independent AR transactivation by sequestering AR in the cytoplasm. Loss of αSGT increases AR nuclear localization in the absence of ligand (Buchanan et al. 2007).

Cross-talk between growth factor pathways and AR can stimulate proliferation in hormone-refractory prostate cancer cells. Growth factors such as insulin-like-growth-factor 1 (IGF-1), keratinocyte growth factor (KGF) and epidermal growth factor (EGF) can all increase ligand-independent transactivation by phosphorylating AR at specific serines (Culig et al. 1994). The EGF pathway induces selective phosphorylation of Ser 578 in the AR DBD by protein kinase C (PKC) (Ponguta et al. 2008), which is important for appropriate nuclear-cytoplasmic shuttling. Activation of Erk and Akt leads to ligand-independent but AR-dependent proliferation in a mouse model of prostate cancer, Nkx3.1;Pten mice (Gao et al. 2006). AR phosphorylation by AKT is associated with decreased survival time in hormone-refractory prostate cancer (McCall et al. 2008).

Somatic *AR* gain of function mutations can have effects on AR activity and stability similar to the previous mechanisms discussed above. A link between gain of function *AR* mutations and treatment evasion was first suggested for the LNCaP cell line,

where a mutation in the LBD, T877A, creates a promiscuous receptor able to be activated by noncanonical ligands including the antiandrogen hydroxyflutamide (Gaddipati et al. 1994; Krishnan et al. 2002). Antiandrogens, such as flutamide and bicalutamide, are synthetic non-steroidal ligands that bind within the ligand binding pocket and competitively inhibit AR activity by disrupting formation of AF-2. The promiscuity of AR-T877A demonstrates that slight alterations in structure can alter the LBD to accommodate antiandrogens while still allowing the formation of an active AF-2. Gain of function mutations in *AR* have since been reported in many clinical cases, particularly in progressive disease after antiandrogen treatment (Buchanan et al. 2001; Gottlieb et al. 2004). Although many of the mutations that have been characterized are gain of function, they vary in their effect on AR activity (Chen et al. 2005). Some even appear to be partial or complete loss of function mutations (Shi et al. 2002).

The prevalence of *AR* mutations in treatment resistance has been debated. Mutations are estimated to occur in ~8% of prostate tumors (Lamb et al. 2003), but are more common in late stage tumors and metastases, with mutations in 30-50% of these cases (Marcelli et al. 2000; Chen et al. 2005). Furthermore, they have been found in up to 50% of hormone-resistant prostate cancers suggesting that these mutations may be selected during treatment (Chen et al. 2005) (Taplin et al. 1995; Taplin et al. 1999). Half of the studies to date have omitted sequencing exon 1 due to repetitive polyamino acid encoding tracts and high GC content. Sequencing exons 2-8 revealed mutations in 21% of patients with late metastatic disease (Marcelli et al. 2000). Evidence suggests that androgen independent AR activity may rely on the N-terminus rather than the LBD (Dehm et al. 2006). Investigators who sequence the entire *AR* find mutations spread

throughout the coding region with 50% of the mutations occurring in the NTD (Tilley et al. 1996; Hyytinen et al. 2002).

Modeling prostate cancer in the mouse

Patient studies are complicated by genetic heterogeneity, small sample size, and variability in tumor progression and treatment. In Chapter 2, a mouse model of prostate cancer expressing the human *AR* was used in order to examine the prevalence of treatment-selected *AR* mutations in prostate cancer in an experimentally controlled context.

Mice do not naturally develop prostate cancer, so to encourage tumor formation, a transgenic oncogene construct carrying the SV40 early genes (T and t antigens) under the control of the minimal rat probasin promoter was expressed in the prostate creating the *tr*ansgenic *a*denocarcinoma of *m*ouse *p*rostate (TRAMP) model (Greenberg et al. 1995; Gingrich et al. 1996). Transgene expression is upregulated in the prostate at puberty and remains active throughout adult life. While cancer is artificially induced, TRAMP tumor development follows a similar progression to that seen in patients. Cells originating from the normal epithelial prostate form multiple hyperplastic foci that develop from low grade prostatic intraepithelial neoplasia (PIN) to high grade PIN. PIN progresses to prostate adenocarcinoma invading the basement membrane and metastasizing. TRAMP tumors also exhibit androgen-independent growth after castration enabling the study of therapy resistance in a mouse model (Greenberg et al. 1995).

A previous experiment in the TRAMP mouse examined the prevalence and location of somatic *Ar* mutations in prostate cancer under normal versus castrate

conditions. Mutations localized to different receptor domains depending on treatment. Mutations from castrated mice occurred in the N-terminal activation domain while those from intact mice were in the LBD (Han et al. 2001). One of the mutations identified in the NTD fell in a highly conserved motif that binds the COOH-terminus of Hsp70-Interacting Protein (CHIP) ubiquitin ligase (He et al. 2004). Disruption of this motif might prevent ubiquitination and proteasome degradation and increase AR stability. Unlike overexpression of wild type *AR*, expression of this mutant, AR-E231G, as a prostate-specific transgene caused prostate cancer, importantly showing that an aberrant AR can be oncogenic (Han et al. 2005).

The human and mouse androgen receptors share 100% identity at the protein level in the DBD and LBD, but differ significantly in the NTD with only 85% homology, including the position and length of the polyamino acid tracts (Gaspar et al. 1990). In order to examine somatic *AR* mutations that may have relevance in human disease, the human *AR* was introduced into the mouse locus by swapping human exon 1, which encodes the entire NTD, into the mouse gene creating the humanized AR mouse (h/mAR) (Albertelli et al. 2006). In studies detailed in Chapter 2, the h/mAR-TRAMP model was used to determine the prevalence of *Ar* mutations in hormone-dependent versus hormone-refractory disease. Because this study examined a large number of mice, we were able to look at the distribution of mutations that occur within and between treatment groups and identify regions of the *Ar* where mutations occur more often. This analysis was then extended to human metastatic prostate cancer samples in Chapter 3. Although the small sample size limited broad characterization of mutations, individual mutations from

patients fell in functional motifs and the mutant receptors demonstrated altered AR activity, providing compelling evidence for treatment selection.

AR in breast cancer

Two rare *AR* mutations have also been identified in male breast cancer patients hinting at a role for AR in this hormone-responsive disease. Interestingly, the two *AR* mutations fall within adjacent arginine residues in the second zinc finger of the DBD. In these patients, the mutant ARs also cause partial androgen insensitivity syndrome (PAIS), suggesting that reduced AR function may contribute to male breast cancer (Wooster et al. 1992; Lobaccaro et al. 1993). While AR is directly implicated in prostate cancer progression, its role in breast cancer is much less obvious. Hormone imbalances affect male breast cancer risk. For instance, men with Klinefelter Syndrome (XXY), who have both high estrogen and low testosterone levels, have a 50-60-fold increased risk of breast cancer compared to normal men (Hultborn et al. 1997; Swerdlow et al. 2005), but it is unclear how these hormone levels translate to increased risk. The androgen axis is generally thought to oppose the estrogen axis through their respective receptors. However, recent work has revealed more complex interactions between androgens and estrogens in hormone responsive tissues (Ellem et al. 2007). Is androgen action, through AR, protective against breast cancer, or can high levels of estrogen alone account for increased risk?

AR is also present in breast cancer in women. In fact, more breast cancers are AR positive (70-90% of all breast cancers and 50% of ER negative tumors) than ER positive (70-80%) (Birrell et al. 1998; Agoff et al. 2003). Testosterone is the precursor of

estrogen. Although serum testosterone levels are ten times lower in women than in men, synthesis of active androgens from adrenal precursors in peripheral target tissues such as the breast may be as much as 71% of that in men (Labrie 2006). Both AR and the steroidogenic enzymes needed to convert adrenal precursors to testosterone are present in breast ductal epithelia (Ruizeveld de Winter et al. 1991; Labrie et al. 2003), suggesting that androgens could influence breast cancer initiation and progression. Expression of AR target genes such as PSA and Kallikrein 15 are positive prognostic factors (Yu et al. 1995; Yousef et al. 2002). When androgens are administered along with antiestrogens, they increase treatment response (Tormey et al. 1983; Ingle et al. 1991). Recent evidence suggests that the synthetic progestin, medroxyprogesterone acetate (MPA), used in breast cancer therapy, may be acting through AR to reduce growth (Buchanan et al. 2005).

Parallels can be drawn between androgen action in prostate cancer and estrogen action in breast cancer. For instance, most breast cancers are estrogen responsive and the first line of treatment is antiestrogen therapy (Pichon et al. 1996). Like prostate cancer, metastatic breast cancer often becomes resistant to endocrine therapy and, in rare cases, resistance has been linked to changes in ER expression and activity. Alternatively spliced *ER* variants that exhibit altered function have been identified in breast cancer (McGuire et al. 1992; Fuqua et al. 1993). ER amplification is also found in 20% of breast tumors (Holst et al. 2007). However, the effect of the opposite receptor on sex-specific development and cancer initiation has not been fully examined. In Chapter 4, the *AR* mutations identified in male breast cancer were functionally characterized revealing promoter-specific differences in AR transactivation. These mutants may thus be activating a subset of targets that encourage breast cancer growth.

The presence of *AR* mutations in male breast cancer, and the general link between hormone imbalance and male breast cancer suggests that an active AR might be protective against breast cancer. In Chapter 5, the initiation of mammary gland tumors was examined in AR-null (testicular feminized male (*tfm*)) mice to see whether the absence of AR increased the rate of tumor development or had any effect on breast cancer initiation and progression. Over the course of these studies, a possible direct effect of AR in mammary gland development was uncovered in this model, since the failure of *tfm* mice to contract breast cancer was linked to their surprising inability to support mammary development.

AR in mammary gland development

Mammary gland development begins with formation of the ductal bud *in utero* but the majority of its development takes place postnatally. At birth, the mammary gland consists of a rudimentary ductal tree extending from the nipple. Prepuberty, ducts grow isometrically in proportion to the mouse. This is followed by allometric growth at puberty characterized by a burst of proliferation and extension of the ductal tree into the fat pad. Proliferation is concentrated in specialized structures at the tips of the mammary ducts, called terminal end buds (TEBs), which invade the fat pad until it is completely filled by a mature ductal tree at which point the TEBs regress. Finally, during pregnancy the mammary gland differentiates into milk-producing glands (Hennighausen et al. 1998; Watson et al. 2008).

Genetic studies with mouse knockout models have determined many of the factors involved in mammary gland development. Hormone receptors, particularly

estrogen receptor α (ERα) and progesterone receptor (PR), play key roles in the development and maintenance of the mammary gland. The AR is also expressed in the mammary gland. Its expression during fetal mammary ductal development is responsible for regression of the male mammary rudiment and nipple (Kratochwil et al. 1976).

AR is also expressed in adult mammary gland, but little is known about its function. Studying mammary development in AR knockout models is complicated by the fact that the *Ar* gene is located on the X chromosome. Because males are hemizygous, XY AR null mice are infertile, preventing the conception of homozygous female mutants. However, the mutant XY mice do not undergo normal male nipple regression and retain the mammary ductal rudiment allowing the study of mammary development in AR-null ducts. Classic mammary gland transplant experiments with *tfm* and female mice (Chapter 5) examined mammary gland development in the absence of functional AR. Results suggested both extrinsic and intrinsic factors are responsible for the *tfm* mammary gland phenotype. Developmental pathways are often harnessed to promote proliferation in cancer. Thus, understanding function and regulation of pathways during normal development can often provide insight into carcinogenesis.

The work presented in this thesis provides insight into how AR mutations can alter AR activity in both prostate cancer and breast cancer. Use of a mouse model of prostate cancer expressing the human AR identified mutations relevant to human disease, but with the added experimental control of an animal model (Chapter 2). Sequencing prostate cancer metastases allowed the comparison of treatment-selected AR mutations in genetically heterogeneous samples (Chapter 3). Functional characterization of AR

mutations in male breast cancer suggests how these mutations may influence disease (Chapter 4), while examination of mouse mammary gland development in the absence of AR (Chapter 5), begins to address the lesser-known role of AR in mammary ductal morphogenesis.

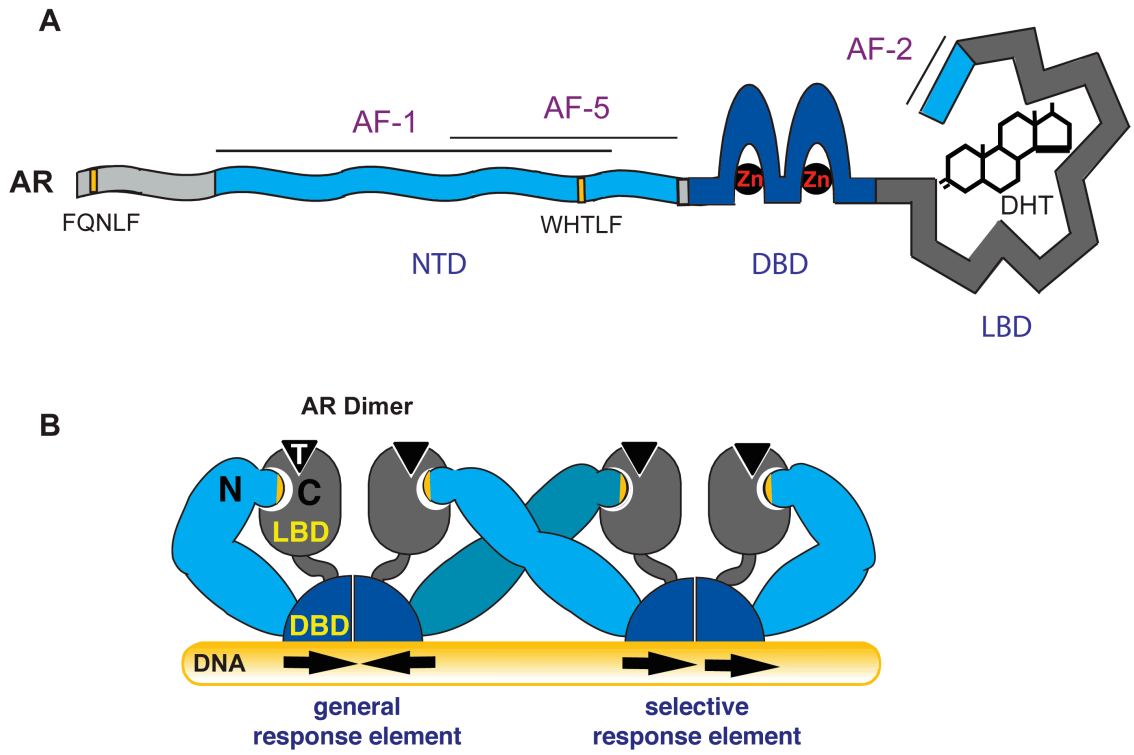

Figure 1.1. Structure of the androgen receptor protein.

A. AR, like other nuclear receptors, consists of modular functional domains: the N-terminal domain (NTD), DNA binding domain (DBD) consisting of 2 zinc fingers (dark blue) containing zinc (Zn) atoms, and the ligand binding domain (LBD) (grey) here binding dihydrotestosterone (DHT). AR has three interaction surfaces for coregulator binding, or activation functions (AFs) (light blue) that increase AR activity. Overlapping AFs, AF-1 and AF-5, make up the majority of the NTD and function independent of ligand binding. AF-2 is only exposed upon binding of ligand to the LBD. Two motifs in the NTD, FQNLF and WHTLF (yellow), participate in intramolecular interactions, shown in B, by binding to AF-2 and stabilizing ligand-bound AR. **B.** Upon ligand binding to the LBD, ARs dimerize and translocate into the nucleus where they bind to androgen response elements (AREs) in the promoter region of target genes. AREs can be either general elements consisting of inverted repeats or selective elements consisting of direct repeats. Promoters often have more than one ARE, and ARs may interact with each other through N/C interactions in which the FQNLF motif (yellow) in the NTD binds to its own AF-2 or the AF-2 of an adjacent AR. (Modified from Robins, 2005)

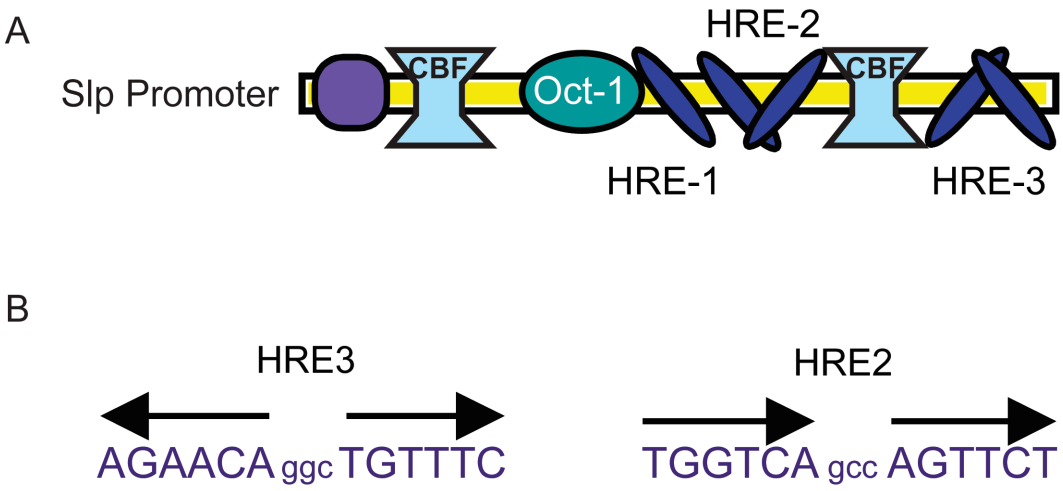

Figure 1.2. Schematic of the complex androgen-responsive Slp promoter.

A. The Slp promoter contains multiple hormone response elements (HREs): one half site (HRE1) and two repeats (HRE2 and HRE3) where AR (represented by blue ovals) can bind. AR cooperates with other transcription factors, such as Oct-1 and CBFα1, to transactivate target genes. **B.** Sequence of HRE3, a canonical response element with an inverted repeat and a three nucleotide spacer between the half sites (left). Sequence of HRE2, an AR-selective response element consisting of two half sites arranged as direct repeats (right). Arrows indicate the orientation of the half sites. (Modified from Robins, 2004.)

Chapter 2

Profiling Human Androgen Receptor Mutations Reveals Treatment Effects in a Mouse Model of Prostate Cancer[1]

Abstract

Gain of function mutations in the androgen receptor (AR) are found in prostate cancer and have been implicated in the failure of hormone therapy. Most studies have emphasized the importance of the ligand binding domain (LBD) where mutations can create promiscuous receptors, but mutations in the N-terminal transactivation domain (NTD) have also been found. To assess AR alterations as a mechanism of treatment resistance, a mouse model (h/mAR-TRAMP) was used in which the murine AR coding region is replaced by human sequence and prostate cancer initiated by a transgenic oncogene. Mice received either no treatment, androgen-depletion by castration or treatment with antiandrogens, and twenty AR transcripts were sequenced per end-stage tumor. All tumors expressed several mutant alleles, although most mutations were low frequency. Some mutations that occurred multiple times within the population were differentially located dependent on treatment. Mutations in castrated or

[1] This chapter represents the contents of a published manuscript: O'Mahony, O. A., Steinkamp, M. P., Albertelli, M. A., Brogley, M., Rehman, M. and Robins, D. (2008). Profiling human androgen receptor mutations reveals treatment effects in a mouse model of prostate cancer. Mol Cancer Res **6** 1691-1701. The first two authors contributed equally to this work.

antiandrogen-treated mice were widely dispersed but with a prominent cluster in the LBD (amino acids 736-771), while changes in intact mice centered near the N-terminal polymorphic glutamine tract. Functional characterization of selected LBD mutant alleles showed diverse effects on AR activity, with about half of the mutations reducing transactivation *in vitro*. One mutant receptor, AR-R753Q, behaved in a cell and promoter-dependent manner, even though as a germline mutation it causes androgen insensitivity syndrome. This suggests that alleles that are loss of function during development may still activate a subset of AR targets to become gain of function in tumorigenesis. Mutant ARs may thus utilize multiple mechanisms to evade cancer treatment.

Introduction

Somatic mutations are a hallmark of cancer initiation, progression and metastatic disease. During tumorigenesis, genomic instability leads to a mutator phenotype in which it is estimated that each cancer cell may harbor as many as 1,000 mutations (Bielas et al. 2006). While most mutations likely are "passengers" with little effect on selection, some may be "drivers" that provide a growth advantage (Greenman et al. 2007). In the case of prostate cancer, numerous mutations in AR have been identified. Intriguingly, many of them are gain of function (Shi et al. 2002), but the extent to which they influence disease progression has been debated.

Prostate cancer is initially androgen-dependent and responds to treatments that inhibit androgen synthesis and/or antagonize AR action. However, tumors ultimately recur and AR remains present and active despite hormone therapy (Scher et al. 1997).

Numerous mechanisms have been proposed for AR activation following androgen depletion, including *Ar* gene amplification, AR activation by growth factors or altered levels of coregulators. Mutations within the receptor itself have also been found that allow androgen-independent activation, increase sensitivity to low androgen, and alter ligand specificity (Feldman et al. 2001).

A paradigm of how gain of function mutations may allow treatment evasion is illustrated by the mutant AR, AR-T877A, found in the LNCaP cell line and some advanced prostate cancers (Taplin et al. 1995). For wild type AR, hormone binding alters conformation of the ligand binding domain (LBD) to create a coactivator interaction surface, activation function 2 (AF-2), which is not formed with bound antiandrogen. The subtle shift in structure due to T877A, proximal to AF-2, permits an active conformation with various noncanonical ligands, including the antiandrogen hydroxyflutamide (Hur et al. 2004). This, and other mutations that allow promiscuous AR activation, may underlie the phenomenon of flutamide withdrawal syndrome in which tumors regress after antiandrogen treatment is stopped (Hara et al. 2003). Because ligand is key in AR transactivation, the search for AR mutations in prostate cancer has focused on the LBD (Shi et al. 2002). However, the DNA binding domain (DBD) and the large N-terminal transactivation domain (NTD) also influence hormone-dependent function, and as importantly, may enter into ligand-independent activation (Shen et al. 2005). Unfortunately, the NTD is often ignored since its high GC content and polymorphic repeats impede sequencing.

The prevalence of *AR* mutations in prostate cancer and their possible association with specific treatments has been difficult to evaluate because of human genetic

heterogeneity, disparate patient treatment, lack of biological samples, and the small sizes of most clinical studies. Mouse models help circumvent these issues, providing an opportunity to study somatic mutations in cancer. The *tr*ansgenic *a*denocarcinoma of *m*ouse *p*rostate (TRAMP) model (Greenberg et al. 1995) has been used to compare *Ar* mutations in tumors from intact (untreated) versus castrated (androgen-ablated) mice. Although a small study, location of *Ar* missense mutations in primary tumors varied with hormonal status, with seven of nine mutations from castrated mice occurring in the NTD and all mutations from intact mice confined to the LBD (Han et al. 2001). One of the mutants identified, AR-E231G, is sufficient to cause cancer when expressed as a prostate-specific transgene, highlighting the oncogenic potential of *Ar* mutations (Han et al. 2005).

To examine whether somatic mutations in prostate cancer correlate with treatment in the context of human AR, we utilized a knock-in mouse in which the human *AR* exon 1 was swapped into the mouse locus to create an AR nearly identical to human (Albertelli et al. 2006), bred to TRAMP to initiate prostate cancer. Our objective was two fold: 1) to determine whether somatic mutations in the humanized AR (h/mAR) are random or are selected by treatment and 2) to examine whether different treatments select for distinct mutation clusters in functional AR domains. Sequencing the entire coding region from tumors of mice in varied treatment groups confirmed by an unbiased approach that mutation of AR was common overall but few events achieved high frequency in the tumor cell population. Nevertheless, some mutations reflected treatment and some had context-dependent functions, further delineating the role of AR in cancer progression.

Materials and Methods

Mice

Female h/mAR mice (Albertelli et al. 2006) were mated to TRAMP males on a C57BL/6J background. Short-term treatments of 12-week-old males were castration by surgical orchiectomy or treatment with bicalutamide (Bic) or flutamide (Flu). Bic was compounded with food pellets and administered ad lib for a dose of 50 μg/g based on average food consumption. Flu (25 μg/g) was administered in food pellets or by a 75 mg 60 day slow release subcutaneous pellet (Innovative Research, Sarasota, FL). Age- and gender-matched intact mice served as controls. After 4 weeks, animals were sacrificed. AR N20 antibody (Santa Cruz Labs) was used to detect AR in formalin fixed, paraffin embedded prostate tissue. Serum T levels were measured by RIA (DSL, Webster, TX).

For tumor analysis, h/mAR-TRAMP males were randomly assigned to 4 treatment groups (9-10 mice/group): castration at 12 weeks of age, treatment with 50 μg/g Bicalutamide or 25 μg/g Flutamide upon tumor detection, or no treatment. Tumors were monitored by MRI or abdominal palpation and mice were euthanized when moribund as described (Albertelli et al. 2008). Primary prostate tumors, metastases and testes were harvested into RNAlater buffer (Ambion, Inc., Austin, TX) or flash frozen in liquid N_2. All mouse procedures were approved by the University of Michigan Committee on Use and Care of Animals, in accordance with the NIH guidelines for the Care and Use of Experimental Animals.

RNA and DNA isolation

Tumor RNA was isolated with RNeasy kits (Qiagen Inc, Valencia, CA) and 1 µg was reverse transcribed using Superscript II RT (Invitrogen, Carlsbad, CA) with 0.5 µg oligo(dT) in a 20 µl reaction. Two RT reactions were performed per sample to control for enzyme error. Testis RNA from 17 mice was reverse transcribed and select fragments of AR were amplified and sequenced as controls. DNA was extracted as previously described (Miller et al. 1988). Briefly, tissue was digested overnight at 37^{o}C in Lysis Buffer (10 mM Tris HCl, 400 mM NaCl, 2 mM Na_2EDTA, pH 8.2) with 250 µg/ml proteinase K and 0.5% SDS. Proteins were removed by precipitation with NaCl and the DNA was precipitated with 2 volumes 100% ethanol.

Amplification, subcloning and sequencing of the *Ar* coding region

The *Ar* coding region was amplified in 4 fragments, three from RNA (proximal NTD, DBD and LBD) and one from DNA (NTD). PCR primers for h/mAR samples are listed below. PCR amplifications were performed in 25 µl reactions containing 2.5 units Platinum *Pfx* DNA polymerase (Invitrogen), 2X Buffer and 1X GC enhancer (supplied by the manufacturer), 1.5 mM $MgSO_4$, 0.3 mM dNTPs, 0.5 µM each primer, and 1-3 µl of the RT reaction or 100 ng genomic DNA. PCR conditions optimized for each primer pair were: 94^{o}C for 5 min, 25-35 cycles of 94^{o}C for 30 sec, 55^{o}C (57^{o}C for primer pair 1) for 30 sec, and 68^{o}C for 90 sec, with a final extension step at 68^{o}C for 10 min.

h/mAR 1 Sense 5’ TCGGTGGAAGCTACAGACAA 3’
h/mAR 1 Antisense 5’ CCGACACTGCCTTACACAAC 3’

h/mAR 2 Sense	5’ TTCGACCATTTCTGACAACG 3’
h/mAR 2 Antisense	5’ TTGGTCAAAAGGAGGCATTT 3’
h/mAR 3 Sense	5’ AGTGTGGTACCCTGGTGGAG 3’
h/mAR 3 Antisense	5’ TTGTGCATGCGGTACTCATT 3’
h/mAR 4 Sense	5’ CAACTTGCATGTGGATGACC 3’
h/mAR 4 Antisense	5’ TCTGGAAAGGGAACAAGGTG 3’

Products were visualized on 1% agarose gels and bands were excised and purified with the QiaexII gel extraction kit (Qiagen). 3’-A overhangs were added to the blunt-ended product by incubation with *Taq* polymerase (Invitrogen) at 70^{o}C for 30 min. Products were ligated into the pGEM-T easy vector (Promega, Madison WI) and transfected into DH5α chemically competent bacterial cells (Invitrogen). DNA from 20 clones /sample (10 clones/RT reaction) was purified with QIAprep Spin Miniprep columns (Qiagen) or with the MacConnell Mini-Prep 24 Machine (MacConnell Research, San Diego, CA) according to the manufacturer’s directions and submitted to the University of Michigan DNA Sequencing Core for analysis.

Sequence Analysis

Sequence was compared to the human *AR* sequence (Genbank Accession# NM_000044) using Sequencher software (version 4.1, Gene Codes, Ann Arbor, MI). Putative mutations were then checked against the Androgen Receptor Gene Mutations Database (Gottlieb et al. 2004).

Mutagenesis of AR expression plasmids

Six mutations (M524T, S741F, M750I, W752C, R753Q, and R761G) were introduced into pCMV5-hAR using the Quickchange Site Directed Mutagenesis kit (Stratagene) and the primer pairs below containing each mutation (underlined):

M524T Sense:	CCACTTGTGTCAAAAGCGAAA<u>C</u>GGGCCCCTGGA
M524T Antisense:	TCCAGGGGCCC<u>G</u>TTTCGCTTTTGACACAAGTGG
S741F Sense:	GCTGTCATTCAGTACT<u>T</u>CTGGATGGGGCTCATG
S741F Antisense:	CATGAGCCCCATCCAG<u>A</u>AGTACTGAATGACAGC
M750I Sense:	GCTCATGGTGTTTGCCAT<u>T</u>GGCTGGCGATC
M750I Antisense:	GATCGCCAGCC<u>A</u>ATGGCAAACACCATGAGC
W752C Sense:	TGTTTGCCATGGGCTG<u>T</u>CGATCCTTCACCAATG
W752C Antisense:	CATTGGTGAAGGATCG<u>A</u>CAGCCCATGGCAAACA
R753Q Sense:	TGTTTGCCATGGGCTGGC<u>A</u>GTCCTTCACCAATGTCAAC
R753Q Antisense:	GTTGACATTGGTGAAGGAC<u>T</u>GCCAGCCCATGGCAAACA
R761G Sense:	CACCAATGTCAACTCC<u>G</u>GGATGCTCTACTTCGC
R761G Antisense:	GCGAAGTAGAGCATCC<u>C</u>GGAGTTGACATTGGTG

The mutant synthesis, DpnI digestion, and transformation were performed as detailed in the manual. DMSO was added to the mutant strand synthesis reaction to prevent CAG and GGN repeat contraction. Plasmids were sequenced to verify the presence of the mutation and retention of the original number of repeats within the polyamino acid tracts.

Transactivation assays

CV-1 cells were cultured in DMEM + 10% fetal bovine serum, 1% Glutamax and 1% penicillin/streptomycin. PC-3 cells were cultured in RPMI + 10% fetal bovine serum, 1% Glutamax and 1% penicillin/streptomycin. The day before transfection, cells were seeded at 5 x 10^4 (CV-1) or 1 x 10^5 (PC-3) cells/well in a 12-well plate. Four hrs before transfection, media was replaced with DMEM or RPMI + 2.5% charcoal-stripped NuSerum, 1% Glutamax. Cells were transfected using Fugene 6 reagent (Roche) at 3 µl Fugene/µg DNA with 4 ng pCMV5-hAR (wild type or mutant), 400 ng luciferase reporter plasmid and 100 ng promoterless renilla (Promega) for normalization. 24 hrs post-transfection, cells were rinsed in 1X PBS and fed with phenol red-free DMEM or RPMI media + 10% charcoal-stripped Nuserum +/- hormone. Cells were harvested 48 hrs post-transfection. The PSA-luc reporter (Perez-Stable et al. 2000) was a gift from K. Burnstein.

Western blotting

CV-1 cells were seeded at 4 x 10^5 cells/ 60 mm dish the day before transfection. Four hrs before transfection cells were rinsed in 1X PBS and fed with phenol red-free DMEM + 10% charcoal-stripped NuSerum, 1% Glutamax +/- 1 nM R1881. Cells were transfected with 100 ng receptor (hAR or mutant) and 1.9 µg empty vector (pCMV5) with Fugene 6 (3 µl/µg DNA). 24 hrs after transfection cells were rinsed in ice cold 1X PBS and harvested in 100 µl RIPA buffer + protease inhibitors. Cell lysates were incubated at 4^{o}C for 10 min and then centrifuged at 4^{o}C for 10 min to pellet cell debris. Protein quantification was performed using the Dc Protein Assay (Bio Rad). 20 µg

protein lysate was run on an 8% SDS-polyacrylamide gel and transferred onto a nitrocellulose membrane. The blot was probed with antibody N20 to the AR NTD (Santa Cruz, CA) at 1:500 dilution and incubated with HRP-conjugated anti-rabbit IgG at 1:5,000 dilution for 45 min. Bands were detected with ECL western blotting reagents (Pierce, Rockford, IL).

3D structure representations

LBD mutations were examined by homology to the X-ray structure of AR complexed to the FXXLF motif (Hur et al. 2004) using the SWISS-MODEL automated protein structure homology-modeling server (Arnold et al. 2006). 3-D structures were viewed in Protein Explorer (Martz 2002).

Statistics

Significance of differences in disease length between treatments was determined using a Bonferroni multiple comparison adjustment ($p<0.01$).

Results

Treatment affects tumor progression in h/mAR-TRAMP mice

To examine whether somatic mutations correlate with treatment in the context of human AR, the h/mAR model was used, in which homologous recombination replaced the mouse *Ar* exon 1 with the corresponding human sequence (Albertelli et al. 2006).

The murine NTD differs from human by 15% in amino acid sequence and lacks the polymorphic glutamine (Q) and glycine (G) tracts that affect AR activity and are implicated in prostate cancer progression (Albertelli et al. 2008). Exchanging the NTD creates a hybrid gene within the mouse genomic locus that is 97% identical in coding sequence to *hAr*. These humanized AR mice were crossed to TRAMP mice that express a prostate-specific SV40 T-antigen oncogenic transgene (Greenberg et al. 1995; Gingrich et al. 1996), allowing examination of mutations in human *Ar* that arise in prostate cancer in genetically homogeneous mice.

To ensure that the h/mAR-TRAMP mice responded to hormone ablation similarly to wild type mice, short-term effects of androgen blockade were assessed in 12-week-old males treated for 4 weeks by castration or with antiandrogens (flutamide or bicalutamide). Prostatic AR protein detected by immunohistochemistry (IHC) showed nuclear localization in intact mice, while in castrated mice most AR was cytoplasmic indicative of the unliganded state (Figure 2.1A). In antiandrogen-treated mice, most AR was nuclear since these antagonists permit nuclear transit and DNA binding but not target gene activation (Marcelli et al. 2006). Both antiandrogens reduced serum testosterone (T) to less than 25% of intact levels (Figure 2.1B) unlike in men where androgen synthesis inhibitors are necessary to reduce hormone levels. This likely reflects differences in the hypothalamo-pituitary-gonadal axis and adrenal androgen synthesis in mice and men.

In end-stage primary tumors from intact, castrate, or antiandrogen-treated mice AR localization was similar to that of short-term treatment, being nuclear in intact and antiandrogen-treated mice, but scant in castrates (Figure 2.1C). However, AR staining

was heterogeneous by end-stage, in all treatment groups. The time from tumor detection by palpation to death revealed differences in survival with disease in treated compared to intact mice (Figure 2.1D). In TRAMP mice, castrates survive only a short time once tumors are detected, suggesting that in this model early reduction in androgen synthesis encourages growth of aggressive androgen-independent tumors (Johnson et al. 2005). Bicalutamide or flutamide treatment after tumor detection significantly extended survival with disease (flutamide versus control, $P < 0.008$, bicalutamide versus control, $P < 0.0001$ using a Bonferroni multiple comparisons adjustment).

Analysis of mutation frequency in h/mAR-TRAMP tumors

To detect mutations in *Ar* mRNA transcripts that may be present in only a subset of tumor cells, a reverse transcription (RT)/amplification/sub-cloning strategy was used (Figure 2.2). Sequencing the equivalent of 20 *Ar* mRNAs per primary tumor (10 from each of two independent (RT) reactions, 760 clones total) identified 994 changes from the reference sequence. 808 of these putative mutations were single base changes. Variation in Q or G tract codon numbers was common and was analyzed separately. Based on the total number of nucleotides sequenced, prostate tumors had an average of 4.0 changes/10,000 bp of *Ar* coding region. To obtain a baseline mutation rate for the methodology, *Ar* was sequenced for 17 of these mice from testes where AR but not the T-antigen oncogene is expressed. 33 base substitutions were identified from 230 clones, or about 2.2 changes/10,000 bp. This likely represents the combined error of RT (1/15,000 bp per the manufacturer), the polymerase (1.58/100,000 per the manufacturer) and subcloning and sequencing errors. This error rate may be an overestimate since many of

the testis clones included the error-prone Q-tract region (see below). Nevertheless, tumor samples had twice as many sequence changes as non-tumor samples. Of these putative mutations, 54.1% were missense, 8% base deletions, 4% codon deletions, 1.6% base insertions, 4.7% nonsense and 27.4% silent mutations (Table 2.1). The distribution of mutation types across treatment groups did not differ significantly (Table 2.1).

Different cancer types often display a unique mutation spectra favoring one type of base pair change over another (Greenman et al. 2007). Analysis of the h/mAR-TRAMP prostate tumor spectrum revealed a preponderance of mutations at C:G sites that was not seen in the testis. Prostate cancer mutations showed high C:G to T:A transitions (41.0%) and C:G to A:T transversions (21.3%) but low G:C to C:G transversions (1.9%) (data not shown), unlike the reported breast cancer spectrum which has frequent G:C to C:G transversions (Greenman et al. 2007).

The majority of mutations were identified in one or two clones per tumor. Consistent with the previous report on TRAMP mice, this represents a mutation frequency of 5-10% of the cell population (Han et al. 2001). However, considering that samples often contain malignant and normal cells and that prostate cancer is multifocal, mutation frequency within the tumor may be higher. As evidence, 24 mutations were present in multiple clones from a single tumor, with four (Q58L, R102X, S324G, A385T) occurring in four clones (20%) each from an independent tumor.

Recurring mutations in h/mAR-TRAMP tumors

To further exclude possible random errors, only codons mutated at least twice were further analyzed. Missense mutations in multiple clones of a single tumor (23

codons) or in multiple tumors (109 codons) occurred at an overall rate of 0.53/10,000 bp. Figure 3A depicts a Venn diagram of mutations that recurred within or between treatment groups. Only four mutations occurred in all groups (Q58L, G228S, R544G and A764S) three of which were in the NTD. Tumors from flutamide-treated mice bore the most unique mutations (11) whereas those treated with bicalutamide shared most mutations with the flutamide-treated group.

Missense mutations mapped throughout *Ar* (Figure 2.3B) but many clustered within regions mutated in prostate cancer patients, such as a proximal region of the LBD (residues 700-800) (Gottlieb et al. 2004). Mutations around the Q-tract were found in all groups but most commonly in intact mice. Mutations in three activation function (AF) domains reflected treatment, with the antiandrogen groups carrying many more in the distal NTD region of AF5, while the intact and castrated mice had more mutations in AF1. Overall there were few mutations in AF2, with the least in the castrated group, as might be expected for tumorigenesis under androgen-depleted conditions.

Recurring mutations subdivide into two sets: substitutions at the same codon to different amino acids (e.g., R13Q, R13W), which might represent selection against wild type, and substitutions in one codon to the same residue (e.g., 2 tumors with L110P), perhaps indicating selection for a specific change. 70 codons were mutated to different residues, and 84 codons to the same amino acid (Figure 2.3C). Remarkably, only one mutation to different amino acids recurred in testis and none to the same amino acid, suggesting this conservative analysis excluded most of the base changes due to methodology. Each tumor averaged 5 recurring mutations to the same amino acid, with

most in amino acids conserved between mouse and man. In the NTD, only 13 mutations recurred in nonconserved residues, of which 10 occurred in or near the Q or G tracts.

The prevalence of missense compared to silent mutations within a domain can suggest positive selection (Tarraga et al. 2007). Graphing the frequency of recurring missense and silent mutations in 50 amino acid segments along the AR shows variation over the length of the protein (Figure 2.5). The polyamino acid tracts have an increased frequency of mutation with the Q tract having increased missense mutations and the G-tract increased silent mutations. This is likely due to the nature of the repeat sequence where Q to R mutations are common in the CAG repeat. Other areas that show a larger proportion of missense mutations may suggest areas where mutations may be advantageous.

Although silent mutations are less likely to alter AR function, they can affect splicing or mRNA stability, as well as protein folding due to altered codon usage (See discussion). Recurring silent mutations were distributed throughout the AR coding region and showed no apparent differences between treatment groups. However, a few interesting observations were noted. First, the majority of the silent mutations altered a more abundant codon to a less abundant codon. Only silent mutations in proline, serine and alanine changed a rare codon to a more abundant codon. Both proline and serine silent mutations were over represented within the recurring silent mutations. Further, the distribution of silent proline mutations along the AR protein was confined to the first 172 amino acids even though there are 38 additional prolines in the sequence, including a run of eight prolines beginning at amino acid 374. This may suggest that while the early prolines within the disorganized NTD are unconstrained, the codon choice of the later

prolines may be more controlled. Three of the eight prolines that carried silent mutations changed from the most rare codon (CCG with a frequency of 6.2/1000 codons) to one of the more abundant codons (between 17.3-18.4/1000 codons).

Mutations in or near the NTD polyamino acid tracts

Contraction of the Q tract occurs clinically (Alvarado et al. 2005) and expansion and contraction of both Q and G tracts by one or two codons was common in the mouse tumors. While all testis clones, and 96% of those from prostate, had 21 or 22Qs, 2.1% of the tumor clones had 19-20 Qs and 2.3% had 22-31 Qs. The G tract also varied – most clones (84.3%) had the original 23 Gs, but 12.4% lost one and 3.3% lost 2 to 6 Gs. Although there were no large alterations in Q tract length, Q to R substitutions within the tract were common in all groups, occurring in 23 clones from 12 tumors, with none in testis. One such mutation, Q65R, was reported in a clinical sample (Gottlieb et al. 2004). While a functional significance of disrupting the Q tract with arginine is unknown, disruption by leucine elevates transcriptional activation despite limiting N/C interaction (Buchanan et al. 2004).

A stretch of six Qs (amino acids 86-91) of unknown function just beyond the major Q-tract showed contraction to five or four Qs in 22 mice from all groups (ΔQ86), but not in testis. The most common mutation in this study, Q58L, occurred next to 4 leucines just before the Q tract in which mutation of the first Q codon expands the L tract from 4 to 5 residues. This was found in 16 mice representing all groups, and was in two or more clones in 4 of these mice, as well as in one clone from a testis control. Interestingly, this tract has expanded from one L in mouse and dog, to three in

chimpanzee, and four in man. Whether or not this expansion affects AR activity is unknown.

Ar mutations that may affect AR function

Previously identified as well as novel mutations within functionally significant regions were found in multiple tumors. In the NTD, few of the recurring mutations had been identified previously since few studies have systematically sequenced this region. However, Q114L, found in two castrated mice (one primary tumor and one lymph node metastasis) was noted in a primary prostate tumor (Tilley et al. 1996). This same study also reported L575P, which we found in one bicalutamide- and one flutamide-treated mouse. A novel NTD mutation, M524T, is located in AF5, an area that interacts with p160 coactivators and is involved in ligand independent activation (Shen et al. 2005). M524T occurred in 3 flutamide- and 2 bicalutamide-treated mice but not in intact or castrated mice. Four of 7 mutations previously identified in patients with flutamide withdrawal symptoms were located in this area, between residues 502 to 535 (Tilley et al. 1996).

Within the LBD, three novel mutations, R711M, H715Y and W719C, were identified within the most highly conserved segment, the signature sequence (Figure 2.3C), where other mutations alter ligand specificity (Culig et al. 1996; Fenton et al. 1997; Zhao et al. 2000). All three mutations lie on the same surface of helix three, adjacent to AF2, where they may influence protein-protein interactions. Of the remaining LBD mutations, 10 clustered between amino acids 736-771 (Figure 2.3C) where they might affect ligand specificity. 8 of these were common, occurring in 3 or more mouse

tumors (Figure 2.3C). M750I, F755L and V758I, were identified previously in patients (Gottlieb et al. 2004). In particular, M750I was identified in disease recurring after orchiectomy and bicalutamide treatment (Haapala et al. 2001). Here, M750I was found in two mice, one treated with flutamide and one with bicalutamide.

Three novel mutations in this cluster were of particular interest based on their presence in treatment groups or their location. S741F lies adjacent to W742 where a mutation allows bicalutamide, but not flutamide, to act as an agonist (Bohl et al. 2005). This mutant was identified only in antiandrogen-treated mice, in two each per treatment. W752C might expand the base of the binding pocket to accommodate other ligands, and was found in two clones from a castrated mouse, and one each from a flutamide- and a bicalutamide-treated mouse. R753 contacts androgen and its mutation to Q previously was shown to cause complete androgen insensitivity (CAIS) in man and rat (Gottlieb et al. 2004), but had not been noted in prostate cancer. R761G was unique to the castrated group, in two primary tumors and a metastasis.

Some *Ar* mutations are treatment group-specific

Substitutions that occurred more than once within a group, either in more than one mouse of a group (29 mutations) or multiple times in a single tumor (25 mutations), revealed treatment effects (Figure 2.3D). 14 of these mutations also occurred once in other groups. Few substitutions overlapped between groups, with only Q58L and ΔQ86 occurring in all groups and only G209R occurring in both castrated and intact mice. Nine of 11 substitutions recurring in the intact group clustered around the Q tract, with 4 Q to R substitutions within the tract itself. Most recurring mutations in the castrated group (13

of 20) were in the NTD, as noted previously (Han et al. 2001), and six occurred more than once within a tumor. Two mutations were found proximal to the first zinc finger of the DBD (S542G and T543A) and 5 clustered in the LBD between residues 736 - 771.

The two antiandrogen treatment groups showed distinct mutation patterns, perhaps due to differences in structure of the ligands. There were many more recurring mutations with flutamide than with bicalutamide, and most (10 of 16) were in the DBD and LBD. One of three substitutions in the DBD, C563R, mutated a zinc-chelating cysteine in the first zinc finger and is likely to be a loss of function. Another, G578C, altered a conserved base in the P-box important for DNA binding specificity (Nguyen et al. 2001), and the last, R616L, contacts the phosphate backbone (Freedman 1992). Four missense mutations were located in the LBD where they could affect ligand-dependent activation (see below). The flutamide group also had many more nonsense mutations (5 out of 16) than other groups. The bicalutamide-treated group had few recurring mutations: 3 were unique and 2 overlapped with only the flutamide-treated group.

Transcriptional activity of select AR mutants

Mutations clustered in the proximal portion of the LBD included novel as well as previously reported but uncharacterized mutations. For functional analysis, five LBD mutations (S741F, M750I, W752C, R753Q and R761G), and M524T that was specific to the antiandrogen groups, were introduced into an AR expression vector. Wild type and mutant residues in the LBD cluster are represented in Figure 2.4A. All mutant ARs expressed at levels equivalent to wild type when transfected into CV-1 cells (Figure 2.4B). M524T migrated more slowly, possibly due to differential protein modification.

Treatment with phosphatase did not abolish the M524T size difference indicating it is likely not due to altered phosphorylation (data not shown).

Mutant transactivation was tested in CV-1 cells on C'Δ9-luc, a luciferase reporter driven by the AR-specific enhancer of mouse *Slp* (Robins 2004). Three types of response to the synthetic androgen R1881 were exhibited: M524T was as active as wild type, R753Q and R761G were less responsive at lower ligand concentrations, and S741F, M750I and W752C were inactive even at 1 nM R1881 (Figure 2.4C). None of the mutants responded to either hydroxyflutamide or bicalutamide at doses of hydroxyflutamide that strongly activate AR-T877A (data not shown).

To compare transactivation in prostate cancer cells, mutants were transfected into AR-negative PC-3 cells along with C'Δ9-luc or PSAe1p-luc, containing the prostate specific antigen (PSA) upstream enhancer and proximal promoter (Perez-Stable et al. 2000). M524T and R761G had wild type activity with 1 nM R1881 for both reporters (data not shown). S741F, M750I, and W752C that were inactive in CV-1 cells were also weak in PC-3 cells. However, increasing R1881 concentration to 1 μM rescued receptor activity for all but S741F (Figure 2.4D). Interestingly, R753Q, which had very low activity in CV-1 cells, was more potent in PC-3 cells, with half the activity of wild type AR on C'Δ9-luc and as much activity as wild type on PSAe1p-luc (Figure 2.4E). The differential response of R753Q could reflect promoter-specific differences in AR response elements or interactions with other factors.

Androgen response elements are either canonical inverted repeats of a TGTTCT half-site that can bind multiple steroid receptors or direct repeats of the half-site that selectively bind AR but confer weak activation (Robins 2004). Both PSA and Slp

enhancers consist of a complex mix of canonical and selective elements, as well as binding sites for other factors. To determine whether the differential activity of AR-R753Q depended on the response element, activity was tested on either canonical (HRE3) or AR-selective (HRE2) elements from the *Slp* enhancer. While R753Q was able to transactivate the HRE3 reporter at wild type levels, it showed little activity on the AR-selective HRE2 (Figure 2.4F). This is intriguing since the equivalent mutation in rat, R734Q, is the germline mutation accounting for CAIS in the *tfm* rat (Yarbrough et al. 1990). Characterization of this subset of mutants suggests that some mutations have subtle, but potentially important, affects on AR function that can be cell and promoter context dependent. In particular, loss of function mutations such as those identified in AIS may, in the context of prostate cancer, be gains of function by differentially activating a subset of AR targets.

Discussion

This study queried somatic *hAr* mutations expressed in h/mAR-TRAMP mouse prostate cancer for evidence of selection due to treatment. Numerous alterations were present at a low frequency, in part reflecting increased mutation during oncogenesis (Bielas et al. 2006). Based on an error rate estimated from testis cDNA, about half of the AR changes in tumors are putative somatic mutations arising during disease. Restricting analysis to recurring mutations highlighted those with a possible selective advantage as evidenced by their variation in position and frequency with treatment.

The number of *Ar* mutations identified was higher than in previous studies, although most mutations were only present in one or two clones of the twenty sequenced

per tumor. While accumulation of rare mutations may be a general characteristic of tumor genomes, mutations in *AR* are more phenotypically evident because the gene is monoallelic. Many of these mutant alleles may confer similar growth advantages, resulting in heterogeneous cell subpopulations within a tumor. Multiple mutations in a single tumor have been reported in hormone-refractory prostate cancer (Hyytinen et al. 2002). In one case, two mutations were identified in a single transcript and both influenced AR function (Monge et al. 2006). Because cDNAs in this study were amplified in fragments, it is not possible to determine whether mutations in different segments exist in a single transcript.

Among studies, differences in the number of mutations detected likely reflect the methodology, disease stage, and experimental model. By amplifying and subcloning Ar cDNA, sequence changes are evident in as few as 5% of the transcripts, while genomic DNA, examined in most clinical studies, can only reveal mutations present in a majority of cells. Analyzing the entire *Ar* coding region showed that about half of the mutations occur in the usually ignored NTD. The prior TRAMP study examined earlier stage tumors and identified fewer mutations per mouse but all were also at low frequency, suggesting that mutation abundance may be influenced by the model (Han et al. 2001). The survival benefit of individual mutations may be modest relative to the strong proliferative drive conferred by T-antigen. We have gone on to analyze AR mutations from the cDNA of human metastases using the same method and have found a similar mutation rate in the AR (Chapter 3). However, more AR mutations from the patient metastases were found in more than one clone per sample suggesting that end stage

primary tumors from TRAMP mice may be more heterogeneous than patient metastases that are more clonal in nature.

Clustering of recurring *Ar* mutations in distinct functional domains highlights the influence of therapy. Mutations are least frequent in the intact mice, in accord with clinical studies that find fewer AR mutations in untreated or androgen-responsive tumors (Marcelli et al. 2000; Chen et al. 2005). In the previous TRAMP study (Han et al. 2001), most mutations in intact mice occurred in the AR C-terminus, in contrast to their NTD location here. This could reflect AR species differences, particularly since mutations in intact h/mAR tumors centered around the Q-tract that is poorly conserved in mice. On the other hand, mutations after castration are found primarily in the NTD similar to the earlier study (Han et al. 2001). This may be because all NTD mutations in the castrate group occurred in residues conserved between mouse and man, suggesting a role for these residues in androgen-independent activation.

Mutations in antiandrogen-treated mice overlap little with those in the castrate group, indicating that early depletion of androgen leads to tumor development distinct from that of antagonist treatment. Two mutations, M524T and S741F, occurred in multiple mice for both flutamide and bicalutamide treatments, and thus may affect interactions particular to antiandrogen-bound AR. Since M524T had altered electrophoretic mobility, post-translational modification may influence differential AR activity. Numerous protein modification sites are nearby, including ones for Erk2 phosphorylation at S515, RACK1 phosphorylation at Y535, and ligand-dependent SUMOylation at K520 (Callewaert et al. 2004; Kraus et al. 2006; Funderburk et al.

2008). The other shared mutation, S741F, is transcriptionally inactive; the presence of stable cytoplasmic protein suggests ligand binding is defective.

Many more recurring mutations were identified in flutamide- than in bicalutamide-treated mice. Since flutamide is a partial agonist of AR at high concentrations *in vitro*, lower concentrations such as those found in patients may activate mutant alleles (Suzuki et al. 1996). Altering the LBD to achieve activation by the bulkier bicalutamide may be more difficult, but has been reported for AR-W742L (Bohl et al. 2005). Flutamide-treated mice also express several nonsense mutants. Whereas the N-terminal AR-R102X most likely is a loss of function allele, other mutants terminating within the DBD or LBD may produce constitutive receptors (Gao et al. 1996; Ceraline et al. 2004). Moreover, some truncated transcripts may have paracrine effects, promoting androgen-independent activation of wild type AR in adjacent cells (Lapouge et al. 2007). Reduced AR activity may promote growth of late stage tumors that have amassed other mutations, especially when antiandrogen treatment inhibits AR activation. In fact, AR expression is reduced late in disease (Shah et al. 2004). There may be an early window when AR gain of function mutations are advantageous but become less so as other growth factor pathways predominate.

Certain areas within the AR carried many more recurring mutations indicating potential hotspots for mutation or selection. One cluster identified within the LBD in all treatment groups has also been reported in clinical studies of prostate cancer, with mutations affecting AR function in diverse ways. AR-A749T identified in an untreated metastasis reduces receptor stability (James et al. 2002). Modeling of AR-V758I, found in a patient after orchiectomy and in this study, predicts a distortion that alters ligand

specificity (Hyytinen et al. 2002). Likewise, M745I that leads to CAIS as a germline mutation allows activation of AR by estradiol (Bonagura et al. 2007). None of the mutations from this cluster characterized in this study allow AR activation with noncanonical ligands or antiandrogens in transfection. Instead, they exhibit varying degrees of reduced transactivation. Three of the mutations, M750I, W752C, and R753Q, reside at the bottom of the ligand binding pocket within the same alpha helix as the loss of function mutation A749T. All three showed lower activation than wild type at 1 nM R1881 in CV-1 cells, but normal to higher activation at increased ligand levels. This is intriguing since intracrine hormone synthesis may maintain intraprostatic androgen levels in hormone-refractory prostate cancer (Titus et al. 2005). This might provide sufficient stimulus for these alleles to activate at least a subset of AR targets.

An indication that differential activation of AR targets might enhance cancer progression is the context-dependent function of R753Q. As a germline mutation, R753Q causes CAIS in patients and in rats (Yarbrough et al. 1990; Gottlieb et al. 2004). Previous characterization of this mutant revealed reduced androgen binding capacity, reduced N-C interaction, and reduced activation in CV-1 cells (Yarbrough et al. 1990; Langley et al. 1998). This study has shown both cell-specific and promoter-dependent effects of R753Q, since activation is near wild type in PC-3 cells and robust for canonical HREs but impaired on AR-selective HREs. These effects may be accounted for at least in part by the altered N-C interaction which may destabilize AR binding on selective elements (He et al. 2002). An inability to activate AR-selective elements due to DBD differences in a knock-in mouse model leads to reduced fertility (Schauwaers et al. 2007). Although germline AR-R753Q may not activate genes critical in male development,

partial function of somatic AR-R753Q may activate a subset of promoters in prostate cancer. This residual activity may favor target genes involved in proliferation over those involved in differentiation. There may even be an optimal oncogenic AR activity that promotes proliferation over differentiation and can be achieved either through a reduction in androgen levels or reduced activity of AR. In support of this idea, *Nkx3.1;Pten* mutant mice treated with low doses of testosterone (T) develop more aggressive disease than mice treated with either no or normal levels of T (Banach-Petrosky et al. 2007). Moreover, h/mAR mice with Q tract variant alleles that differ in AR transactivational strength show poorer response to hormone therapy with weaker AR alleles (Albertelli et al. 2008).

In conclusion, this study has identified a diverse group of *Ar* mutations in both the NTD and LBD of the AR that fall within functionally important domains. While different treatments favored certain mutations, all tumors carried numerous overlapping mutations. The presence of so many AR mutations at low levels has implications for treatment, suggesting that, while targeting the AR may slow disease progression, treatment will ultimately select for different cell populations allowing hormone-refractory growth. Furthermore, functional characterization of mutants from this study indicates that partial loss of function mutations that differentially activate AR targets may be selected during tumorigenesis. These partial loss of function alleles may tip the balance between proliferation and differentiation to confer a gain of function advantage in the context of tumor growth.

Acknowledgements

We thank Dr. Norman Greenberg (Fred Hutchinson Cancer Center, Seattle) for advice throughout this study, and Drs. Andy Lieberman and Chris Krebs (University of Michigan) for helpful discussions. This work was supported by grants to D.M.R. (DOD17-02-1-0099, NIDDK-RO1-56356 and NCI-P50 CA69568). O.A.M. was supported by a DOD fellowship W81XWH-05-1-0105, M.P.S. by the Organogenesis Training Grant (NIH-T32-HD075005) and M.A.A. by NCRR/NIH-T32-RR07008. Additional support came from the University of Michigan Cancer Center Support Grant (5 P30 CA46592) and the Michigan Diabetes Research and Training Center (NIH5P60 DK20572).

Table 2.1. Distribution of *Ar* mutation types within h/mAR-TRAMP treatment groups.

	Treatment Groups				
	Intact	**Castrated**	**Flutamide**	**Bicalutamide**	**Testis Control**
Mutations/10,000 bp	3.6	3.3	4.4	4.0	2.2
Missense (%)	55.0%	46.6%	57.2%	47.3%	61.0%
Silent (%)	26.8%	24.1%	24.0%	31.1%	31.0%
Nonsense (%)	8.2%	5.1%	5.3%	5.8%	3.0%
Codon deletion (%)	2.3%	2.8%	3.2%	6.6%	0
Base pair deletion (%)	7.7%	7.9%	10.2%	7.9%	6.0%
Base pair insertion (%)	0	0	0	0.8%	3.0%

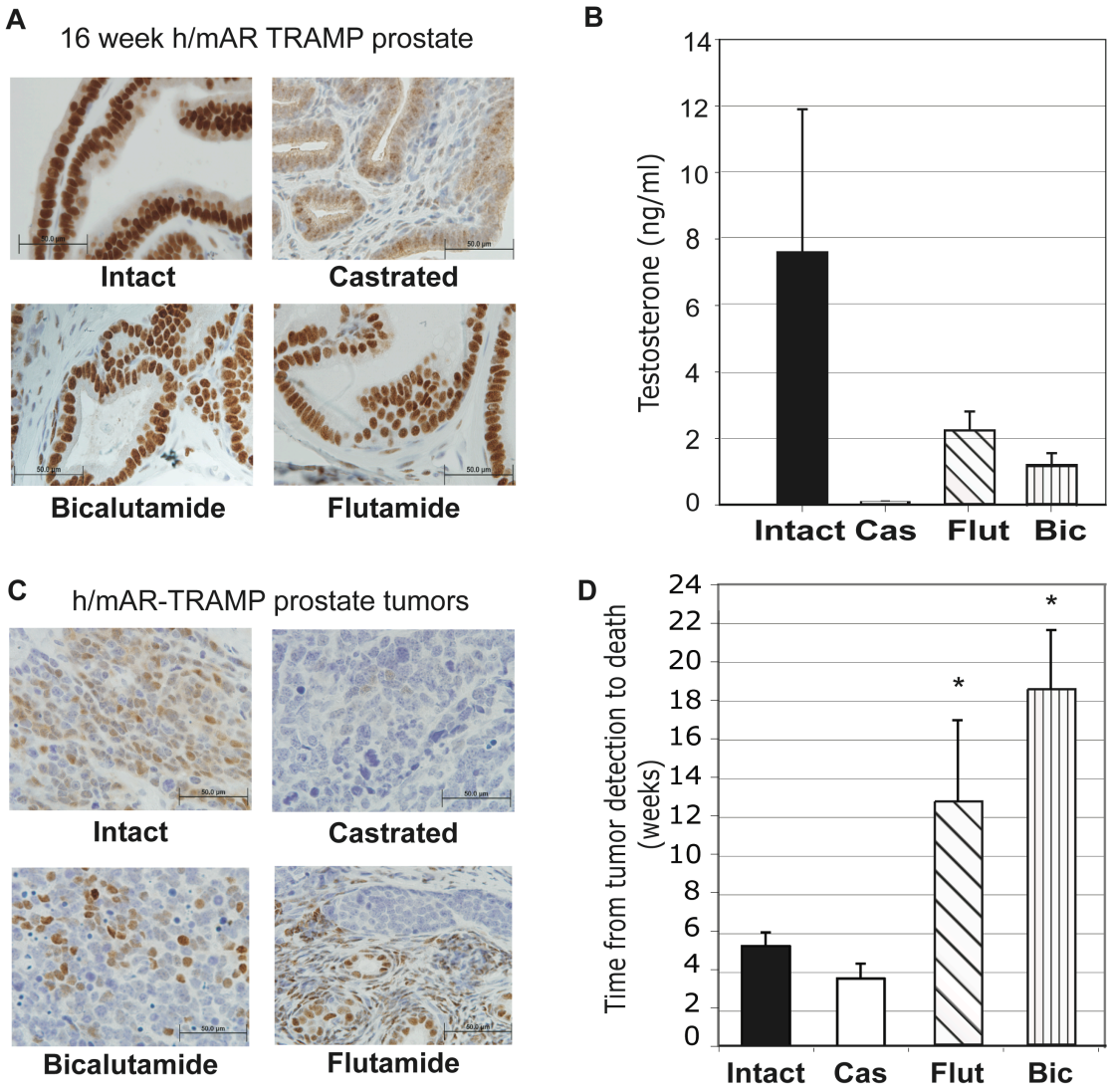

Figure 2.1. Effects of treatment on the androgen axis in h/mAR-TRAMP mice.

A. Immunohistochemical localization of AR in h/mAR-TRAMP prostates 4 weeks after castration or treatment with the antiandrogens flutamide or bicalutamide. Intact prostate is shown as a control. Bar indicates 50 μm. **B.** The effect of 4 weeks castration or anti-androgen treatment on serum testosterone levels. **C.** Localization of AR in representative end stage h/mAR-TRAMP prostate tumors from each treatment group. **D.** Treatment alters disease length in h/mAR-TRAMP mice. Average length of disease from detection of a palpable tumor to death is plotted for each treatment group. Error bars are the standard error of the mean. * significant difference in length of disease compared to intact by Bonferroni multiple comparison adjustment $p<0.01$

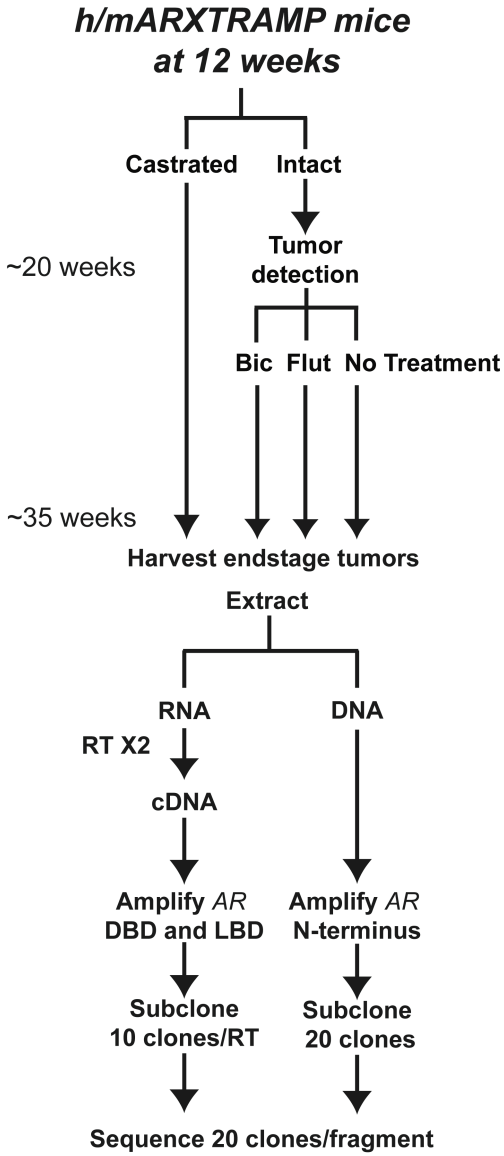

Figure 2.2. Treatment Schematic.

h/mAR-TRAMP mice were randomly assigned to treatment groups (9-10 mice/group). At 12 weeks of age, mice were either castrated or left intact. Upon tumor detection by palpation, intact mice either received no treatment or were treated with the antiandrogens bicalutamide (Bic) at 50 μg/g or flutamide (Flut) at 25 μg/g. End stage tumors were harvested and RNA and DNA extracted. *Ar* was amplified in 4 fragments from cDNA (DBD and LBD) or DNA (NTD). Products were subcloned and 20 clones/ fragment sequenced (10 clones from 2 separate RT reactions for RNA).

Figure 2.3. Analysis of *Ar* mutations from h/mAR-TRAMP tumors.

A. Venn diagram of *Ar* missense mutations recurring in h/mAR-TRAMP tumors grouped by treatment. Numbers represent the mutations shared by overlapping treatment groups. Analysis included only mutations occurring more than once within the entire population. This included all substitutions at the same residue (e.g. R31C and R31H). **B.** The number of mice per treatment group with missense substitutions in the same residue (Y-axis) positioned along the AR protein (amino acids 1-920; X-axis). The position of the activation functions (AF) 1, 2, and 5 involved in cofactor recruitment are shown above. Arrows indicate Q58L, the most common mutation. AR domains and repeats are shown below. Q: Polyglutamine tract, NTD: N-terminal domain, G: Polyglycine tract, DBD: DNA binding domain, H: Hinge region, LBD: Ligand binding domain. Primer positions are indicated by arrows. Primer 1F is located in the 5' UTR, 4R in the 3' UTR and 2R (not shown) in intron 1. Primer pair 2 amplifies the C-terminal half of the NTD including the glycine repeat from genomic DNA. Primer pairs 3 and 4 cross exon/intron boundaries and are used to amplify from cDNA. C, D. Schematics of the amino acid substitutions identified in h/mAR-TRAMP tumors and their relative location within the AR protein domains. **C**. Amino acid substitutions occurring in more than one mouse within the population or in more than one clone in a single tumor. Mutations underlined in blue occurred in three or more tumors. **D.** Amino acid substitutions identified in more than one tumor within a treatment group or in more than one clone in a single tumor. Underlined mutations occurred in three or more tumors within a treatment group. Δ: A base deletion within the codon of the specified amino acid causing a frameshift and subsequent premature stop codon.

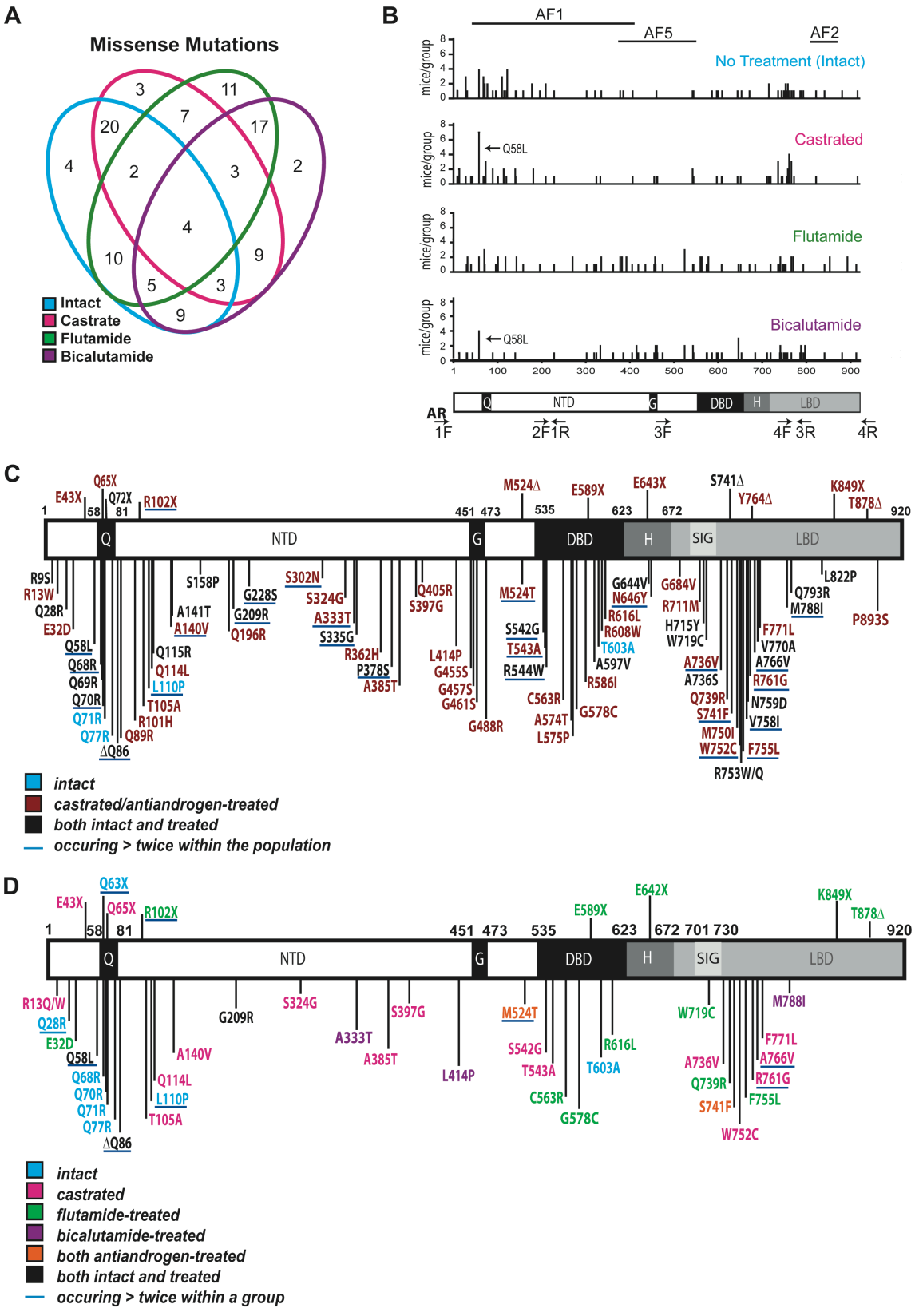

Figure 2.3. Analysis of *Ar* mutations from h/mAR-TRAMP tumors.

Figure 2.4. Functional characterization of mutant ARs from mouse prostate tumors.

A. Protein structure model of the AR LBD representing the five residues (left) and the h/mAR- TRAMP mutations (right) introduced into expression vectors. **B.** Western blot of 20 µg of whole cell protein lysates from CV-1 cells transfected with 100 ng expression vector containing wild type or mutant AR and treated for 24 hours with 1 nM R1881. Arrow - nonspecific band; ß-tubulin was used as a loading control. **C.** Transactivation of wild type and mutant receptors (4 ng) transfected into CV-1 cells along with 400 ng of the C'Δ9 luciferase reporter and 100 ng of promoterless renilla. Cells were harvested 24 hours after treatment with the indicated concentration of R1881 and assayed for firefly and renilla luciferase activity. The average normalized values of at least three trials are represented as the fraction of wild type activity at 1 nM R1881. Error bars are the standard error of the mean (SEM). **D.** Transactivation of wild type and mutant ARs transfected into PC-3 cells with the PSA-luciferase reporter. Cells were harvested as in C. after treatment with 10 or 100 nM R1881. Average normalized values of at least three trials are shown +/- SEM. Values are the fraction of wild type activity at 10 nM R1881. **E, F**. Transactivation of R753Q in PC-3 cells is promoter-dependent. PC-3 cells were transfected with wild type *Ar*, *Ar*-R753Q or *Ar*-R761G, and reporters with complex enhancers (**E**) or with tandem repeats of single HREs (**F**). Normalized values are as in C. * $p<0.05$ *** $p<5x10^{-5}$ based on Student's t-test.

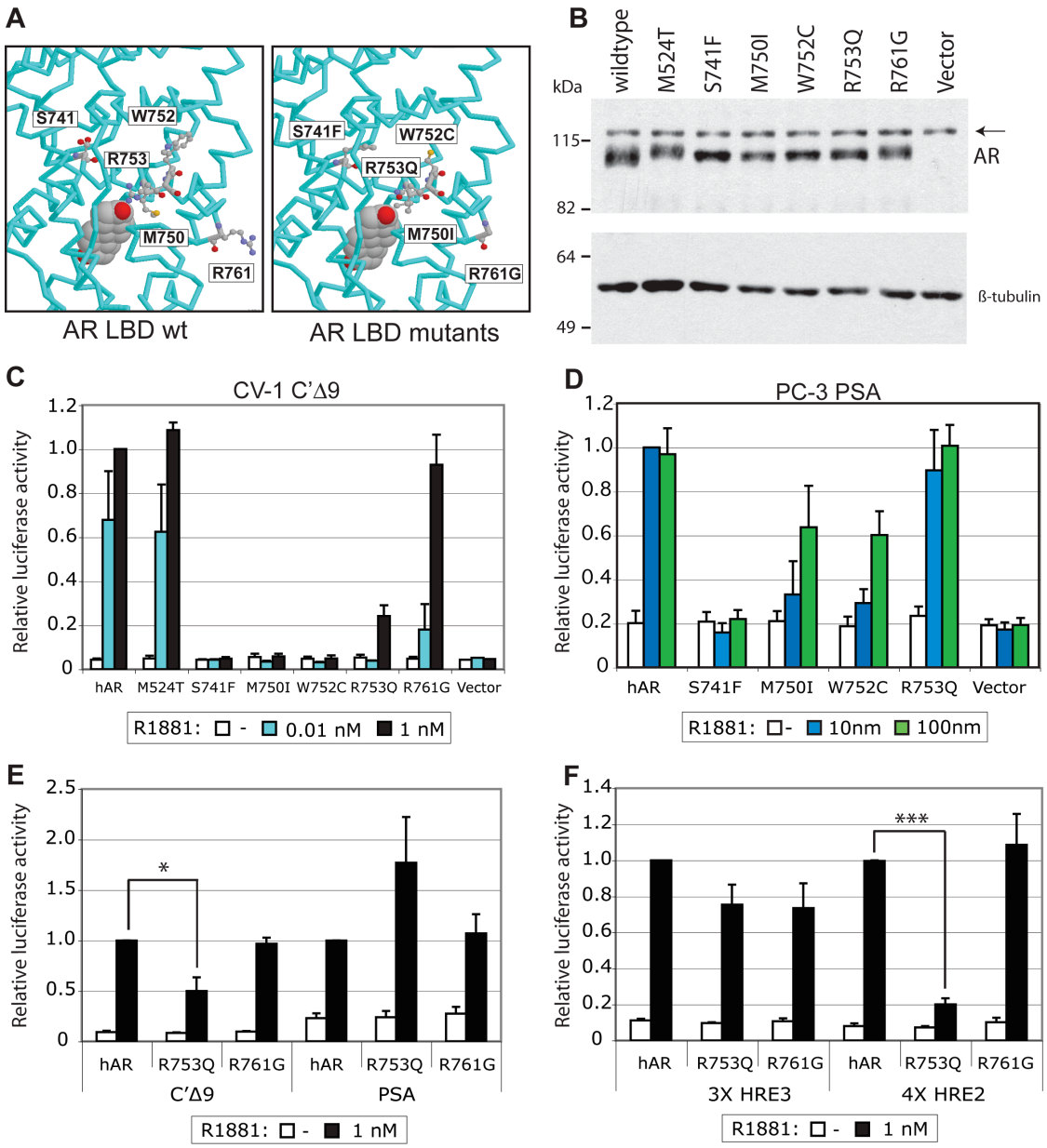

Figure 2.4. Functional characterization of mutant ARs from mouse prostate tumors.

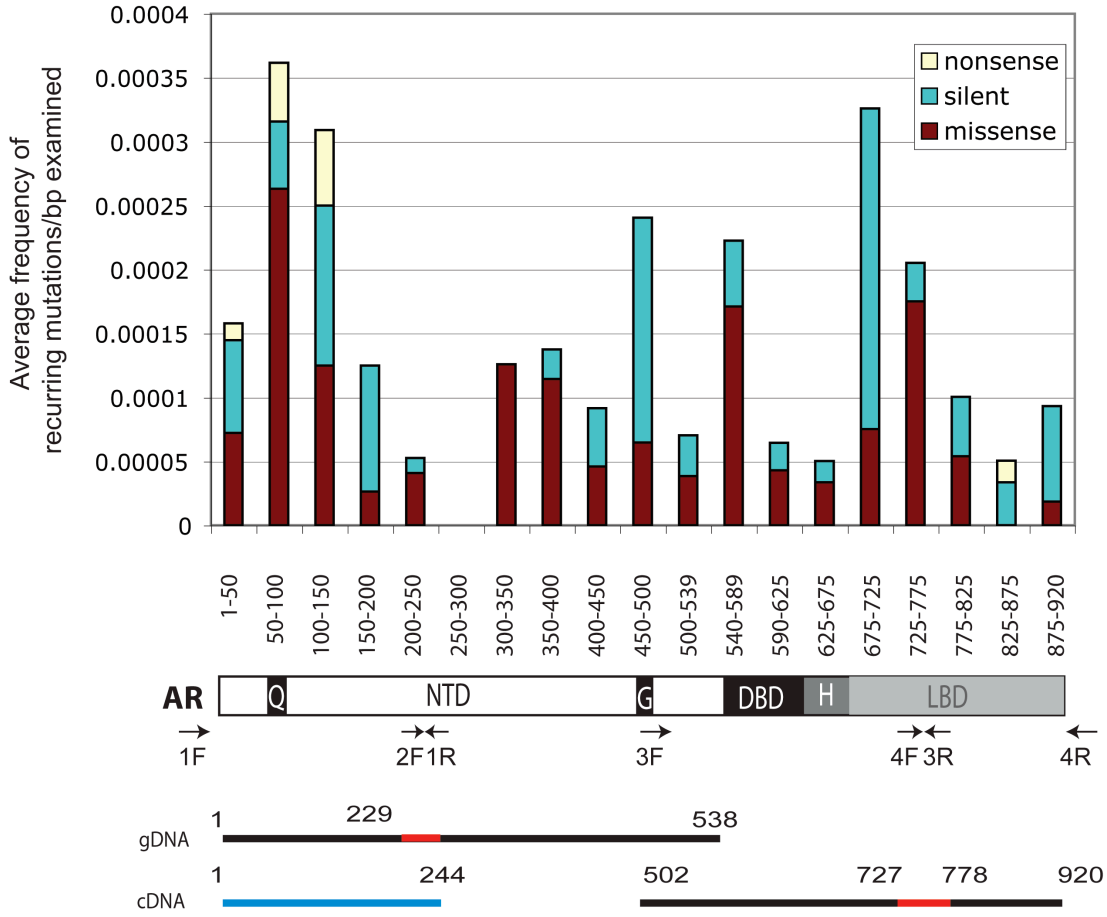

Figure 2.5. Frequency of recurring mutations from h/mAR tumors.

Frequency of mutations is partitioned into 50 amino acid segments along the entire *Ar* coding region. A diagram of the AR protein with its domains is aligned below the graph. Polyamino acid tracts have relatively high mutation frequencies. Mutations are divided into missense, silent, and nonsense mutations within each 50 aa. window. Due to the degenerative amino acid code, approximately one third of the mutations are expected to be silent by random chance. Missense mutations are over or underrepresented in certain segments. Primer pairs (1-4) used to amplify the *Ar* are shown as arrows. Primer 2R lies in intron 1 and is not shown. Lines at the bottom indicate the sequence amplified from genomic DNA (gDNA) and complementary DNA (cDNA). Black lines indicate fragments that were amplified in all treatment groups. The blue line is a portion of exon 1 amplified from cDNA and gDNA in intact and castrate groups but only amplified from gDNA in antiandrogen-treated groups. Red lines indicate places where amplification fragments overlap. This overlap was taken into account for frequency calculations.

Chapter 3

Treatment-Dependent Androgen Receptor Mutations in Prostate Cancer Exploit Multiple Mechanisms to Evade Therapy[2]

Abstract

Mutations in the androgen receptor (AR) that enable activation by antiandrogens occur in hormone-refractory prostate cancer, suggesting mutant ARs are selected by treatment. To validate this hypothesis, we compared AR variants in metastases obtained by rapid autopsy of patients treated with flutamide or bicalutamide, or lymph node metastases of hormone-naïve (i.e. untreated) patients. AR mutations occurred at low levels in all specimens, reflecting genetic heterogeneity of prostate cancer. Base changes recurring in multiple samples or multiple times per sample were considered putative selected mutations. Of 26 recurring missense mutations, most in the N-terminal domain (NTD) occurred in multiple tumors, while those in the ligand binding domain (LBD) were case-specific. Hormone-naïve tumors had few recurring mutations and none in the LBD. Several AR variants were probed to assess mechanisms that might underlie treatment resistance. Selection was evident for the promiscuous receptor AR-V716M, which dominated three metastases from one flutamide-treated patient. For the inactive and cytoplasmically restricted splice variant AR23, co-expression with wild type

---

[2] This chapter represents the contents of a manuscript submitted for publication:
Mara P. Steinkamp, Orla A. O'Mahony, Michele Brogley, Haniya Rehman, Saravana Dhanasekaran, Matthias D. Hofer, Rainer Kuefer, Arul Chinnaiyan, Mark A. Rubin, Kenneth J. Pienta and Diane M. Robins. Androgen receptor mutations in human prostate cancer metastases vary with treatment. submitted to Cancer Research.

AR enhanced activity, supporting a decoy function. A novel mutation within the NTD (W435L) fell in a motif involved in intramolecular interaction and influenced promoter-selective, cell-dependent transactivation. AR-E255K, mutated in a domain that interacts with an E3 ubiquitin ligase, led to increased protein stability and nuclear localization in the absence of ligand. Thus treatment with antiandrogens selects for gain of function AR mutations with altered stability, promoter preference, or ligand specificity. These processes reveal multiple targets for effective therapies regardless of AR mutation.

Introduction

Tumors arise through the accumulation of somatic mutations that allow uncontrolled growth and lead to general genomic instability and acquisition of random mutations (Bielas et al. 2006). This creates a heterogeneous tumor population that is able to adapt to changes in the environment (Loeb et al. 2008). In the case of prostate cancer, this "mutator phenotype" may contribute to the short time to treatment resistance.

Because prostate cancer is initially androgen responsive, standard treatment consists of combined androgen blockade: reduction of testicular androgen synthesis and direct antagonism of the androgen receptor (AR) with antiandrogens such as flutamide or bicalutamide (Labrie et al. 1983). However, therapy ultimately fails, indicated by increasing prostate specific antigen (PSA) levels and recurrent tumor growth (Pienta et al. 2006). Despite castrate androgen levels, AR is still highly expressed and active in hormone-refractory tumors implying a switch to alternative mechanisms of activation (Scher et al. 2004). Among mechanisms proposed for AR activation at no or low hormone levels are *AR* gene amplification, increased coactivator expression, activation by growth factors and selection of somatic *AR* mutations (Feldman et al. 2001). Therapy-

specific selection of *AR* mutations may underlie antiandrogen withdrawal syndrome where tumors regress upon cessation of treatment (Scher et al. 1993; Hara et al. 2003), and may also explain why tumors that are resistant to hydroxyflutamide often respond to treatment with bicalutamide and vice versa (Taplin et al. 1999; Suzuki et al. 2008).

In clinical prostate cancer, many *AR* mutations have been reported, but their prevalence and influence on disease progression are unclear due to few comprehensive sequencing studies, variability in treatment regimens, and limited access to high-quality tumor samples. Many previous studies focused on the ligand binding domain (LBD), although recent examinations of the entire AR coding region have identified mutations in the N-terminal domain (NTD) as well (Bentel et al. 1996; Hyytinen et al. 2002; Chen et al. 2005). Apart from the T878A mutation that has been reported in up to one-third of hormone-refractory prostate tumors (Gaddipati et al. 1994; Taplin et al. 1999), most mutations appear to be rare (Gottlieb et al. 2004).

Studies in mouse models of prostate cancer where treatment is experimentally controlled have added compelling evidence for treatment selection. In the *tr*ansgenic *a*denocarcinoma of *m*ouse *p*rostate (TRAMP) model, intact or castrate hormonal status selects for *Ar* mutations in different domains (Han et al. 2001). Our lab recently identified *Ar* mutations in tumors from TRAMP mice expressing a “humanized" AR (h/mAR-TRAMP) (O’Mahony et al. 2008). Mutations in *Ar* were frequent but at low levels, generally comprising 10% or less of the tumor RNA population. Examination of recurring mutations between antiandrogen-treated groups identified distinct mutations within the flutamide- and bicalutamide-treated mice, as well as clusters of mutations

shared among groups. Characterization of select mutants revealed altered AR function, including differential activation of androgen-responsive promoters.

Here we extend this analysis to a set of high quality patient samples with detailed treatment records from the University of Michigan Specialized Program of Research Excellence (SPORE) in Prostate Cancer rapid autopsy program. To determine whether antiandrogens impose a treatment-specific selection pressure, *AR* mutations from flutamide-treated, bicalutamide-treated, and hormone-naïve (i.e. untreated) patients were compared. Further functional analysis of some known as well as novel variants provides insight into alternative mechanisms of antiandrogen resistance including alterations in AR stability and localization in the absence of ligand.

Materials and Methods

Patient samples

RNA from metastases of prostate cancer patients treated with bicalutamide or flutamide were obtained from the University of Michigan SPORE in Prostate Cancer rapid autopsy program; tissue was procured as described (Shah et al. 2004). Tumor biopsies of hormone-naïve lymph node metastases were obtained from the University Hospital in Ulm, Germany (Hofer et al. 2006) as part of the UM SPORE-Ulm Cooperative Collaborative Clinical Case Procurement Program.

Reverse transcription, amplification, subcloning and sequencing

1 µg of RNA was reverse transcribed using SuperscriptII reverse transcriptase (Invitrogen, Carlsbad, CA) with 0.5 µg oligo (dT) in a 20 µl reaction. Two reverse transcription (RT) reactions were performed per sample to control for error. The entire coding region of *AR* was amplified in 5 fragments. PCR amplifications (primers listed below) were performed in 25 µl reactions containing 2.5 units Platinum *Pfx* DNA polymerase (Invitrogen), 2X Buffer and 1X GC enhancer (supplied by the manufacturer), 1.5 mM $MgSO_4$, 0.3 mM dNTPs , 0.5 µM each primer, and 1-3 µl of the RT reaction. PCR conditions were optimized for each primer pair.

Primer Pairs:

AR1 Forward, position 1074: 5' CGGGGTAAGGGAAGTAGGTG 3'
AR1 Reverse, position 1732: 5' CTGCCTTCGGATACTGCTTC 3'

AR2 Forward, position 1689: 5' CAACTCCTTCAGCAACAG 3'
AR2 Reverse, position 2448: 5' CAGTTGTATGGACCGTGT 3'

AR3 Forward, position 2412: 5' TCATCCTGGCACACTCTCTTCACA 3'
AR3 Reverse, position 2693: 5' GGGGCCCATTTCGCTTTTGACACA 3'

AR4 Forward, position 2639: 5' GGTGAGCAGAGTGCCCTATC 3'
AR4 Reverse, position 3399: 5' TCCTGGAGTTGACATTGGTG 3'

AR5 Forward, position 3312: 5' GACCAGATGGCTGTCATTCA 3'
AR5 Reverse, position 3982: 5' GAAATTCCCCAAGGCACTG 3'

Products were processed as described in (O'Mahony et al. 2008). Briefly, products were visualized on 1% agarose gels; bands were excised and purified with the

QiaexII gel extraction kit (Qiagen, Valencia CA). 3'-A overhangs were added to the blunt-ended products by incubation with Taq polymerase (Invitrogen) at 70°C for 30 min. Products were ligated into the pGEM-T easy vector (Promega, Madison WI) and transfected into DH5α chemically competent bacteria (Invitrogen). DNA from 20 clones/sample (10 clones/RT reaction) was purified with QIAprep Spin Miniprep columns (Qiagen) or with the MacConnell Mini-Prep 24 Machine (MacConnell Research, San Diego, CA) according to the manufacturer's directions and sequenced by the University of Michigan DNA Sequencing Core.

Sequence analysis

Sequence was compared to the human *AR* sequence (Genbank Accession# NM_000044) using Sequencher software (version 4.1, Gene Codes, Ann Arbor, MI). Putative mutations were checked against the Androgen Receptor Gene Mutations Database (http://www.androgendb.mcgill.ca/) (Gottlieb et al. 2004).

Mutagenesis of AR expression plasmids

Mutations E255K and W435L were introduced into the pCMV5 hAR expression vector using the Quickchange Site Directed Mutagenesis kit (Stratagene, La Jolla CA) and the primer pairs below. DMSO was added to the mutant strand synthesis reaction to prevent Q and G tract contraction. Plasmids were sequenced to verify presence of the mutation and retention of the original number of Q and G codons.

Mutation primers:

E255K Sense: 5’ GTGTGGAGGCGTTGAAGCATCTGAGTCCAGGG 3’
E255K Antisense: 5’ CCCTGGACTCAGATGCTTCAACGCCTCCACAC 3’

W435L Sense: 5’ CGCTTCCTCATCCTTGCACACTCTCTTCACAGC 3’
W435L Antisense: 5’ GCTGTGAAGAGAGTGTGCAAGGATGAGGAAGCG 3’

A mutant with the 69 bp DBD insertion was constructed by ligating a HindIII/TthIII 1 fragment into pCMV5-hAR. The insert and junction points were verified by sequencing.

Transfection assays

CV-1 cells were cultured in DMEM and PC-3 cells in RPMI, supplemented with 10% fetal bovine serum, 1% Glutamax, and 1% penicillin/streptomycin. RWPE cells were grown in complete keratinocyte-serum free media (KSFM). CV-1 cells act as a control non-prostate cell line that does not express AR. RWPE cells have characteristics of normal prostate epithelial cells, while PC-3 cells are androgen-independent prostate tumor cells. Cells were seeded at 5×10^4 (CV-1) or 1×10^5 (PC-3, RWPE) in 12-well plates. Four hours before transfection, media was replaced with standard media (DMEM or RPMI) + 2.5% charcoal-stripped NuSerum + 1% Glutamax. Cells were transfected with Fugene 6 reagent (Roche, Nutley, NJ) at 3 volumes of Fugene/µg DNA with 4 ng pCMV5-AR (wild type or mutant), 400 ng luciferase reporter plasmid and 100 ng promoterless renilla (Promega) for normalization. The PSA-luciferase plasmid includes the distal PSA enhancer (-5323 to –4023) linked to its promoter (-542 to +12) (Perez-Stable et al. 2000). C’Δ9, HRE3 and HRE2 reporters have been described (Robins 2005). 24 hours post-transfection, cells were rinsed in 1X PBS and fed with phenol red-free

media + 10% charcoal-stripped Nuserum +/- hormone. Cells were harvested 48 hours post-transfection into 1X Passive Lysis Buffer (Promega). Luciferase activity was measured using the Dual Luciferase Reporter Assay System (Promega) on a Veritas Microplate Luminometer (Turner Biosystems Inc., Sunnyvale CA).

Western blotting

CV-1 or PC-3 cells were seeded at 4 x 10^5 cells/ 60 mm dish, fed phenol red-free media +/- 1 nM R1881 four hours before transfection and transfected as above with 100 ng receptor (hAR or mutant) and 1.9 µg empty vector (pCMV5). 24 hours after transfection, cells were rinsed in cold 1X PBS and harvested in 100 µl RIPA buffer + protease inhibitors, lysed at 4^{o}C for 10 minutes and centrifuged at 4^{o}C for 10 minutes. Protein was quantified by the Dc Protein Assay (Bio-Rad, Hercules CA). 20 µg protein was run on a 5% stacking/8% separating SDS-polyacrylamide gel and transferred to nitrocellulose. The blot was probed with antibody to the AR N-terminus (N20, Santa Cruz Biotechnology, Santa Cruz, CA) (1:500) and incubated with HRP-conjugated ECL anti-rabbit IgG (GE Healthcare, Piscataway, NJ) (1:5,000) for 45 minutes. Bands were detected with ECL western blotting reagents (Pierce Biotechnology, Rockford IL). For lactacystin treatment, cells were transfected as above but after 24 hours cells were treated with 10 µM lactacystin (Cayman Chemical, Ann Arbor MI) for 18 hours before harvesting.

Cycloheximide assay and lactacystin treatment

CV-1 cells were transfected with hAR or E255K as above. After 24 hours, cells were rinsed with 1X PBS and incubated in media containing 30 μM cycloheximide (Sigma, St. Louis MO) +/- 1 nM R1881 (a dose which triggers maximum transactivation *in vitro*) for up to 24 hours. At indicated times, cells were rinsed in ice-cold 1X PBS and lysed in RIPA buffer plus inhibitors as above. Westerns to determine AR protein levels were performed as above; bands were quantitated by densitometry using ImageJ (NCBI). AR levels were normalized to ß-tubulin and % protein remaining determined relative to amount at time 0 (100%).

Immunocytochemistry

PC-3 cells were seeded at 4 x 10^4 cells onto 4-chamber slides and transfected with 100 ng receptor in phenol red-free RPMI + 10% charcoal stripped Nuserum. 24 hours after transfection, cells were fed fresh media +/- 10 nM R1881and incubated another 24 hours at 37ºC. Cells were rinsed in ice-cold PBS, fixed on ice in 4% paraformaldehyde for 5 minutes, permeabilized in 0.1% triton-X PBS for 10 minutes, blocked in 5% heat inactivated goat serum (Invitrogen) in 0.1% Triton-X PBS for 1 hour, incubated in AR N20 antibody (Santa Cruz Biotechnology) (1:500) overnight and FITC-conjugated goat anti-rabbit secondary antibody (1:1000) for 1 hour. Slides were mounted with Prolong Gold plus DAPI (Invitrogen). Images were captured using an Olympus BX-51 microscope linked to an Olympus DP-70 high-resolution digital camera.

Results

Identification of *AR* mutations in prostate cancer metastases

To examine directly whether *AR* mutations differ between treated and untreated tumors, whether frequency of mutations increases following antiandrogen treatment, and whether different antiandrogens select for distinct mutations, the *AR* coding region was sequenced from metastatic prostate tumors collected in the University of Michigan Rapid Autopsy Program (Shah et al. 2004). Samples were selected from patients who had been treated with only one antiandrogen. Because secondary hormone therapy is often used after relapse, only eight of thirty patients, 4 treated with flutamide and 4 with bicalutamide, met this criterion (Table 3.1). AR from 3 hormone-naïve lymph node metastases from patients at the University of Ulm Hospital (Ulm, Germany) was sequenced for comparison (Hofer et al. 2006). RNA from all samples was reverse transcribed and the entire *AR* coding region amplified, subcloned, sequenced and *AR* mutations compared within and between groups.

Sequencing the equivalent of 20 full-length *AR* mRNAs per metastasis (10 from two independent RT reactions) identified 280 single base pair changes in 191 codons. The average alteration rate within the population was 4.1 base changes/10,000 bps, which is comparable to the rate observed in the h/mAR-TRAMP tumors using the same method (O'Mahony et al. 2008).

For that study, baseline error due to the nature of the sequence (e.g., trinucleotide CAG and GGN variability in polyQ and G tracts and error in areas of high GC content)

and the methodology (e.g., RT and subcloning error) was established by sequencing *Ar* from mouse testis RNA. Testis samples carried 2.2 base changes/10,000 bp indicating that about half the differences in tumor samples by this approach are likely somatic mutations during tumorigenesis. A similar level of error has been reported in comparable studies using RT and PCR amplification (Arezi et al. 2007).

Of the total base alterations, 160 were missense with 10% falling in the polyQ and G-tracts, and 69 were silent mutations, 30% of which were located in the polymorphic G-tract. A breakdown of mutation types per treatment group is shown in Table 2. There were no significant differences between treatment groups in total number or types of mutations. Mutations in the NTD (amino acids 1-535) were over-represented relative to AR length, accounting for 73% of mutations from all groups (excluding the polyamino acid tracts) (data not shown). The majority of mutations were present in one or two clones per sample, or 5-10% of the RNA population, similar to the mutation frequencies in mouse (Han et al. 2001; O'Mahony et al. 2008; O'Mahony et al. in press). Since it is difficult to distinguish between true mutations that occur in a single clone and errors due to methodology, analysis was restricted to mutations that occurred in more than one clone.

Treatment-specific patterns of recurring mutations

Mutations that provide a growth advantage are likely to be more common within the tumor. There were 36 codons where mutations occurred more than once either in more than one case (24 codons) (Figure 3.1A) or in more than one clone within a tumor (17 codons) (Figure 3.1B). Recurring missense mutations include those that mutate a

codon to different residues (selection away from wild type, e.g. L194F/R) or to a new residue (selection for a particular change, e.g. Q58L). Both types could be functionally significant. All but two missense mutations identified in multiple cases were located in the NTD, with few specific to a single treatment group - half occurred only with antiandrogen treatment and half were shared by treated and untreated patients (Figure 3.1A). In contrast, the 13 missense and 2 nonsense mutations present in multiple clones from a single case were case-specific and not restricted by AR domain (Figure 3.1B). 10 silent mutations recurred, six of which were in the G-tract. Another silent mutation at E213 is a known polymorphism (Riva et al. 2004) and occurred in all 20 clones from 3 samples, but also in four and seven clones from two other samples.

Differences between treatments were most apparent for mutations that occurred more than once per tumor (Figure 3.1B). Only two of these mutations were found in the hormone-naïve samples, while the flutamide-treated and bicalutamide-treated tumors carried eight and seven mutations, respectively. Three antiandrogen-treated tumors carried most of the recurring mutations (Table 3.1). Length of treatment had no obvious effect on the number of mutations although power was limited by the small sample size.

All recurring mutations in the LBD were from antiandrogen-treated tumors, suggesting selection for altered conformation of, or ligand contacts within, the binding pocket. Half of the antiandrogen-treated tumors carried at least one recurring mutation in the LBD, but none overlapped between the flutamide and bicalutamide groups, indicating distinct selection conferred by each antiandrogen. The flutamide-treated group had three missense mutations in the LBD, V716M, L798P, and L874P (Figure 3.1B). V716M, discussed below, creates a promiscuous receptor (Culig et al. 1993). L798P is a novel

mutation that falls within an E3 ubiquitin ligase interacting area (Rees et al. 2006). L874P, another novel mutation, lies near codons H875 and T878 that when mutated allow activation of AR by flutamide (Veldscholte et al. 1990; Fenton et al. 1997).

Multiple metastases from one patient express only the promiscuous AR-V716M

The mutation, V716M, was present in all 20 clones sequenced from the lung metastasis of a flutamide-treated patient (Table 3.1, patient 28). To rule out a germline mutation, 281 bps around V716M were amplified and sequenced from genomic DNA of the patient's normal kidney. Only the wild type G at position 3255 was identified indicating that the mutation was somatic (Figure 3.1C). Additional amplification and sequencing of cDNA and/or genomic DNA from two other metastases from this patient yielded only mutant sequence with no detectable wild type (Figure 3.1C and data not shown), indicating that a clonal population carrying AR-V716M accounted for all three metastases. No other mutations occurred more than once in this sample. In accord with reports that AR-V716M is activated by a wide array of hormones and antagonists (Culig et al. 1993), its predominance in all metastases from this patient supports its role in treatment resistance.

The splice variant AR23 was found only in antiandrogen-treated cases

A variant generated by the use of a cryptic splice site in intron 2 was identified in one or more clones in 5 of 8 tumors from treated patients, but in none of the hormone-naïve tumors. Alternative splicing inserted 69 bps of intron 2 in frame creating a 23

amino acid extension between the two zinc fingers of the DNA binding domain (DBD) (Figure 3.2A). This variant, AR23, was previously found in Androgen Insensitivity Syndrome due to a mutation upstream of exon 3 that altered splicing (Bruggenwirth et al. 1997). Recently, AR23 was identified in a hormone-refractory prostate metastasis from a bicalutamide-treated patient suggesting a possible role in cancer (Jagla et al. 2007). AR23 was engineered into an expression plasmid and its activity assayed after transfection. We confirmed by immunohistochemistry that AR23 did not localize efficiently to the nucleus in the presence of hormone but rather appeared as speckles in the cytoplasm (Figure 3.2B) (Jagla et al. 2007), and was incapable of activating androgen-responsive reporters (Figure 3.2C). AR23 could not repress NF-κB-induced transcription, unlike wild type AR (Figure 3.2D). It was noted previously that AR23 increases endogenous AR-T877A activity when over expressed in LNCaP cells (Jagla et al. 2007). To further explore how AR23 acts, equimolar ratios of *AR*23 and wild type *AR* were co-transfected into PC-3 cells. *AR*23 co-expression increased ligand-dependent transactivation of the PSA-luciferase reporter 2.5-fold above wild type AR alone (Figure 3.2C). Furthermore, AR23 increased transactivation with the antiandrogens hydroxyflutamide and bicalutamide above wild type AR alone (Figure 3.2E). Because AR23 was incapable of transactivation on its own, it is possible that AR23 enhanced activity of correctly processed AR via cytoplasmic activity.

Novel mutations in the AR NTD in conserved functional motifs

The AR NTD is largely unstructured and contains two activation functions (AF) 1 and 5 that bind coactivators and are critical for AR activity (Figure 3.1A) (Shen et al.

2005). The NTD also directs intramolecular amino-carboxy (N/C) interactions, via FQNLF and WHTLF motifs, that stabilize ligand-bound AR. In this study, 14 of 19 mutations in the NTD fell into four regions: the polymorphic Q-tract, the COOH-terminus of Hsp70-Interacting Protein (CHIP) interaction domain, the WHTLF motif, and the end of AF5 involved in coactivator interactions (Irvine et al. 2000) (Figure 3.1). Mutations in the CHIP interacting domain were previously discovered in the TRAMP model: E231G causes cancer as a prostate-specific transgene, highlighting the oncogenic potential of AR mutants (Han et al. 2001; Han et al. 2005). The novel mutations W435L and E255K were engineered into expression vectors for functional characterization.

W435L alters a motif involved in AR N-C interaction

The mutation, W435L, was identified in one clone each of two antiandrogen-treated metastases. Due to its position within the conserved WHTLF motif, this mutation may influence AR intramolecular interactions, positively or negatively dependent on its mechanism of action. To determine the effect on transactivation, AR-W435L was co-transfected into CV-1 fibroblasts, immortalized prostate RWPE cells, and prostate cancer PC-3 cells along with representative androgen-responsive reporters. Androgen responsive elements are of two types: canonical inverted repeats of a TGTTCT half site that bind multiple steroid receptors (e.g., HRE3), or direct repeats that are weaker but AR-selective elements (e.g., HRE2) (Robins 2004). Natural promoters often contain both element types as well as binding sites for other transcription factors. AR-W435L showed increased transactivation in CV-1 and RWPE cells that was promoter-dependent (Fig 3.3). Some complex promoters worked preferentially, e.g. MMTV in CV-1 cells and

PSA in RWPE, likely due to the greater efficacy of AR-W435L on the AR-selective 4X HRE2. This promoter-specific effect was cell-type dependent as well since transactivation was not affected by W435L in PC-3 cells (data not shown).

Mutations in the highly conserved CHIP interacting domain

Two mutations from treated patients, A253V and E255K, lie adjacent to the most highly conserved portion of the NTD (Han et al. 2001). This region interacts with an E3-ubiquitin ligase that reduces steady state AR levels by promoting degradation (He et al. 2004). To determine whether E255K enhances AR stability, CV-1 cells transfected with wild type or E255K AR were treated with cycloheximide to inhibit protein synthesis and cells harvested at times thereafter to detect protein degradation. R1881 greatly stabilized AR protein in both mutant and wild type as expected (Figure 3.4A). However, AR-E255K had an extended half-life compared to wild type AR, particularly noticeable in the absence of ligand. While AR half-life without ligand was 5.2 hours, the half-life of AR-E255K was 12.5 hours. E255K migrated slower than wt AR, which may be due to differential protein modification. This was also seen with another NTD mutant, M524T, identified in the h/mAR-TRAMP mice (O'Mahony et al. 2008).

To explore whether stabilization of E255K was due to reduced degradation by the 20S proteasome, cells were treated with the proteasome inhibitor lactacystin. In the absence of ligand, inhibition of the proteasome increased wild type AR steady state protein levels as expected (Lin et al. 2002). However, E255K levels remained constant, indicating that proteasome activity has little impact on this mutant (Fig 3.4B).

Because both the proteasome and chaperones are implicated in nuclear transit, AR-E255K localization was examined by immunocytochemistry. In the absence of R1881, the majority of wild type AR was cytoplasmic as expected. However, AR-E255K showed significant nuclear localization even in the absence of ligand (Figure 3.4C). Tallying the localization in cells showed skewing of AR-E255K localization to the nucleus in the absence of ligand compared to wild type AR (Figure 3.4C).

AR-E255K induced reporter gene expression similarly to wild type AR in CV-1 and PC-3 cells with no greater activity in the absence of androgen or with added coactivators ARA70 and SRC-1 (data not shown). However, in RWPE cells, AR-E255K increased transactivation of PSA 2.5-fold relative to wild type AR (Figure 3.4D). This may be due in part to cofactor differences between cell types, as well as somewhat greater activity on canonical elements like HRE3. Thus AR-E255K yielded a functional receptor that exhibits increased stability, substantial nuclear localization in the absence of hormone, and differential promoter activation dependent on host cell characteristics.

Discussion

This study has revealed a low level of mutation throughout the *AR* coding region in metastases from antiandrogen-treated as well as hormone-naïve patients, providing evidence for genetic heterogeneity and a "mutator phenotype" in prostate cancer (Bielas et al. 2006). Very few mutations in the hormone-naïve samples occur in more than one clone per case suggesting that most provide little growth advantage and may be random "passenger" mutations. However, antiandrogen treatment leads to more mutations present in greater abundance, suggesting that treatment selects for a subset of AR mutations within this diverse population.

Examination of recurring mutations within and between samples indicates specific codons that may provide a selective advantage during cancer progression. Interestingly, the majority of mutations recurring in multiple samples are located in the NTD and are shared by tumors from different treatment groups. This emphasizes the broad function of the NTD in growth factor and coactivator interactions and receptor stability, and suggests AR variants may provide general growth advantages regardless of treatment. In contrast, all missense mutations in the LBD are case-specific and are only found in samples from antiandrogen-treated patients, evidencing their likely selection by treatment. Further, the lack of overlap between LBD mutations following either bicalutamide or flutamide treatment suggests these antagonists select for distinct variants.

Our h/mAR–TRAMP study examined 40 tumors from intact, castrated or antagonist-treated mice (O'Mahony et al. 2008). Although the patient samples are fewer and are metastases rather than primary tumors, similarities emerge. Overall mutation frequency is similar, although there are more mutations present in multiple clones per human sample, likely reflecting the clonal nature of metastases and the extended length of time with disease. The two most common mouse *Ar* mutations encode AR-Q58L and AR-ΔQ86, and are also common in man regardless of treatment, occurring 5 and 7 times respectively. As in mice, there are fewer recurring mutations in human hormone-naïve tumors, substantiating selection pressure during treatment.

Mutations also occur in similar functional domains in human and mouse ARs, whether primary tumor or metastatic sample, particularly following flutamide treatment. Mutations in flutamide-treated tumors occur in two regions that are important for ligand specificity: the highly conserved signature sequence (i.e., mAR-W719C, hAR-V716M)

and the distal region where some mutations allow promiscuous ligand recognition (i.e., mAR-P893S, hAR-L874P) (Culig et al. 1996; O'Mahony et al. 2008; O'Mahony et al. in press). While this study did not find the common T878A variant, L874P may act similarly (Bohl et al. 2005). In wild type AR, T878 extends into the ligand pocket and contacts ligand. The L874P mutation may displace the T878 residue to accommodate the larger hydroxyflutamide.

The capacity of LBD mutations to affect disease progression is highlighted by the dominance of the V716M mutation in all three metastases examined from a single flutamide-treated patient. From analysis of multiple metastases we infer that V716M arose either within the primary tumor or early in metastatic invasion. This sample had no other recurring mutations suggesting that an effective variant reduces the selective value of other AR mutations. Interestingly, this patient survived much longer than the other cases. Fixation of an AR mutation like V716M occurred in only one of eight antiandrogen-treated patients, indicating that this is a relatively rare event and that most cancers instead may have subsets of cells with different AR mutations, each providing a similar growth advantage.

Only one LBD mutation recurred in a bicalutamide-treated patient, which may reflect structural differences between antiandrogens. Bicalutamide is much bulkier than hydroxyflutamide, making it unlikely that a single residue change can convert its effect into that of an agonist. Only mutation of W742 has been shown to allow bicalutamide to activate AR (Yoshida et al. 2005). The single recurring LBD mutation in a bicalutamide-treated patient, R761K, is at a residue commonly mutated in castrated h/mAR-TRAMP

mice (O'Mahony et al. 2008), indicating a mechanism other than antiandrogen agonism must be responsible.

Not only base changes but also alterations in splicing may be subject to treatment selection. The AR23 splice variant found only in antiandrogen-treated patients may be present in cells along with wild type AR. Although inactive on its own, co-expression of this variant in cell culture increases wild type protein levels and activity. In the presence of ligand, AR23 protein aggregates in the endoplasmic reticulum, where it may sequester antiandrogens and/or corepressors via its intact NTD and LBD, allowing wild type AR to function (Jagla et al. 2007). This decoy activity may be valuable in the presence of antiandrogens, supported here by the absence of AR23 in untreated patients.

The W435L mutation increases transactivation of AR-selective promoters in CV-1 and RWPE cells. This contrasts with the phenotype of an h/mAR-TRAMP mutant, AR-R753Q, that lacks function on selective elements but gains function on canonical elements (O'Mahony et al. 2008). Selection for differential promoter usage may change over the course of disease and incorporate multiple mechanisms. The effect of the W435L mutation might also vary with disease stage or cell type. Recently the WHTLF motif has been implicated in ligand-independent AR activation (Dehm et al. 2007). The W435L mutation, which creates an LXXLF motif, could weaken the motif's competition with FQNLF for AF-2 and thus increase ligand-dependent activity, while also increasing ligand-independent function by mimicking coactivator binding motifs. Alternatively, W435L may affect AR stability via altered interaction with FQNLF, which helps target AR to the proteasome (Chandra et al. 2008). Since steady-state levels of AR-W435L

appear unaffected, it is more likely that W435L impacts transcription and coactivator interactions, either directly or via influence on FXXLF function.

Mutation of the highly conserved CHIP interaction domain in both murine and human tumors underscores the importance of this region. It also illustrates the utility of mouse models for obtaining clinically relevant insights. E255K stabilizes AR and increases nuclear localization in the absence of hormone thus increasing the amount of steady-state AR protein. This may have a similar effect to *Ar* gene amplification, which occurs in metastatic prostate cancer and is associated with increased proliferation (Haapala et al. 2007). Increased AR levels may enhance response to low concentrations of ligand, increase ligand-independent activation, or promote conversion of antiandrogens to agonists (Chen et al. 2004). Although transactivation by AR-E255K is similar to wild type in transfection, overexpression may mask differences due to stability. The analogous mAR-E231G shows modest differences in activity in transfection assays but is oncogenic as a prostate-specific transgene (Hara et al. 2005).

In summary, this study identified a greater number of recurring mutations in metastases from treated compared to untreated prostate cancer patients. Furthermore, the variety of mutations identified indicates that treatment with antagonists does not select for a few common mutations, but instead selects for a number of rare mutations all of which may affect AR function and may be overlooked using bulk sequencing methods. Combining the novel mutations identified here with those from previous studies begins to highlight AR domains within which mutations share a similar phenotype (Buchanan et al. 2001). What is more, these mutations affect diverse AR processes in addition to transcriptional potency, including cell localization, stability, and promoter-selectivity.

Better understanding of these processes may present novel interacting protein targets for new therapies that may obviate AR's ability to evade antiandrogen treatment.

Acknowledgements

Many lab members contributed to this project. Michele Brogley prepared the patient samples for sequencing and performed the original analysis to identify mutations. Orla O'Mahony was involved in the initial examination of the *AR* mutations. Haniya Rehman did the bulk of the AR immunocytochemistry, and Beth Stairns helped with transfections. We also thank Dr. Norman Greenberg (Fred Hutchinson Cancer Center, Seattle, WA) for advice throughout this study and Drs. Andy Lieberman and Chris Krebs (University of Michigan) for helpful discussions.

Table 3.1. Summary of sample information.

Patient # *	Tissue source of metastasis	Hormonal therapy	Time on hormonal therapy (months)	TMPRSS2-ETS gene fusions†	Base pair changes	
					more than 1 clone	more than 1 patient
5	Liver	Flutamide	22	No	ΔQ86 AR23	Q58L, ΔQ86 T440P,G456S, 69bp ins
12	Liver	Flutamide	36	Yes	E255K, L446S K610E, L798P L874P	R485C, 69bp ins R787X
28	Lung	Flutamide	12	Yes	V716M	ΔQ86 G457D 69bp ins
18	Liver	Flutamide	48	Yes	none	Q58L, T229C A253V, W435L
23	Soft tissue	Bicalutamide	48	No	none	V509L, 69bp ins
24	Liver	Bicalutamide	10	Yes	Q58L, L595M, Q262X	Q58L, ΔQ86 69bp ins, E666D
26	Kidney	Bicalutamide	60	Yes	ΔQ86, G456S, R761K	Q58L, ΔQ86 A253V, G456S
30	Soft tissue	Bicalutamide	18	No	Q868X	ΔQ86, T229C W435L, T440P T498I, V509L Q828X
LK8	Lymph node	Hormone-naïve	0	N/A**	T440I	Q58L, ΔQ86 G457D
2C	Lymph node	Hormone-naïve	0	N/A	none	R485C, T498I
12A	Lymph node	Hormone-naïve	0	N/A	ΔQ86	ΔQ86, R787X Q868X

∗Patient numbers for antiandrogen-treated patients correspond to the numbers listed in Shah et al., 2004 (18).

† TMPRSS2-ETS gene fusion data from Mehra et al., 2008 (44).

** N/A (not applicable): these samples were not examined for gene fusions

Table 3.2. Distribution of mutation types within treatment groups.

	Hormone Treatment		
	Flutamide	**Bicalutamide**	**Hormone-Naïve**
Mutations/10,000 bp	4.4	3.9	3.9
Missense	60.6%	57.2%	55.7%
Silent	28.3%	23.1%	18.4%
Nonsense	2.2%	4.9%	8.0%
Codon deletion	2.4%	2.9%	3.1%
Base pair insertion	2.4%	4.5%	5.4%
Base pair insertion	4.3%	7.6%	9.3%

Figure 3.1. Recurring codon mutations found in prostate cancer metastases.

A. Mutations that occur in more than one case. For codons that have mutations to different amino acids, both mutant amino acids are shown. **B.** Mutations that occurred in more than one clone in a sample. Mutations are arranged as in A. Note that only the ΔQ86 mutation was shared among groups. AR domains and repeats are boxed. In both A and B, mutations above the boxed domains are silent or nonsense mutations while mutations below the boxed domains are missense. Codons are color coded as to treatment group. Q: Polyglutamine tract, NTD: N-terminal domain, G: Polyglycine tract, DBD: DNA binding domain, H: Hinge region, LBD: Ligand binding domain. **C.** V716M occurred in all sequenced metastases from patient 28, but not in genomic DNA from normal kidney. Electropherograms of sequence amplified from 3 samples are shown: sequence from one of the twenty clones amplified from metastasis 1 cDNA carrying the mutation G3261A (numbering from Genbank NM_000044) resulting in the amino acid substitution V716M (*far left)*; sequence from genomic DNA extracted from normal kidney carrying a wild type sequence (*left)*; sequence from cDNA *(right)* and genomic DNA (*far right*) of metastasis 2. Green arrow: mutated base; black arrow: wild type base.

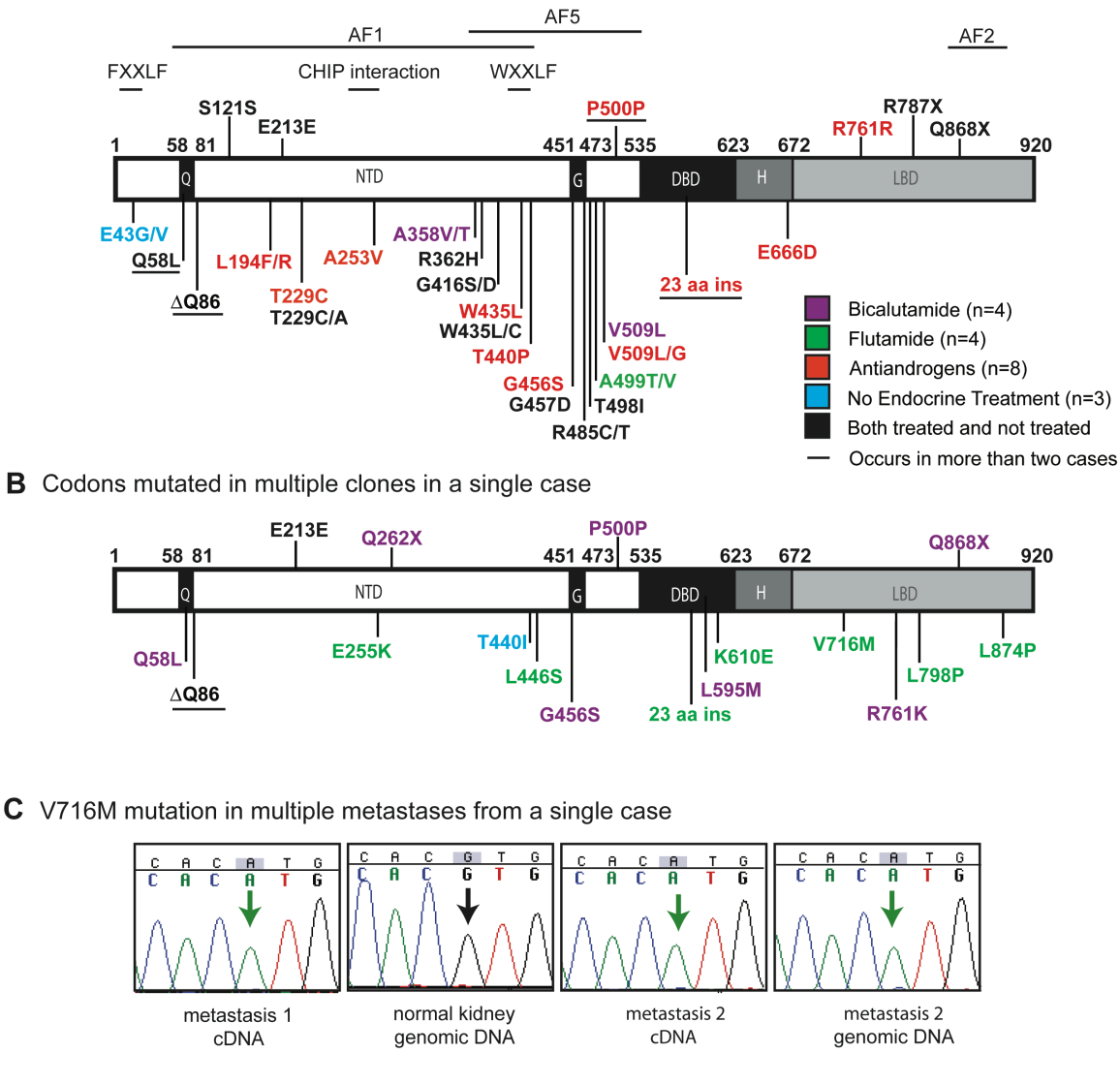

Figure 3.1. Recurring codon mutations found in prostate cancer metastases.

Figure 3.2. The splice variant, AR23, has altered subcellular localization and enhances wild type AR activity.

A. Schematic of the AR23 DBD with an extra 23 amino acids inserted in frame between the two zinc fingers. **B.** Punctate cytoplasmic localization of AR23 protein. PC-3 cells were transfected with wild type AR (*left*) or AR23 (*right*) and treated 24 hours later with or without 10 nM R1881. AR23 shows diffuse cytoplasmic localization in the absence of R1881 similar to wild type AR (*top row*). In the presence of R1881, wild type AR localizes to the nucleus (*bottom left*), while AR23 localizes to cytoplasmic puncta (*bottom right*). AR was detected with AR N20 antibody and a FITC-conjugated secondary antibody. **C.** Transactivation of wild type AR (4 ng), AR23 (4 ng), or a 1 to 1 mix of wild type AR and AR23 (4 ng each) transfected into PC-3 cells along with 400 ng of the PSA luciferase reporter and 100 ng of promoterless renilla. Cells were harvested 24 hours after treatment with 1 nM R1881 and assayed for firefly and renilla luciferase activity. The average normalized values of at least three independent trials are represented as the percent of wild type transactivation at 1 nM R1881. Error bars indicate the standard error of the mean (SEM). Significant p-values are shown for indicated comparisons and are based on analysis by Student's t-test. **D.** Repression of NFκB activity by wild type AR or AR23. Wild type or mutant AR was transfected along with an NFκB reporter. NFκB was activated with the TPA. Wild type AR reduces NFκB activity to 20% of the control (no AR) in the presence of 10 nM R1881, while NFκB activity remains high, 80% of control, in the presence of AR23. **E.** Activity with antiandrogens. Transactivation assays were performed as in B. Cells were treated with no ligand (-), 1 or 10 μM hydroxyflutamide (HOF), or 1 μM bicalutamide. P-values are shown for significant differences as in C. * $p<0.05$, ** $p<0.005$, *** $p< 5x10^{-5}$ Significance based on Student's t-test.

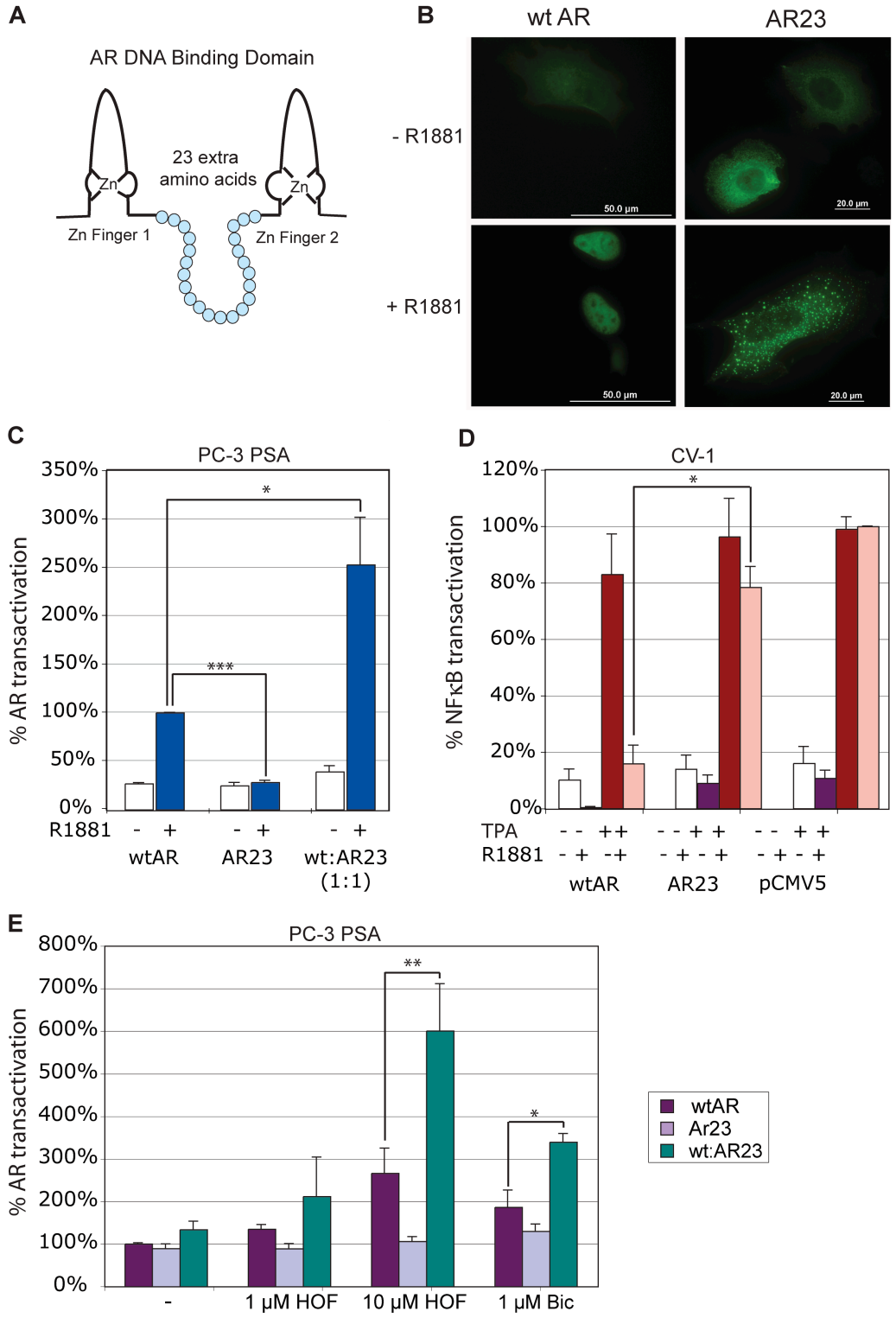

Figure 3.2. The splice variant, AR23, has altered subcellular localization and enhances wild type AR activity.

Figure 3.3. Promoter- and cell-context dependent effects of AR-W435L. Transactivation of AR-W435L was assessed in CV-1 (**A**), RWPE (**B**), and PC-3 cells (**C**), revealing similar promoter-specific increases that were more pronounced in RWPE cells, and absent from PC-3 cells. Cells were transfected with 4 ng wild type AR (wtAR) or AR-W435L and 400 ng of the indicated androgen-responsive luciferase reporters. PSA activates poorly in CV-1 cells so the complex MMTV promoter was tested instead. 100 ng promoterless renilla was cotransfected to control for transfection efficiency. After 24 hours cells were fed with phenol red free medium +/- 1 nM R1881. The average normalized values of at least three trials are represented as the fraction of wild type activity at 1 nM R1881. Error bars are the standard error of the mean (SEM).

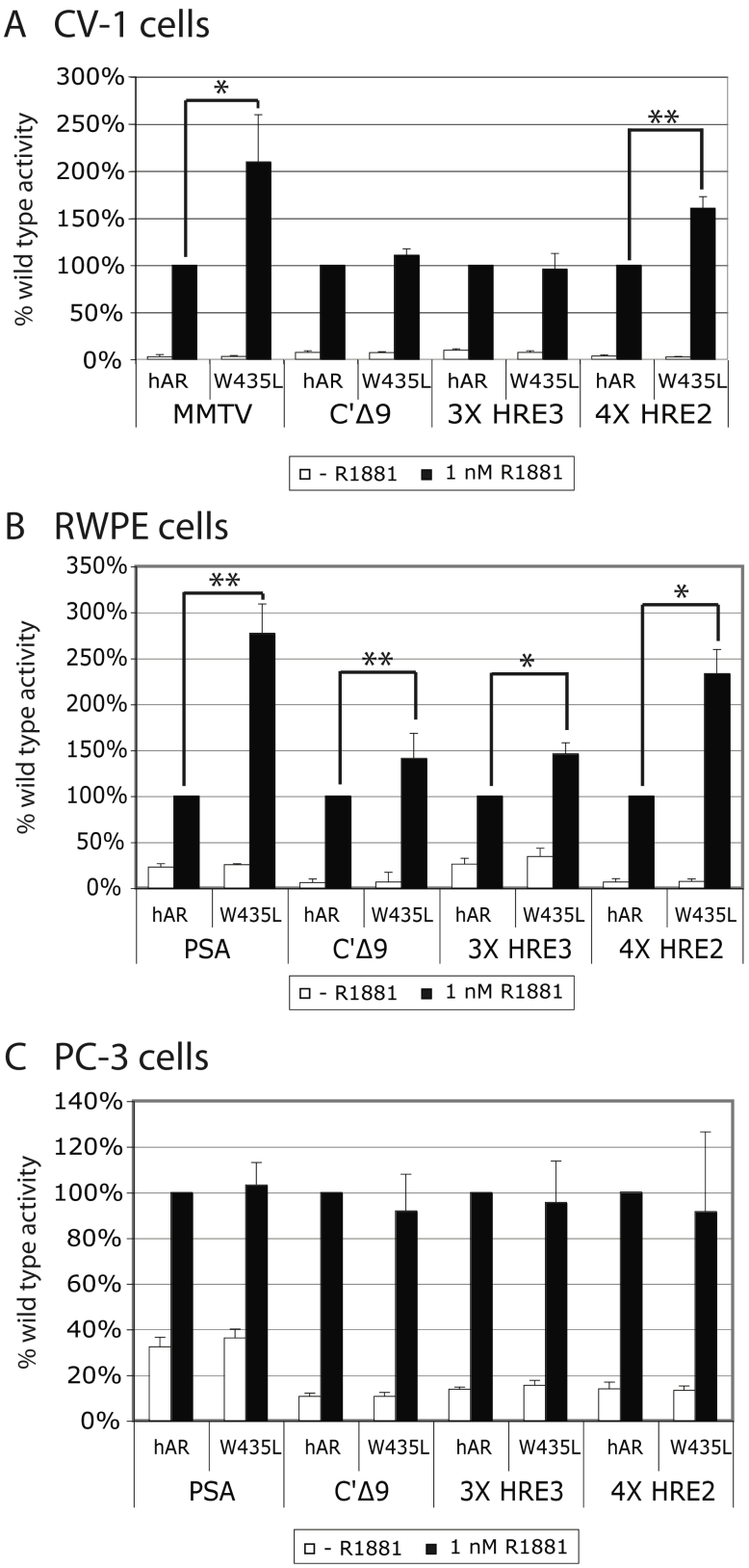

Figure 3.3. Promoter- and cell-context dependent effects of AR-W435L.

Figure 3.4. AR-E255K has increased stability and ligand-independent nuclear localization.

A. Immunoblots of AR from a representative cycloheximide degradation assay (*right*). 100 ng of wild type AR (wtAR) or AR-E255K was transfected into CV-1 cells, which were treated after 24 hours with 30 μM cycloheximide to inhibit protein synthesis. Cells were harvested at times indicated and 20 μg of total protein was run on an SDS/polyacrylamide gel. AR bands from scanned immunoblots were quantified using ImageJ, values normalized to the amount of protein at time 0 and plotted for wtAR and AR-E255K in the absence of hormone (*left*). AR-E255K shows a longer half-life ($t_{1/2}$= 12.5 hrs) than wtAR ($t_{1/2}$=5.2 hrs). Full gels are included in Supplementary Data. **B**. Proteasome inhibition with lactacystin in the absence of hormone increases wtAR but not AR-E255K protein levels. CV-1 cells were transfected as in A, treated after 24 hours with 10μM lactacystin, harvested 18 hours later, and immunoblotted as in A. **C**. Immunofluorescence of wtAR and AR-E255K transfected into PC-3 cells reveal wtAR largely cytoplasmic in the absence of hormone (*top left*) while the majority of cells transfected with AR-E255K show more nuclear staining (*bottom left*). Full color images and composite are in Supplementary Data. AR was detected using N20 anti-AR and a FITC-conjugated secondary antibody. Percent of cells with cytoplasmic to nuclear AR localization are graphed as follows: C, exclusively cytoplasmic; C>N, cytoplasmic fluorescence greater than nuclear fluorescence; C=N, equal cytoplasmic and nuclear fluorescence; N>C, nuclear fluorescence is greater; N, exclusively nuclear fluorescence. n= the number of cells counted for all three trials. The mean percentages +/- SEM for 3 experiments are shown. **D.** AR-E255K shows increased transactivation of a PSA reporter in RWPE cells. Transactivation by wtAR or AR-E255K of representative androgen-responsive promoters is shown. Bars are the average % of wild type activation of three or more trials +/- SEM. ** $p<0.005$ based on Student's t-test.

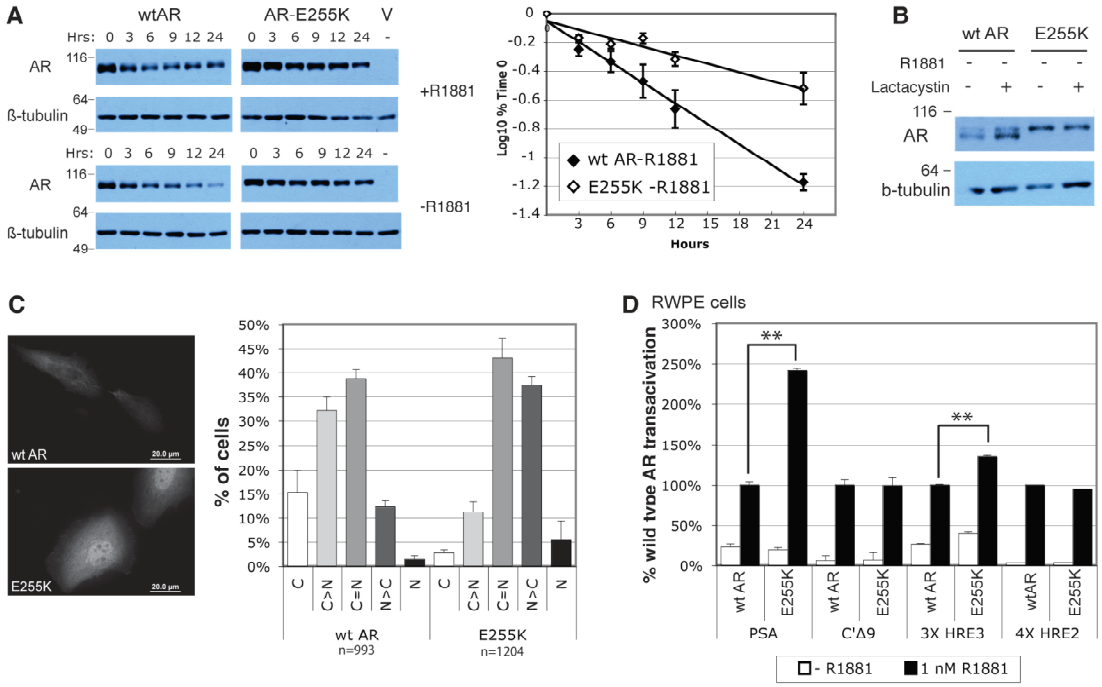

Figure 3.4: AR-E255K has increased stability and ligand-independent nuclear localization.

Table 3.3. Summary of functionally characterized mutants indicating multiple mechanisms involved in therapy resistance.

Mutation	Domain	Function
V716M	LBD	Promiscuous receptor
AR23	DBD	Altered splicing, decoy receptor
W435L	NTD	Promoter-selective activation
E255K	NTD	Increased stability Androgen-independent nuclear localization

Chapter 4

Androgen Receptor Mutations Identified in Male Breast Cancer May Promote Tumorigenesis Through Differential Promoter Transactivation

Abstract

Male breast cancer is rare, accounting for less than 1% of all cases of breast cancer. However, male breast cancer risk is greatly influenced by conditions that reduce androgen or increase estrogen levels or efficacy. Two germline mutations, R607Q and R608K, in adjacent arginine residues of the androgen receptor (AR) DNA binding domain have been identified in men with partial androgen insensitivity and breast cancer. Here, characterization of these mutants' transactivational activity on androgen-responsive promoters in CV-1 fibroblasts as well as normal and malignant breast cancer cell lines, MCF10A and MCF-7 respectively, revealed promoter and cell-specific activation. The mutant receptors were more active than wild type AR in both breast cell lines. AR-R607Q was consistently more active than AR-R608K. However, both mutant receptors were able to activate a reporter with canonical response elements similar to wild type AR, but were deficient in transactivating reporters with AR-specific response elements. The promoters of AR targets often contain a variety of response elements that cooperatively activate transcription. Therefore a subset of targets may be more sensitive to these *AR* mutations. In the case of male breast cancer, differential promoter transactivation by AR-

R607Q and AR-R608K may favor targets that encourage proliferation in concert with estrogen stimulation.

Introduction

Breast cancer in men is rare affecting only 1 per 100,000 men (Giordano et al. 2004) compared to 100 per 100,000 women. Risk of male breast cancer often correlates with alterations in hormone balance suggesting that the ratio of estrogen to androgen may be an important factor in risk assessment for breast cancer in general (Seralini et al. 2001). Men with Klinefelter Syndrome (XXY) that have both increased estradiol and decreased testosterone levels, which may be associated with gynecomastia, have a 60 fold higher rate of breast cancer, than normal men (Swerdlow et al. 2005). In epidemiological studies, long AR polyglutamine tracts (ie. weaker ARs) are seen more often in men with breast cancer compared to controls (Young et al. 2000; Maclean et al. 2004). Furthermore, two mutations in AR that lead to partial androgen insensitivity (PAIS) have been independently identified in male breast cancer patients (Wooster et al. 1992; Lobaccaro et al. 1993). These mutations are particularly interesting because they occur in two adjacent arginines, R607 and R608, in the AR DNA binding domain and may disrupt a single "enhancement region" as suggested in the same region of GR (Schena et al. 1989) (Figure 4.1A). Mutations throughout the AR gene have been identified in complete and partial androgen insensitivity (Gottlieb et al. 2004) and yet, only these two mutations have been found in male breast cancer, suggesting that mutations in this specific area of the DNA binding domain (DBD) may increase risk of male breast cancer, perhaps through altered AR function rather than simply reduced AR activity.

The AR DBD consists of two zinc fingers. The first makes direct contacts with the DNA and is involved in site recognition, while the second stabilizes the DBD and forms the homodimer interface (Verrijdt et al. 2006). AR and GR bind canonical hormone response elements (HREs) consisting of inverted repeats of a 5' TGTTCT 3' half site (Truss et al. 1993). However, AR, and not GR, can bind a second type of response element consisting of partial direct repeats of the half site termed androgen-selective response elements (Robins 2004). Studies using chimeric GR/AR receptors have demonstrated that AR residues within the second zinc finger and its C-terminal extension facilitate AR binding to these androgen-selective response elements (Schoenemakers et al. 1999).

Based on the Partial Androgen Insensitivity Syndrome (PAIS) phenotype of the patients carrying R607Q and R608K and based on the fact that these residues are conserved within the steroid receptor family, it would be expected that these mutations are loss of function. Indeed these mutants show reduced DNA binding to an HRE (Poujol et al. 1997). A mutation in the GR equivalent of R608, GR-R489Q has a cold-sensitive phenotype when cultured in yeast, which often suggests altered protein-protein interactions (Schena et al. 1989). A mutation in the equivalent residue of the thyroid hormone receptor, R158G, prevents homodimer formation on a direct repeat, but maintains heterodimer formation with retinoid-X receptor α (RXRα) (Nagaya et al. 1996). However, AR-R607Q and AR-R608K exhibit normal transactivation on the aldo-keto-reductase 1B7/mouse vas deferens protein (MVDP) promoter at high concentrations of the non-metabolizable androgen, methyltrienolone (R1881), and only show diminished activity at concentrations below 0.1 nM R1881(Poujol et al. 1997). Similar experiments

with the rat equivalent of AR-R607Q, AR-R590Q, show reduced function on a reporter with a single HRE from the probasin promoter, but not on the complete probasin promoter (Aarnisalo et al. 1999). Furthermore, R608K has been shown to exhibit increased activation of Mitogen-Activated Protein Kinase (MAPK) in MCF-7 breast cancer cells (Yeh et al. 2003). Though hinting at the importance of these two arginines in activity, none of the previous studies has determined the mechanism for how these two mutations might predispose males to breast cancer.

To understand the mechanism of action of these mutants, either R607Q or R608K or both were engineered by site-directed mutagenesis into an AR expression plasmid and their activity was assessed on a variety of androgen-responsive promoters in both CV-1 cells and in breast cell lines. Cell and promoter-specific responses suggest that hyperactivity on canonical HREs in combination with reduced activity on androgen-selective AREs in breast cells may encourage cell growth.

Methods

Cell lines

The human breast cancer cell line derived from a plural effusion, MCF-7 (Dickson et al. 1986), was obtained from Dorraya El-Ashry, University of Michigan. The spontaneously immortalized human breast epithelial cell line from a fibroadenoma, MCF10A (Soule et al. 1990) was obtained from Sophia Merajver, University of Michigan. CV-1 fibroblasts were cultured in DMEM + 10% fetal bovine serum (FBS) (Valley Biomedical) + 1% glutamax (Gibco) +1% Penicillin/Streptomycin (Gibco).

MCF-7 cells were cultured in αMEM +10% FBS + 1% glutamax +1% Penicillin/Streptomycin. MCF10A cells were cultures in DMEM/F12 media supplemented with 5% horse serum (Gibco), 20 ng/ml epidermal growth factor, 100 ng/ml cholera toxin, 10 ng/ml insulin, and 500 ng/ml hydrocortisone.

Site-directed mutagenesis

Mutations R607Q, R608K, and the double mutant were introduced into pCMV5-hAR using the Quickchange Site Directed Mutagenesis kit (Stratagene) and the primer pairs below containing each mutation(s) (underlined):

R607Q F: GATTGCACTATTGATAAATTCCAAAGGAAAAATTGTCCATCTTGTC
R607Q R: GACAAGATGGACAATTTTTCCTTTGGAATTTATCAATAGTGCAATC

R608K F: TTGCACTATTGATAAATTCCGAAAGAAAAATTGTCCATCTTGTCGT
R608K R: ACGACAAGATGGACAATTTTTCTTTCGGAATTTATCAATAGTGCAA

607/8 F: ATTGCACTATTGATAAATTCCAAAAGAAAAATTGTCCATCTTGTCGTC
607/8 R:GACGACAAGATGGACAATTTTTCTTTTGGAATTTATCAATAGTGCAAT

Primers were purified by gel electrophoresis on a 12% polyacrylamide/urea gel, cut out and eluted in elution buffer (0.1% SDS, 0.5 M ammonium acetate, and 10 mM magnesium acetate) for 12 hours at 37˚C. Eluate was spun at 12,000Xg for 5 min. at room temperature and supernatants containing the purified primers were filtered through a 0.45 μ filter. Primers were then extracted by ethanol precipitation and reconstituted in ddH2O. Plasmids were sequenced with primers flanking the mutations to ensure appropriate incorporation of the mutation.

Transient transfections

CV-1, MCF-7 and MCF10A cells were seeded at 1 x 10^5 cells per well into 24-well plates. All cells were transfected with Fugene 6 Transfection Reagent (Roche, Nutley, NJ) at 3 µl of Fugene/µg DNA with 4 ng pCMV5-AR (wild type or mutant), 400 ng luciferase reporter plasmid and 100 ng promoterless renilla (Promega) for normalization. Cells were fed with media + 2.5% charcoal stripped Nuserum 4 hours before transfection. R1881 was added to wells just before transfection. Cells were harvested 48 hours after transfection into 1X Passive Lysis Buffer (Promega) and 10 µl of the lysate was analyzed for firefly and renilla luciferase activity with the Dual Luciferase Reporter Assay System (Promega) on a Veritas Microplate Luminometer (Turner Biosystems Inc., Sunnyvale CA). Normalized values were the ratio of firefly to renilla luciferase compared to wild type transactivation at 1 nM R1881.

Stable infection of tetracycline-responsive AR constructs into MCF10A cells.

Tetracycline-responsive wild type AR and AR-R608K were stably introduced into breast cancer cell lines using the BD RevTet System (BD Biosciences) using a protocol (http://www.stanford.edu/group/nolan/protocols/pro_helper_dep.html) from the Nolan laboratory (Stanford University). Wild type AR was cut out of the pcDNA3.1 hAR plasmid by digesting with BamHI and ligated into the pRev TRE BamHI site upstream of the ATG. AR-R608K was cut out of pcDNA3.1 with ClaI and ligated into the ClaI site of pRev TRE (Figure 4.1). Exon 3 of wild type AR and AR-R608K were sequenced from the pRev TRE-AR plasmids to confirm insertion.

Phoenix ampho packaging cells were used to package the viral vectors. Phoenix cells were seeded at $3x10^6$ cells in T25 flasks and transfected with the Tet-On plasmid (BD Biosciences) using Fugene 6 (Roche) at a ratio of 3 µl: 1 µg DNA. Tet-On containing viruses were then collected in the Phoenix cell media, filtered through a 0.45 µM filter, and 4 µg/ml polybrene was added to increase infection efficiency. This media was mixed 1:1 with MCF10A or MCF-7 media and directly added to MCF10A and MCF-7 cells. Media was replaced with fresh culture media 24 hours after infection. 48 hours after infection, cells were selected by G418 treatment for 7 days and proliferating clones were picked. Clones positive for the neomycin-resistance (neo) gene based on a PCR-based assay, and responsive to doxycycline in transfection with the TRE2-Luc doxycycline-responsive reporter were infected with the pRevTRE hAR or pRevTRE AR-R608K virus or a pRevTRE empty vector virus control. Infected clones were selected with hygromycin for 7 days and proliferating clones were picked. Expression of wild type AR or AR-R608K with or without 1 µg/ml doxycycline was assessed by western blot.

Western blotting

CV-1 cells were seeded at 4 x 10^5 cells/ 60 mm dish, fed phenol red-free media +/- 1 nM R1881 four hours before transfection and transfected as above with 100 ng receptor (wild type AR or mutant) and 1.9 µg empty vector (pCMV5). 24 hours after transfection, cells were rinsed in cold 1X PBS and harvested in 100 µl RIPA buffer + protease inhibitors, lysed at 4^oC for 10 minutes and centrifuged at 4^oC for 10 minutes. Stably transfected MCF10A cells were seeded at 2 x 10^6 cells/60 mm dish. Doxycycline

(1 μg/ml) was administered 24 hours later. Cells were harvested 24 hours after induction into RIPA buffer + inhibitors.

Protein was quantified by the Dc Protein Assay (Bio-Rad, Hercules CA). 20 μg protein was run on a 5% stacking/8% separating SDS-polyacrylamide gel and transferred to nitrocellulose. The blot was probed with antibody to the AR N-terminus (N20, Santa Cruz Biotechnology, Santa Cruz, CA) (1:500) and incubated with HRP-conjugated ECL anti-rabbit IgG (GE Healthcare, Piscataway, NJ) (1:5,000) for 45 minutes. Bands were detected with ECL western blotting reagents (Pierce Biotechnology, Rockford IL).

Results

AR mutations identified in male breast cancer patients are located in adjacent arginines in the second zinc finger of the DBD, suggesting a similar mode of action. To examine how these mutations affect AR activity, both mutants were synthesized and then functionally characterized in CV-1 cells and human breast cell lines. MCF10A, an estrogen receptor (ER) negative immortalized mammary gland epithelial cell line and MCF-7, a well-characterized ER positive breast cancer cell line, were chosen to represent a precancerous and cancer state, respectively.

Although AR-R607Q and AR-R608K show reduced activity on the MVD promoter with reduced activity of both mutants only at low concentrations of androgens (Poujol et al. 1997), both showed reduced transactivation on the androgen-specific promoter C'Δ9 (derived from the sex-limited protein gene [Slp]) at all concentrations of R1881 (Figure 4.2). The two mutants also differed from each other with AR-R607Q about half as active as wild type AR while AR-R608K was completely inactive in this

context. Because results were similar over the range of ligand concentrations, further experiments were performed at maximal transactivation by R1881 (1 nM).

AR can bind to two types of androgen response elements: canonical HREs consisting of inverted repeats of a 5' TGTTCT 3' half-site or AR-selective response elements consisting of partial direct repeats (Verrijdt et al. 2003). Both types of element are present in C'Δ9 (Robins 2004). To determine whether the mutations in the second zinc finger have differential effects depending on the type of element, transactivation was examined on the canonical element from Slp, HRE3, versus the AR-selective Slp element, HRE2, in CV-1 cells (Figure 4.3A). Both mutants were more active on the reporter consisting of multimerized canonical elements (3X HRE3) than on the complex C'Δ9, and AR-R607Q was even more active than wild type AR. Both mutants were less active on the reporter consisting of multimerized AR-selective elements (4X HRE2).

AR can also repress transactivation by other transcription factors such as NFκB, through protein-protein interactions (Palvimo et al. 1996). This repression may contribute to increased apoptosis in AR positive prostate cancer cells (Nelius et al. 2007) and may be particularly important in the breast where AR is thought to counteract ER proliferative signals. Since mutation of the GR equivalent of R608, R488, abolishes GR repression of NF-κB (Liden et al. 1997), AR-R608K could potentially diminish repressor function.

NFκB repression was examined in CV-1 cells cotransfected with wild type or mutant ARs and a reporter driven by multimerized NFκB binding sites (6X NFκB-Luc). Endogenous NFκB was activated with the general activator, TPA, and the extent of androgen-dependent repression was observed. Both mutants were capable of repressing

NFκB activity to wild type levels (Figure 4.3B), indicating that these mutations do not compromise interaction with NFκB.

Previously the activity of these mutants had only been tested in CV-1 cells. However, expression of cell-specific cofactors could greatly alter activity in the hormone-responsive breast epithelia. Therefore, transactivation was examined in both a normal mammary epithelial cell line, MCF10A, and a breast cancer cell line, MCF-7 (Figure 4.3B and C). Interestingly, transactivation on C'Δ9 by AR-R607Q was rescued in the breast cell lines. In MCF10A, R607Q was hyperactive on C'Δ9, which may indicate that additional factors expressed in breast epithelia enhance mutant activity on C'Δ9. Both mutants showed hyperactivity on 3X HRE3, but they still only weakly activated 4X HRE2 suggesting a possible defect in binding or protein-protein interactions on direct repeats.

The R608K mutant demonstrated the greatest difference in transactivation between the general and selective response elements. Therefore, we expressed wild type and R608K ARs stably in the MCF10A cell line. MCF10A cells were infected with the tet-on plasmid and either the wild type AR or AR-R608K driven by a tetracycline responsive promoter. Positive clones were assessed for doxycycline response and AR expression. Three wild type AR clones and two AR-R608K clones showed doxycycline-responsive expression (Figure 4.4A). Clones wtAR#2 and AR-R608K #3 yielded equivalent protein amounts and so were further assessed in transfections. Transient transfection with androgen-responsive reporters confirmed the results of the transient transfections with AR-R608K activating reporters with canonical response elements but not those with AR-selective elements. However, AR-R608K showed reduced activation

on C'Δ9 unlike transient transfection in MCF10A and more similar to transiently transfected MCF-7 cells (Figure 4.4B). This difference in transient versus stable receptor expression may be due to the moderate levels of receptor being produced in the stable cell line compared to possible overexpression in the transient transfections.

Discussion

AR-R607Q and AR-R608K, mutants identified in male breast cancer patients, exhibit promoter-specific and cell-specific differential transactivation suggesting that alterations in AR activity may influence breast tumorigenesis by activating a subset of AR targets. Use of the AR-specific reporter, C'Δ9, reveals important differences in transactivation of AR-R607Q and AR-R608K that were not seen previously. Both mutants show normal to increased activity on canonical AREs and reduced activity on selective AREs, but AR-R608K has a more severe phenotype than AR-R607Q, indicating that these two mutants, though similar, are not equivalent. Both mutants are also more active in breast cell lines showing near normal activity on a complex promoter but reduced activity on a selective ARE.

This reduced activation specifically on AR-selective promoters might account for the partial androgenization of the patients during development, while also explaining why only small differences at low androgen concentrations were noted in transactivation on the MVDP promoter, which contains only a canonical hormone response element (Fabre et al. 1994; Darne et al. 1997). It is possible that the zinc finger mutants may indirectly affect breast cancer risk through weaker opposition to the estrogen axis. In addition,

differential activation of AR targets by these mutants may have a direct effect on breast cancer initiation.

Differential transactivation on canonical versus selective AREs suggests that R607 and R608 may make important contacts when binding to direct repeats, either at the DNA or protein level. Previous work with AR/GR chimeric receptors showed that the AR DBD is necessary for binding to direct repeats (Scheller et al. 1998). Particular residues in the second zinc finger that differ between AR and GR, T603, G628 and L635, allow AR dimerization in a head to head fashion on these direct repeats (Schoenmakers et al. 2000; Shaffer et al. 2004).

Both arginines are highly conserved: R607 within the steroid receptor family and R608 in the entire nuclear receptor superfamily, suggesting that mutation of these residues may have broad effects on DBD function. Since binding studies on direct repeats only examined the effect of swapping sequence from the GR and AR in which R607 and R608 are conserved, the role of these residues is unknown. Modeling of AR shows that R607 makes contact with the other AR monomer of the homodimer on a canonical repeat (Poujol et al. 1997). While it appears that AR can transactivate on canonical response elements without R607, this contact may be necessary for dimerization on the weaker, albeit more specific, direct repeats. Alternatively, mutations in these residues could abolish a protein-protein interaction surface, as suggested by molecular modeling (Poujol et al. 1997), for a cofactor that helps to stabilize AR on direct repeats. A reduction in AR binding to direct repeats may account for reduced transactivation by these mutants of the C'Δ9 complex promoter that requires synergistic binding of AR to both canonical and direct repeats for activation (Scheller et al. 1998).

Interestingly, AR-R607Q and AR-R608K mutants were more active on canonical elements in normally hormone-responsive cells such as MCF10A and MCF-7, amplifying differences in transactivation on canonical versus selective AREs and emphasizing the importance of cell-specific cofactors.

Similar differential promoter activation is observed with a mutant, AR-R753Q, identified in a mouse model of prostate cancer (O'Mahony et al. 2008). As a germline mutation, R753Q results in complete androgen insensitivity in the rat *testicular feminized male* (*tfm*) (Yarbrough et al. 1990). However, in prostate cancer cells, R753Q exhibited decreased activity only on AR-specific response elements and was active on general response elements (O'Mahony et al. 2008).

Since AR target promoters contain multiple AREs along with binding sites for other transcription factors, it is likely that a subset of promoters is more sensitive to loss of function on selective AREs or gain of function on canonical AREs. The affect of these mutations on male virility suggests that they affect expression of genes during male development. Loss of AR binding to selective AREs but not canonical AREs in the Specificity-affecting AR Knockin (SPARKI) mouse model results in undervirilized males (Schauwaers et al. 2007), suggesting that selective AREs may be more important for target genes involved in development and differentiation. Thus differential activation of canonical over selective elements may translate to decreased activation of targets involved in differentiation and increased activation of targets involved in proliferation. Alternatively, the hyperactivity of both mutants on canonical elements specifically in breast cancer cells (Figure 4.3B and C) might be enough to promote tumorigenesis. Because these types of mutations have been found in both male breast cancer and prostate

cancer, a general proliferative cell program may be activated in the case of both breast and prostate tumorigenesis. In the future, the stable breast epithelial cell lines expressing wild type AR or AR-R608K established in this study could be particularly useful for examining the differential expression of AR target genes. These cell lines could be used to differentiate between AR targets that might encourage proliferation versus differentiation and breast cancer promotion versus ER opposition.

In conclusion, functional characterization of two AR mutations identified in male breast cancer patients demonstrate that not just quantitative but qualitative differences in AR activity, here shown by differential regulation of canonical versus AR-specific response elements, may affect both male development and risk of breast cancer. Though these particular mutations have only been identified in a few patients, examination of AR targets in the breast that are differentially activated by these mutant receptors may clarify AR's effects on the breast and reveal ways to harness AR's antiproliferative activities to treat breast cancer.

Acknowledgements

We thank Sophia Merajver for providing the MCF10A breast cell line and Dorraya El-Ashry for the MCF-7 breast cancer cell line. Matthew Butler from the Glover lab provided the Phoenix cells, and the BD RevTet System plasmids into which AR sequence was inserted and showed me how to collect virus particles and infect cells safely.

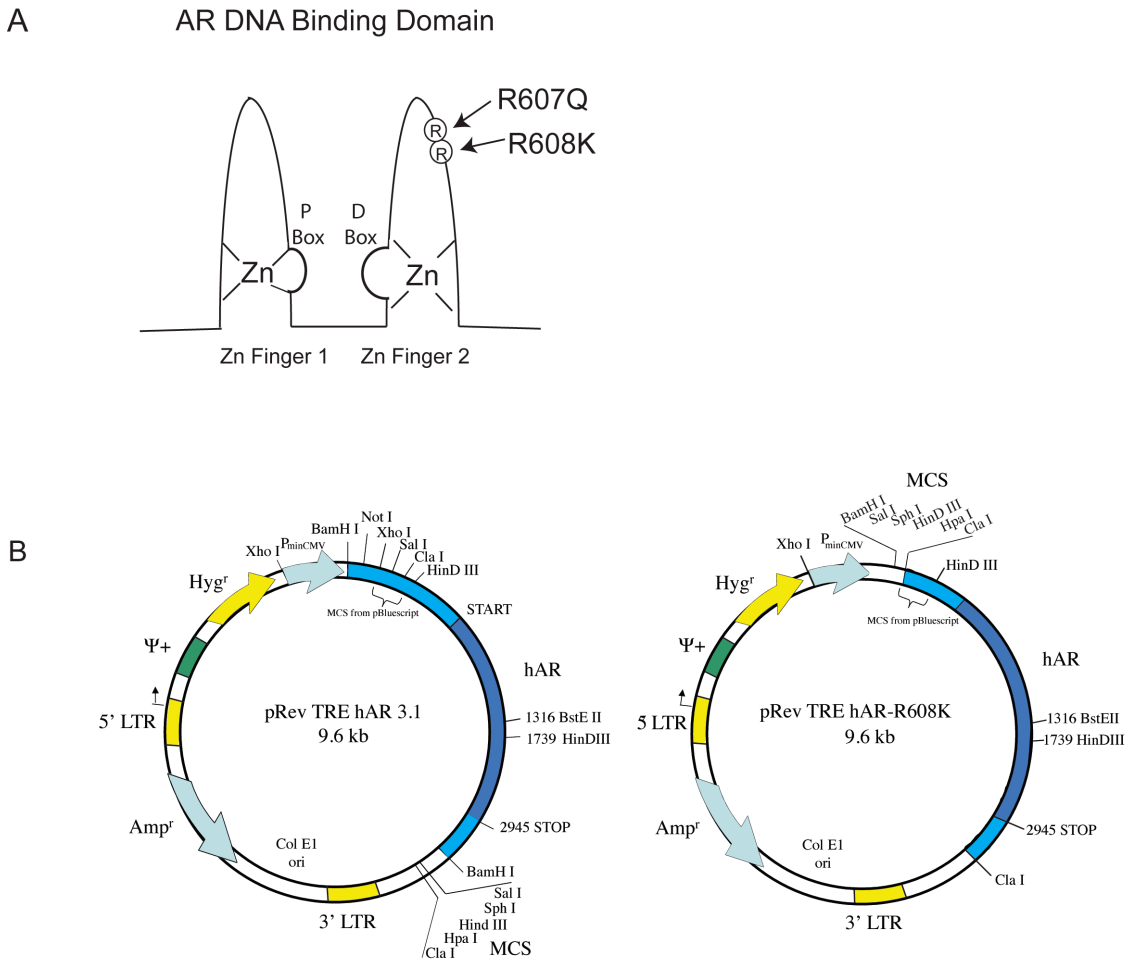

Figure 4.1. AR mutations in male breast cancer.

A. Schematic of the AR DNA binding domain (DBD) containing two zinc (Zn) ions each bound to four cysteine residues to form zinc fingers that directly contact the DNA. Mutations that have been identified in male breast cancer are located in adjacent arginines in the second zinc finger (arrows). Also shown are important elements of the DBD including the P Box, whose residues dictate DNA binding selectivity of steroid receptors, and the D Box, which is the dimerization interface for intermolecular interactions. **B.** Plasmid construct for stable infection of tetracycline-responsive wild type and AR-R608K. Wild type human AR sequence was cut out of the pcDNA 3.1 AR expression plasmid with BamHI and ligated into the BamHI site within the multiple cloning site of the pRev TRE plasmid (BS Biosciences). AR-R608K was cut out of the pcDNA 3.1 AR-R608K expression plasmid with ClaI and ligated into the ClaI site of the pRev TRE plasmid.

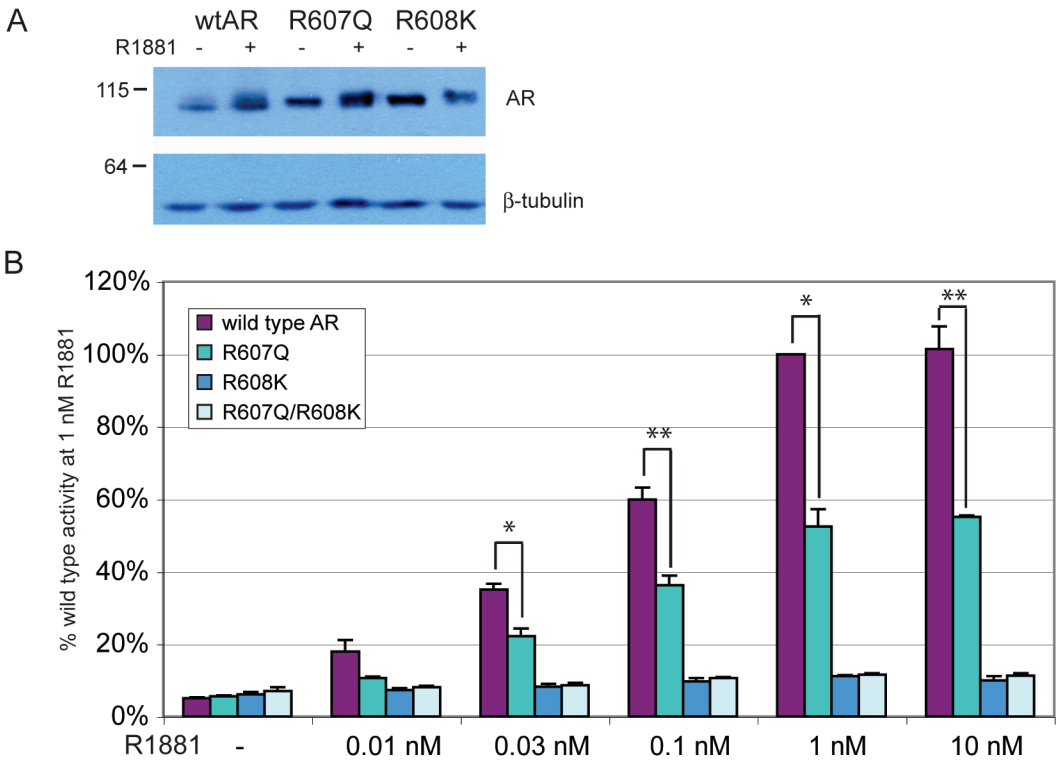

Figure 4.2. Mutant AR levels and activity in transiently transfected CV-1 cells.

A. A western blot for AR protein expressed in transfected CV-1 cells indicated that mutant AR protein levels in transfection are similar to that of wild type AR. CV-1 cells were transfected with wild type or mutant AR and fed with or without 1 nM R1881 24 hours after transfection. Cells were harvested 48 hours after transfection into RIPA buffer and 50 µg total protein was run on a 12% polyacrylamide gel. Westerns were probed with AR antibody N20. ß-tubulin was probed as a loading control. **B.** Transactivation activity of mutant receptors with increasing levels of R1881. CV-1 cells were transfected with wild type or mutant receptors plus the AR-specific fragment of the Slp promoter (C'Δ9) and a renilla luciferase reporter for normalization. 24 hours post-transfection, cells were treated with varying concentrations of the non-metabolizable androgen methyltrienolone (R1881) as labeled. 48 hours post-transfection cells were collected in passive lysis buffer and luciferase activity assayed. Luciferase activity was normalized to the renilla activity to control for transfection efficiency and plotted as the average percent wild type AR activity at 1 nM R1881. AR-R608K and the double mutant showed no response on this promoter while AR-R607Q was partially active. Transactivation activity of AR-R607Q was significantly lower than wild type AR. * $p<0.01$, ** $p< 0.005$. Significance based on Student's t-test.

Figure 4.3. Promoter-specific and cell-specific transactivation of mutant ARs in transient transfections.

AR-R607Q and AR-R608K activity was assessed on the complex promoter C'Δ9 and on tandem repeats of its individual response elements, HRE3 and HRE2, in CV-1 cells (**A**) as well as two human breast cell lines, the non-malignant MCF10A cell line (**B**) and the MCF-7 breast cancer cell line (**C**). Activity was assessed in the absence (-) or presence (+) of 1 nM R1881 as indicated. Both mutants exhibited similar responses on the three reporters, although AR-R608K was less active on all three reporters. Both mutants were more active, particularly on the canonical response element, when transfected into breast cell lines. Luciferase activity is shown as % wild type AR activity. * $p<0.05$, ** $p< 0.005$, *** $p< 5 \times 10^{-5}$ Significance based on Student's t-test.

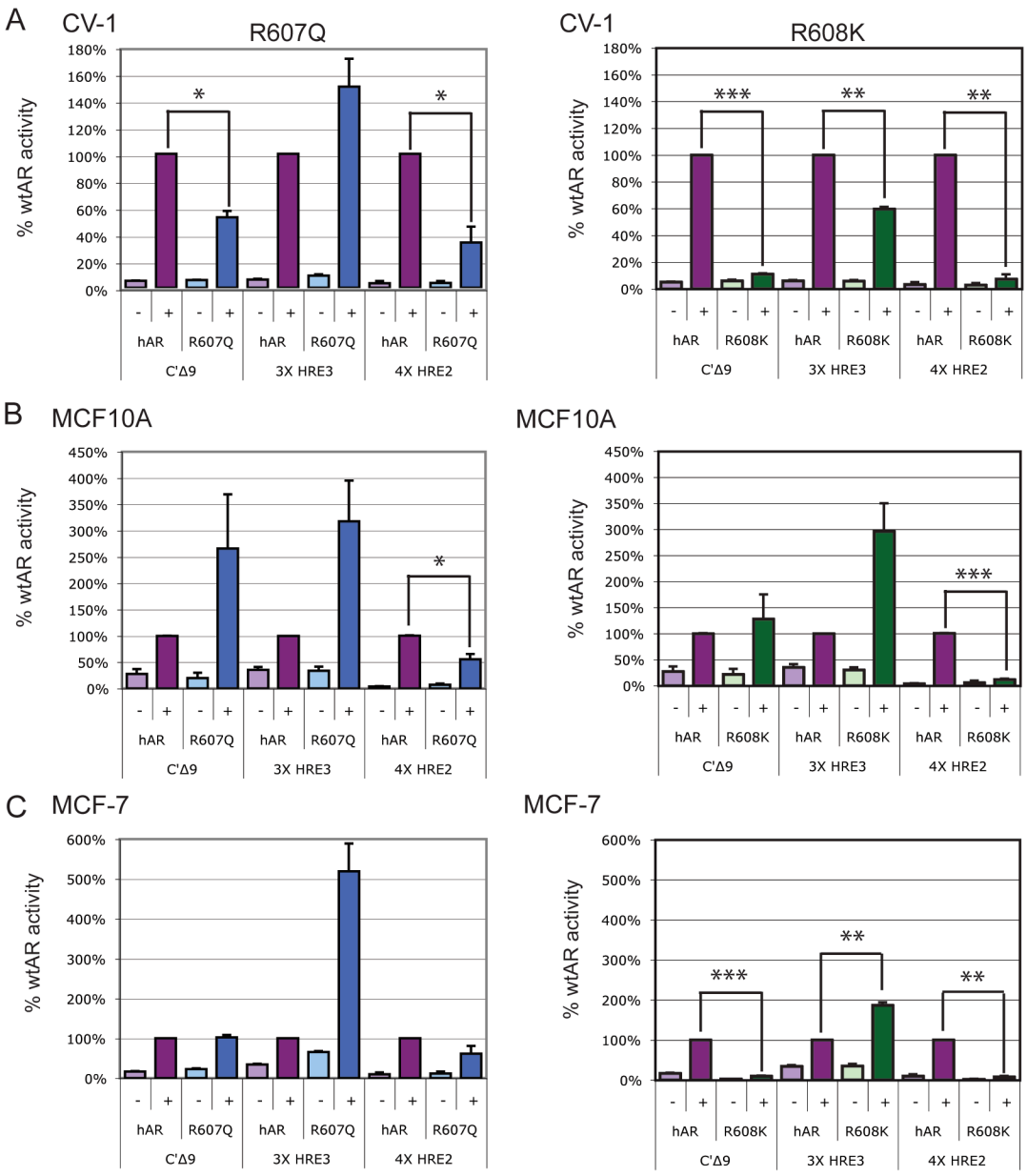

Figure 4.3. Promoter-specific and cell-specific transactivation of mutant receptors in transient transfections.

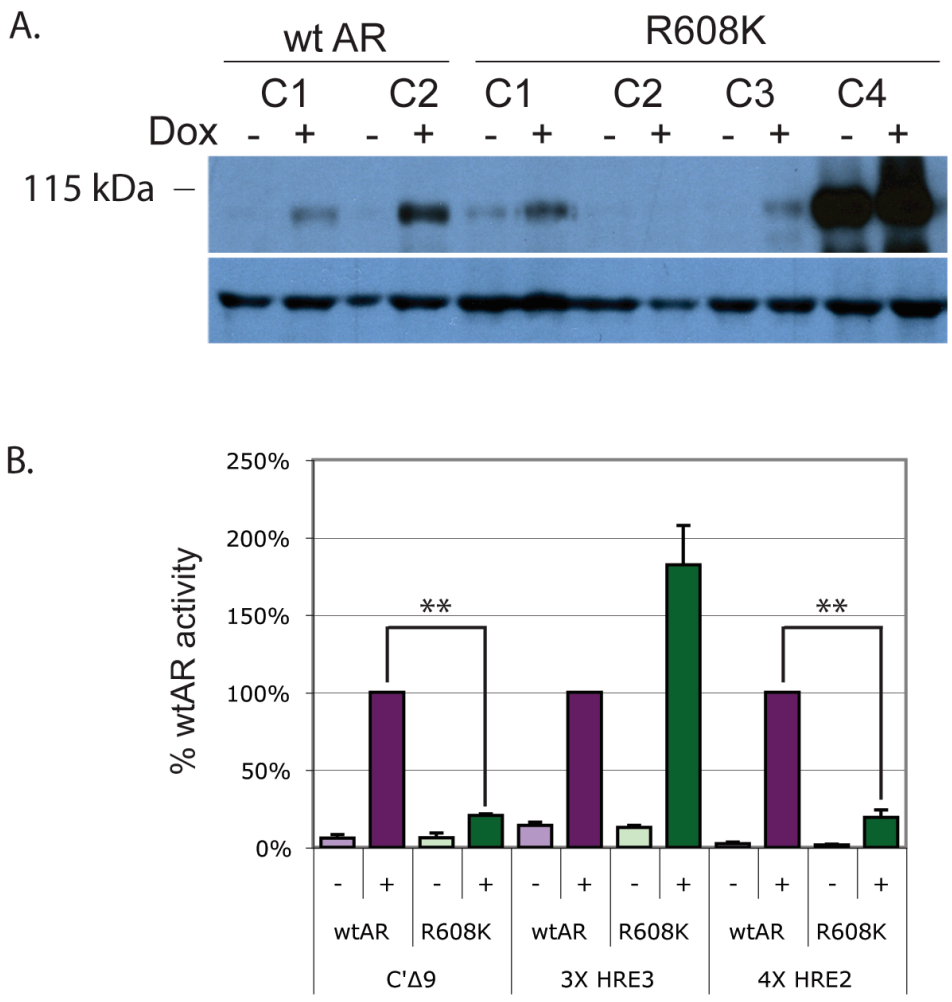

Figure 4.4. AR expression and activity in MCF10A breast cells stably transfected with tetracycline-responsive wild type and AR-R608K expression plasmids.

MCF10A cells were infected in two rounds with the Tet-On plasmid and the wild type or R608K tetracycline-responsive plasmid as detailed in Materials and Methods. **A.** Six clones, two carrying the wild type AR and four AR-R608K were assessed for AR protein and doxycycline responsiveness. One clone, R608K clone 4 expressed copious amounts of AR even in the absence of doxycycline. Wt AR clone 1 and R608K clone 3 expressed equal amounts of AR protein and were responsive to doxycycline. **B.** These two clones were further examined for AR transactivation activity in transient transfections. They were transfected with AR-responsive reporter constructs and the control renilla reporter and then treated with doxycycline with or without 1 nM R1881. MCF10A stably expressing AR-R608K displayed similar promoter-specific differential expression as seen in transient transfections. ** $p<0.005$ Significance based on Student's t-test.

Chapter 5

A Role for the Androgen Receptor in Mammary Gland Development

Abstract

The androgen receptor (AR) is expressed in nearly 70-90% of all breast cancers including 50% of estrogen receptor negative tumors that have a poor prognosis suggesting that AR might be a viable treatment target. In order to effectively utilize AR in novel breast cancer therapies, however, its complex role in proliferation and its interaction with the estrogen pathway must be clearly understood. In this study, the effect of the loss of AR on breast cancer risk was addressed genetically by comparing testicular feminized (*tfm*) mice (AR null) overexpressing the *neu* proto-oncogene in the mammary gland to *neu* positive females. The hypothesis was that if AR protects against breast cancer, then mice lacking AR should present with earlier or more aggressive disease. Instead, the *tfm* mice were resistant to neu-driven tumorigenesis.

Examination of adult *tfm* mammary glands revealed rudimentary ductal outgrowth, suggesting impaired development. Transplanting the immature ductal bud of three-week-old *tfm* mice into the cleared fat pad of a syngeneic female resulted in partial rescue of ductal outgrowth. However, *tfm* ductal trees grew less (based on ductal area) than ducts transplanted from age-matched female controls and terminal end buds from

tfm transplanted ducts had reduced proliferation as indicated by BrdU staining, suggesting that AR may encourage ductal outgrowth in female ducts. A subset of aged *tfm* mice exhibited outgrowth of the ductal tree. AR protein was present in these ducts suggesting that a reversion of the *tfm* frameshift mutation may have contributed to growth in these mice. These results point to a potential proliferative role for AR in breast epithelia and demonstrate the complexity of androgen/estrogen regulation in development as well as in cancer.

Introduction

The androgen receptor (AR) is expressed in 70-90% of all breast cancers including 50% of estrogen receptor negative tumors and 75% of metastases, highlighting its potential as a therapeutic target (Birrell et al. 1998; Agoff et al. 2003). Furthermore, AR can be manipulated, either activated or repressed, with existing AR agonists and antagonists. However, the role of AR and the androgen axis in the breast and in breast cancer has been controversial. Androgens are thought to oppose estrogen action and since cumulative exposure to estrogen is the most important factor in breast cancer risk (Henderson et al. 2000; Yager et al. 2006), androgen action may be protective against breast cancer. High serum testosterone levels correspond to increased breast cancer risk (Onland-Moret et al. 2003) and predict poor survival in breast cancer patients (Micheli et al. 2007). This is likely a result of testosterone aromatization to estrogen in the breast (Thijssen 2004), since an active androgen axis in tumors appears to be beneficial with expression of androgen-responsive genes such as PSA and Kallikrein 15 being positive prognostic factors (Yu et al. 1995; Yousef et al. 2002).

Genetic variation that affects AR activity could be expected to affect breast cancer risk. However, because the *AR* gene is located on the X chromosome and thus subject to random X inactivation, studies of *AR* genetic variation in women with breast cancer have been uninformative (Cox et al. 2006). Male breast cancer is extremely rare, but since males are hemizygous for *AR*, genetic variation is phenotypically evident. An association between weaker AR variants and male breast cancer has been identified (Maclean et al. 2004). More specifically, two mutations in the DNA binding domain of AR have been identified in men with partial androgen insensitivity and breast cancer linking AR reduced function to this disease (Wooster et al. 1992; Lobaccaro et al. 1993).

Animal models have indicated that androgens, acting through AR, can have either proliferative or antiproliferative effects on mammary epithelial cells. AR is also expressed in adult mammary gland where androgens may limit proliferation by counteracting estrogen action. Treatment with androgens limits estrogen-induced proliferation in normal mammary epithelial cells in female rhesus monkeys in part by down regulating estrogen receptor alpha (ERα) (Zhou et al. 2000; Dimitrakakis et al. 2003). However, androgen action can vary depending on context. In the mouse, AR is expressed in the developing fetal mammary gland where androgen expression in males leads to nipple regression (Kratochwil 1977), while in the adult female gland, a synergistic effect is seen with testosterone and estrogen treatment resulting in mammary gland hyperplasia (Zhang et al. 2004). In female rats, pharmacological doses of testosterone and estrogen promote tumorigenesis, decreasing tumor latency time compared to estrogen alone (Liao et al. 1998; Xie et al. 1999).

Androgens also have divergent effects on breast cancer cell lines in culture, reducing proliferation in some but increasing proliferation in others (Birrell et al. 1995). In ZR-75-1 breast cancer cells, androgen-dependent growth inhibition was attributed to androgens preventing ERα upregulation of the pro-apoptotic protein, Bcl-2, through AR (Lapointe et al. 1999). However, proliferation is increased in AR-positive T47D and MCF-7 cells. Changes in androgen dose and ER status can transform androgens from anti-proliferative and pro-apoptotic to proliferative in breast cancer cell lines (Aspinall et al. 2004). Thus there is a fine balance between repressive and proliferative actions of androgens in the breast that appears to depend on the level of both hormones and their receptors.

To determine whether AR is protective in mammary cancer initiation, we chose to look at a mouse model in which the androgen axis was inactivated through a mutation in *Ar*, the testicular feminized (*tfm*) mouse. The *tfm* mouse has a single base deletion in exon 1 of *Ar* that leads to a frameshift and premature termination (Gaspar et al. 1991). X^{tfm} Y mice are phenotypically sterile "females" with cryptorchid testes and a blind vagina (Lyon et al. 1970; Rosenberg 2001). Because they retain nipples, and thus have the potential to retain aspects of mammary gland development, we thought that these mice could be used to examine the effect of AR on breast cancer.

Tumorigenesis was assessed in X^{tfm} Y mice carrying the *neu* proto-oncogene as a transgene (N#202). ErbB2/Her2/Neu is a potent oncogene when overexpressed in the mammary gland with 50% of female mice developing tumors by 205 days (Guy et al. 1992). If AR is protective in the mammary gland, X^{tfm} Y mice lacking AR should develop earlier or more aggressive tumors. Results of this experiment, instead, indicated

a role for AR in mammary gland development. To distinguish effects of hormonal environment from direct effects of AR, mammary gland transplants between X^{tfm} Y and female littermates were performed. These studies indicate that AR may influence mammary epithelial proliferation during development, adding complexity to AR's involvement in mammary tumorigenesis.

Materials and Methods

Mice

Males carrying the MMTV/unactivated *neu* transgene (N#202) (Guy et al. 1992) and $X^{Tabby}X^{tfm}$ heterozygote females were obtained from The Jackson Laboratories (Bar Harbor, ME). C57BL/6 $X^{wild\ type}X^{tfm}$ heterozygous females were obtained from Norman Drinkwater (University of Wisconsin). All mouse procedures were approved by the University of Michigan Committee on Use and Care of Animals, in accord with the NIH guidelines for the Care and Use of Experimental Animals.

Males carrying the MMTV/unactivated *neu* transgene (N#202) (Guy et al. 1992) were crossed to $X^{Tabby}X^{tfm}$ heterozygote females. Female (XX or XX^{tfm}) and X^{tfm}Y *neu*+ progeny were monitored for mammary gland tumors.

Estrogen treatment

X^{tfm}Y Tabby (n=5) or $X^{wt}X^{wt}$ ovariectomized C57/BL 6 (n=7) mice were injected intramuscularly with 0.1 or 1 µg/day estradiol (0.1 ml of 1µg/ml or 10 µg/ml estradiol

dissolved in sesame oil). Mice were sacrificed after 14 days and the fourth inguinal mammary glands collected and prepared as whole mounts.

Bicalutamide treatment

Wild type Balb/c mice received 0.1 ml of 10 mg/ml bicalutamide dissolved in sesame oil (total dosage 50 mg/kg) by intramuscular injection every day for 3 weeks. Mice were sacrificed and the mammary glands were collected as with estrogen treatment above.

Whole mount preparation

After removal, the fourth inguinal mammary glands were pressed between pairs of glass slides and fixed overnight in Carnoy's formula 1 fixative (3 parts ethanol to 1 part glacial acetic acid) or in 10% formalin if being used later for immunohistochemistry. Glands were hydrated in a series of ethanol washes and stained overnight with aqueous carmine alum stain to visualize ducts in whole mounts. Glands were dehydrated in a series of ethanol washes and cleared in methyl salicylate. Whole mounts were submerged in methyl salicylate and photographed on a Leica Stereoscope.

Mammary gland transplants

$X^{wt}X^{tfm}$ heterozygous females were crossed to wild type C57BL/6 males (Jackson Labs) to obtain progeny used in the mammary gland transplant experiments. Mammary gland transplants were performed using a protocol modified from L.Young (Young

2000). At three weeks of age, the fourth inguinal fat pads of an $X^{tfm}Y$ and a female littermate were cleared by removing the ductal anlages between the nipple and the lymph node. The ductal rudiment from the *tfm* was then inserted into a pocket made in the cleared fat pad of the female and vice versa. Four weeks post-operation, animals were injected with BrdU to assess cell proliferation and sacrificed one hour later. Transplanted mammary glands and contralateral control mammary glands were removed, fixed overnight in 10% formalin, and whole mounts were prepared as above. Ductal area of whole mount glands was measured using ImageJ (author Wayne Rasband, the Research Services Branch, National Institute of Mental Health, Bethesda, Maryland).

BrdU detection

Glands were paraffin embedded and sectioned by the Histology Core (University of Michigan Cancer Center). They were then deparaffinized in a series of xylenes and ethanol washes and immunostained for BrdU using the BrdU detection kit (Zymed Laboratories, Inc., South San Francisco, California) as directed. Hematoxylin was used as a counterstain. BrdU positive and negative cells were counted in at least 5 terminal end buds per mammary gland.

Estrogen and testosterone RIA

Blood was collected from $X^{tfm}Y$ as well as female and male controls and centrifuged to separate the serum. Serum was stored at –70˚C until assayed. Estradiol and testosterone levels were measured from serum using the 3rd Generation Estradiol RIA

kit and the Testosterone RIA kit (Diagnostic Systems Laboratories, Inc., Webster, TX) as per instructions.

Real time RT-PCR of *Ar*

Total RNA was isolated from the mammary glands of *tfm* mice (with or without ductal outgrowth) and females using the RNeasy Total RNA Mini Kit (Qiagen, Inc., Valencia, CA). 1 μg RNA was reverse transcribed with the High Capacity cDNA Archive Kit (Applied Biosystems, Foster City, CA). Real time RT-PCR was performed as described in (Albertelli et al. 2008). Briefly, 10 ng cDNA was combined with the SYBR Green PCR master mix (Applied Biosystems) along with 900 nM each of AR primers. Values were normalized to GAPDH and relative expression was calculated by comparison to a standard curve of diluted female mammary gland cDNA.

Statistical analysis

Differences in BrdU counts were assessed by the Wilcoxon rank-sum test. Estradiol level differences and differences in ductal area were assessed by the independent samples Student's t-test.

Results

Lack of tumorigenesis in $X^{tfm}Y$ –*neu* mice

To determine whether AR was protective against mammary tumor development in a mouse model of breast cancer, mice expressing the *neu* proto-oncogene under the control of the MMTV promoter/enhancer were mated to heterozygous $X^{tfm}X^{wt}$ females to obtain $X^{tfm}Y$, $X^{tfm}X^{wt}$, and $X^{wt}X^{wt}$ mice expressing the *neu* proto-oncogene in their mammary glands. Mice were monitored for tumor initiation.

Surprisingly, while 47% of $X^{wt}X^{wt}$ and 56% of $X^{tfm}X^{wt}$ mice developed mammary tumors, only 2% of $X^{tfm}Y$ mice, 1 out of 43, developed a mammary tumor (Figure 5.1A). The reduced number of tumors in the $X^{tfm}Y$ mice suggested that loss of AR might be affecting tumorigenesis completely opposite to what had been thought. Examination of whole mounted fourth inguinal mammary glands from $X^{tfm}Y$ *neu* mice revealed poorly developed mammary glands (Figure 5.1B), which could explain lack of tumorigenesis. While the ductal tree of wild type adult females filled the fat pad, $X^{tfm}Y$ ducts were confined to the area around the nipple. This phenotype is similar to that found in the ERα knockout (ERKO) female (Korach et al. 1996) but more extreme than the AR knockout female, which has ductal outgrowth with reduced branching and reduced size of terminal end buds (Yeh et al. 2003).

The tumors that developed in the $X^{wt}X^{wt}$ and $X^{tfm}X^{wt}$ mice were positive for AR by immunohistochemistry (Figure 5.1C). AR was cytoplasmic in most tumors, but treatment with testosterone resulted in nuclear staining of a subset of cells within the tumor.

Tfm mammary development

The $X^{tfm}Y$ mammary gland phenotype was further examined in $X^{tfm}Y$ mice not expressing the *neu* proto-oncogene. Adult $X^{tfm}Y$ mice have limited ductal outgrowth that does not extend beyond the centrally located mammary lymph node (Figure 5.2A). While mice have a rudimentary ductal bud that extends from the nipple into the fat pad at birth, the majority of mammary gland development occurs at puberty, starting around 4 weeks after birth, when a rise in estrogen levels triggers allometric growth in the ductal bud (Hennighausen et al. 1998). At three weeks of age, before the onset of puberty, the $X^{tfm}Y$ mammary gland is indistinguishable from a wild type gland. To examine $X^{tfm}Y$ development and determine when it fails, mammary glands were collected at 4, 8, and 14 weeks of age from $X^{tfm}Y$ or control $X^{wt}X^{wt}$ littermates. By four weeks of age, wild type females exhibited swollen terminal end buds (TEBs), structures that are a hallmark of allometric growth (Figure 5.2B). They showed extensive branching by 8 weeks, and had mature ductal trees by 14 weeks. In contrast, the $X^{tfm}Y$ ducts showed no growth during this time. The glands lacked TEBs and showed no invasion of the fat pad.

Pubertal development of the mammary gland is triggered by a rise in ovarian hormones including estrogen. To determine whether ductal outgrowth could be rescued by exogenous estradiol, $X^{tfm}Y$ or control ovariectomized C57BL/6 females were treated with daily intramuscular injections of 0.1 or 1 μg estradiol for 14 days and their ductal development was assessed in whole mounts (Figure 5.2C). Administration of estradiol initiated ductal outgrowth in both $X^{tfm}Y$ and ovariectomized controls. However, the $X^{tfm}Y$ ducts appeared more disorganized than the controls with larger TEBs and shorter extension from the nipple (Figure 5.2C).

The role of AR in mammary gland development might be assessed more directly by limiting AR activity in wild type females. To this end, 3-week-old wild type females were treated with the antiandrogen, bicalutamide (0.1 ml of 10 mg/ml bicalutamide dissolved in sesame oil (total dosage 50 mg/kg)), for 4 weeks and mammary glands were harvested to assess ductal outgrowth. Treatment with bicalutamide reduced ductal elongation to varied extents. While the ducts of untreated controls had completely filled the fat pad by 7 weeks of age, the ducts from mice treated with bicalutamide were still extending into the fat pad with visible TEBs and had filled from three-quarters to nearly all of the fat pad (Figure 5.2D). Thus inhibition of AR by antiandrogens appears to retard ductal outgrowth to varying degrees although it does not halt the process.

Mammary gland transplants show reduced growth capacity of *tfm* ducts

Lack of pubertal growth in the $X^{tfm}Y$ could be due to systemic hormone imbalances as suggested by initiation of growth following estradiol treatment. $X^{tfm}Y$ mice have elevated levels of prolactin, LH, and FSH compared to male controls (Amador et al. 1986; Murphy et al. 1991). However, an intrinsic role for AR during mammary gland development could not be discounted. To assess the growth potential of the AR negative $X^{tfm}Y$ duct within a normal hormonal environment, classic mammary gland transplants were performed.

At three weeks of age, the wild type ductal tree has not grown beyond the central mammary lymph node, so removal of the gland between the nipple and lymph node removes the duct thus "clearing" the fat pad. The removed ductal tissue can then be transplanted into the cleared fat pad of a syngeneic mouse. Normal ductal outgrowth will

occur if requisite systemic as well as intrinsic factors are present. Immature ductal buds of $X^{tfm}Y$ mice were implanted into the cleared fat pad of female littermates to assess the growth potential of AR negative *tfm* ducts. Female ducts were also implanted in the cleared fat pad of the $X^{tfm}Y$ to confirm that the *tfm* hormonal environment is not permissive for ductal growth. As controls, female ducts were transplanted into female fat pads. Also, the opposite fourth inguinal mammary gland was left untouched in all mice as a measure of normal ductal outgrowth in that phenotype.

Glands were harvested four weeks after surgery when the ductal network of a normal female C57BL/6 has filled about 3/4 of the mammary fat pad. Representative transplant and contralateral whole mount glands, stained with carmine red, are shown in Figure 3A. Wild type female ducts failed to grow in the *tfm* environment demonstrating the importance of hormonal signals during pubertal development of the mammary gland. The *tfm* duct in the female fat pad demonstrated delayed growth as determined by area filled by the transplanted ductal tree 4 weeks post-transplant (Figure 5.3A). There was no significant difference between the growth of $X^{wt}X^{wt}$ or $X^{tfm}X^{wt}$ female contralateral ducts (t-test, $p<0.57$), or transplanted ducts (t-test, $p<0.22$) based on ductal area, so they were combined in further analyses.

While control female ducts transplanted into a female fat pad filled a median area of 63.5 (+/-5.8 SEM) mm^2, *tfm* ducts in female fat pads filled a median area of 34.9 (+/-6.4 SEM) mm^2 ($p=0.017$, Student's t-test, 2 tailed, equal variance), suggesting that a lack of AR in the ducts delayed or limited their growth. Thus a combination of hormonal imbalance and loss of AR in the mammary gland is responsible for the *tfm* phenotype.

While most of the $X^{tfm}Y$ mice exhibited stalled ductal trees in the contralateral gland, 4 of the 14 $X^{tfm}Y$ mice used as transplant hosts showed evidence of growth in the contralateral gland (Figure 5.3B). The ducts grew beyond the lymph node and 3 of 4 glands had pronounced TEBs indicating allometric growth was occurring. Female ducts implanted in the cleared fat pads of these three $X^{tfm}Y$ mice also had TEBs suggesting that the mammary gland environment of these particular mice was more conducive to ductal elongation. $X^{tfm}Y$ ducts from all four mice with contralateral growth also invaded a greater area of the fat pad when implanted into the cleared female fat pad (Figure 5.3C, open shapes). This observation suggests that there was an alteration affecting growth potential, which occurred in these $X^{tfm}Y$ mice prior to transplantation allowing subsequent ductal growth during puberty.

To assess proliferation occurring in TEBs in transplanted and contralateral glands, BrdU was injected 2 hours prior to harvesting the mammary glands and then detected in paraffin embedded sections by immunohistochemistry (Figure 5.4A). Excluding those $X^{tfm}Y$ transplants that exhibited outgrowth in the contralateral gland, transplanted $X^{tfm}Y$ TEBs showed a significant decrease in proliferation in the terminal end buds based on % BrdU positive cells ($p=0.05$ by 2-tailed Wilcoxon Rank-Sum Test) (Figure 5.4B). This is similar to AR -/- females, which also have reduced TEB proliferation (Yeh et al, 2003).

Stochastic ductal outgrowth in a minority of $X^{tfm}Y$ is associated with AR expression

The rare phenomenon of $X^{tfm}Y$ mice exhibiting mammary gland outgrowth was further examined in a large cohort to determine the incidence in the population. Examination of 111 $X^{tfm}Y$ mammary glands harvested at various ages from 6 weeks to >

three years indicated that outgrowth is stochastic within the population. While outgrowth is found in 5% of mice aged 1 year or less, this percentage increased as mice aged, to 37% of mice over two years old (Figure 5.5A). Of the Her2-*neu* $X^{tfm}Y$ mice aged beyond three years, 57% showed significant outgrowth (n=7).

Two *neu*+ $X^{tfm}Y$ mammary glands are shown in Figure 5.5B. The extent of ductal outgrowth varied, but nearly filled the fat pad in two individuals. $X^{tfm}Y$ estrogen and testosterone levels did not significantly differ between those *neu* $X^{tfm}Y$ mice with and without ductal growth (Table 5.1) although relevant changes may have occurred earlier. In one particular case, swollen TEBs, usually only seen during puberty, were visible suggesting recent growth or persistent TEBs (Figure 5.5B). Surprisingly, this mouse was nearly three years old. Furthermore, in this mouse, growth appeared to originate from a single duct near the lymph node. This suggested that growth might be clonal in nature perhaps stemming from a somatic mutation.

Since the *tfm* mutation is the loss of a single C in a string of Cs, addition of another C, due to polymerase slippage, might occur randomly leading to a reversion. If this reversion occurred early in development it could lead to a functional male despite a tabby coat color, or a later somatic reversion in the mammary gland might trigger AR-driven ductal growth. Ducts present in $X^{tfm}Y$ *neu* mice with outgrowth were positive for AR protein similar to female controls (Figure 5.5C). Because the *tfm* mutation yields C-terminal truncated protein, $X^{tfm}Y$ mice with no ductal growth showed some residual staining with an N-terminal antibody. A C-terminal antibody to AR (C19) stained the epithelia of $X^{tfm}Y$ mammary glands with outgrowth, but did not stain ductal epithelia in the ductal rudiment of an $X^{tfm}Y$ mouse negative for ductal outgrowth (Figure 5.5C). This

suggests that there is expression of a full length AR in some $X^{tfm}Y$ mice, and that this may trigger ductal outgrowth in the *tfm* hormonal environment.

Because the *tfm* frameshift mutation destabilizes the mRNA (Charest et al. 1991), a reversion should stabilize AR mRNA leading to increased mRNA levels in the mammary epithelia. Relative expression levels of AR mRNA from $X^{tfm}Y$ mammary glands with and without ductal outgrowth were assessed by real time RT-PCR (Figure 5.5D). In the absence of microdissection to enrich for epithelial cells, increases in AR mRNA are not evident. Comparable low levels of AR expression were seen in $X^{tfm}Y$ mice, regardless of outgrowth, compared to female expression levels. Because the epithelial cells represent a small proportion of the total cells in the mammary gland, this technique may not be sensitive enough to detect such changes.

Discussion

In this study, we set out to examine the effect of AR on breast cancer initiation and progression in a mouse model of androgen insensitivity. Instead, a surprising role for AR in mammary gland development was revealed. Lack of tumor development in $X^{tfm}Y$ *neu*+ animals led to the discovery of their underdeveloped mammary glands. Although the $X^{tfm}Y$ mouse was discovered in 1970 (Lyon et al. 1970), this is the first detailed report of the $X^{tfm}Y$ mouse mammary gland phenotype. This is likely due to past comparison of the $X^{tfm}Y$ mouse to male mice, which lack mammary glands due to androgen-driven regression of the fetal nipple (Kratochwil 1977). Previously, a few homozygous $X^{tfm}X^{tfm}$ females were created by mating heterozygous females to males chimeric for the *tfm* allele. These *tfm* females showed decreased reproductive fitness,

hinting at a role for AR in female reproductive tissue (Lyon et al. 1980). Female AR knockout (ARKO) mice also have a mammary phenotype with smaller TEBs (Yeh et al. 2003). This phenotype is less severe than that of the *tfm* mice, which show the combined effects of systemic alterations in hormone levels and AR loss in the mammary gland.

The lack of breast tumors in the *neu* $X^{tfm}Y$ mice and the lack of ductal outgrowth in the majority of $X^{tfm}Y$ mice suggest that either the $X^{tfm}Y$ mouse lacks the necessary balance of hormonal signals to initiate mammary gland development (extrinsic factors) or that an active androgen receptor is important for normal growth of the gland (intrinsic factors). Mammary gland transplants revealed that reduced growth in *tfm* mammary glands was dependent on both extrinsic and intrinsic regulatory mechanisms. Female glands fail to grow in the *tfm* fat pad, highlighting the importance of hormonal initiation. However, *tfm* ducts do not grow as well as female ducts even when transplanted into a normal female hormonal environment, due at least in part to reduced proliferation in the TEBs.

Although AR is not required for ductal outgrowth, since the *tfm* ductal anlage can grow in response to exogenous estrogen (Figure 5.2), AR nevertheless influences ductal proliferation. This suggests a new role for AR in addition to its generally accepted role in counteracting estrogen action. AR might stimulate proliferation during ductal outgrowth, but then adopt a new role in the adult where it primarily opposes ER action. This could explain differences in AR function seen in breast cancer cell lines (Birrell et al. 1995). Lines that show activation by AR may have reactivated AR developmental pathways, whereas those cell lines where proliferation is inhibited by androgens may retain the adult regulatory system.

Stochastic ductal outgrowth in a subset of *tfm* mice increasing with age suggests that either altered hormone levels or genetic changes in ductal epithelial or stromal cells occur over time. Serum estrogen and testosterone levels do not differ between *tfm* mice with or without ductal outgrowth, although transient alterations in hormone levels are not ruled out. The fact that female ducts transplanted into *tfm* fat pads show growth only if the contralateral *tfm* gland grows suggests differences in either hormonal milieu or in stromal components between *tfm* mice with outgrowth and those without. Transplanting the whole mammary anlagen does not distinguish between a ductal epithelial or stromal influence of AR on growth. However, there is very little AR expression in mammary stromal cells, and only paracrine effects of epithelial AR activation on stromal proliferation have been reported in rat (Xie et al. 1999).

Further evidence for AR's role in mammary gland development comes from the apparent AR presence in the epithelia of $X^{tfm}Y$ mice with ductal outgrowth. In the absence of AR, ducts do not invade the fat pad. Spontaneous reversion even in a single epithelial cell, which produces full length AR protein, may then trigger proliferation leading to clonal outgrowth of AR-positive ducts. Oddly these ducts are able to grow in a low hormone environment. In the older *neu* positive mice that have little testosterone or estrogen, ligand-independent activation of AR by the *neu*/Akt pathway might further encourage growth (Wen et al. 2000).

To confirm this hypothesis, we have attempted to identify a reversion event in the AR gene. The *tfm* mutation is a spontaneous single base pair deletion resulting in a frameshift and the creation of a premature stop codon within exon 1 (He et al. 1991). Interestingly, the deletion occurs within a string of cytosines where rare polymerase

slippage might add back the missing cytosine in one of two strings of cytosines at the *tfm* mutation site (Figure 5.6). Somatic reversions occurring in single nucleotide strings, though rare, are not unknown. Black spotting in pigs has been attributed to a somatic reversion of a frameshift mutation in a string of cytosines leading to the expression of the full-length melanocortin 1 receptor gene in a subset of melanocites (Kijas et al. 2001). Replication slippage has been implicated in this process and may also be responsible for the *tfm* reversion, although alternative mechanisms including transcriptional frameshifting are also possible (Farabaugh 2000).

Identification of this reversion has been difficult. Amplification with proofreading Platinum *Taq* polymerase of the region around the *tfm* mutation, subcloning, and sequencing of mRNA from one $X^{tfm}Y$ mouse with and one without ductal outgrowth detected 1 wild type sequence in 10 clones from both *tfm* mice (data not shown). PCR amplification may have resulted in slippage at the repeat. Alternatively, $X^{tfm}Y$ mice in general may have low rates of somatic reversion. The reversion may have to occur in a specific cell type such as the ductal epithelia to trigger ductal outgrowth or there may be other specific requirements to for functional reversion. Because AR immunostaining was evident in all ducts of $X^{tfm}Y$ mice with outgrowth and not in those without, the reversion is expected to have occurred early in the ductal tree with clonal expansion of AR positive cells into the rest of the fat pad. Therefore, the reversion should be present at a higher rate in the *tfm* mice with ductal outgrowth.

The apparent contribution of AR to mammary gland proliferation and ductal outgrowth adds a new dimension to ER/AR interactions. Instead of a purely antagonistic relationship, there may be contexts in which both pathways or one or the other elicit

proliferation. Identifying appropriate AR therapies for breast cancer will require stratification of tumors depending on androgen response. For instance, ER negative apocrine breast tumors are often AR and Her2/*neu* positive and apocrine cell lines proliferate in response to androgens making them sensitive to antiandrogen treatment (Doane et al. 2006; Naderi et al. 2008). On the other hand, certain ER positive tumors may benefit from increased activation of AR. Previous treatment for breast cancer was adrenalectomy, which not only depletes the body of estrogen, but also adrenal androgens. New treatment with aromatase inhibitors decreases estrogen while maintaining adrenal androgen levels, which may be beneficial in some cases by increasing the anti-proliferative effect of AR activation (Macedo et al. 2006), but worsen the situation in others.

Acknowledgements

We thank Megan Albertelli for her assistance with the mammary gland transplant surgeries, and Haiyan Pang who examined the time course of *tfm* mammary gland development.

Table 5.1. Serum hormone levels of *tfm* mice with and without ductal branching.

Sample	**Serum estradiol (pg/ml)**		**Serum testosterone (ng/ml)**	
Tfm with branching	7.45 +/- 2.21	n=3	0.42 +/- 0.21	n=3
Tfm without branching	9.37 +/- 1.78	n=5	0.50 +/- 0.19	n=3
Female	12.29 +/- 4.99	n=9	0.14 +/- 0.08	n=3
Male	5.72 +/- 1.02	n=2	2.07 +/- 2.78	n=3

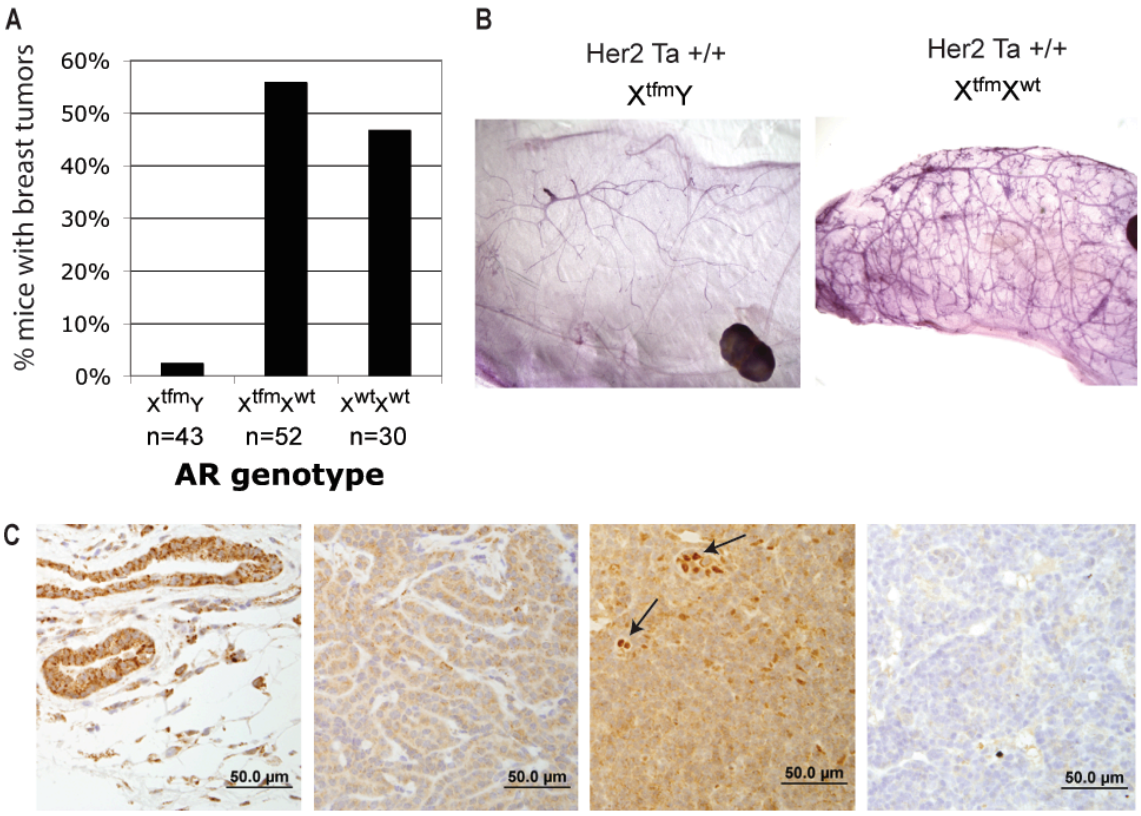

Figure 5.1. AR in breast cancer.

A. Quantification of the percentage of *neu* mice with breast cancer. *neu* expressing $X^{tfm}Y$, $X^{tfm}X^{wt}$ and $X^{wt}X^{wt}$ mice were aged until tumor detection (< 1 year) at which time no $X^{tfm}Y$ mice had developed tumors, while half of the heterozygous and wild type mice had developed cancer. 1 of 43 $X^{tfm}Y$ mice developed a tumor after aging the mice for up to three years. **B.** *neu* $X^{tfm}Y$ mice have poorly developed mammary glands (*left*) compared to an age-matched female (*right*). **C.** AR staining in mammary tumors from neu mice. Normal mammary gland surrounding a tumor (*far left*) and the tumor itself from a *neu* female (*second from left*) showed positive AR staining. Although staining was perinuclear in these tumors, mice injected with testosterone one day prior to tissue collection exhibited nuclear staining (*second from right, arrows*). Competing with PG21 peptide abolished epithelial staining (*far right*).

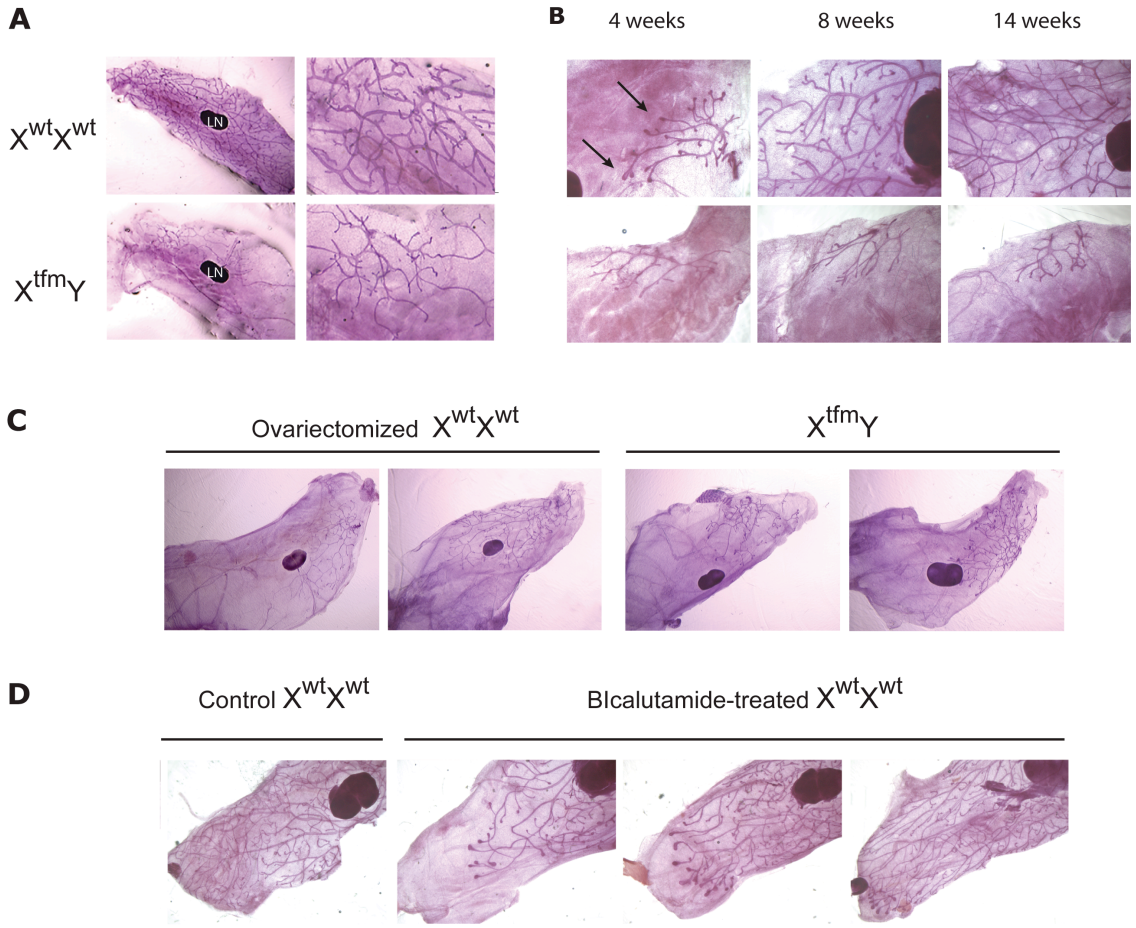

Figure 5.2. $X^{tfm}Y$ mice have poorly developed mammary glands.

A. Whole mounts of adult mammary glands from C57BL/6 +/+ female (*top*) and $X^{tfm}Y$ (*bottom*) mice stained with carmine red to visualize the mammary ducts. The dark oval is the lymph node (LN). Stereoscope images (left, 8X; right, 32X) **B.** $X^{tfm}Y$ mice (*bottom*) failed to develop terminal end buds (TEBs) as seen in wild type mammary glands at 4 weeks of age (*top left*, arrows), nor did they invade the fat pad during pubertal mammary gland development (*bottom*). Wild type glands invaded the fat pad by 8 weeks (*top middle*), and filled it by 14 weeks of age (*top right*). **C.** Treatment with estrogen triggered TEB formation in $X^{tfm}Y$ mammary glands. Representative glands from ovariectomized females (*left*) and $X^{tfm}Y$ mice (*right*) treated with 1 µg/ml/day estradiol in sesame oil administered intramuscularly for 14 days. Ducts from ovariectomized females extended beyond the lymph node while the $X^{tfm}Y$ ducts just reached the lymph node. **D.** Treatment of wild type females with bicalutamide delays ductal extension. Three wild type four-week-old females were treated with 10 mg/ml bicalutamide administered intramuscularly (50 mg/kg/day) for three weeks. A wild type untreated age-matched control gland completely filled the fat pad. Bicalutamide-treated glands had delayed extension and filled the fat pad to varying degrees (*right*).

Figure 5.3. Mammary gland transplants reveal intrinsic and extrinsic effects of AR on mammary gland development.

A. Whole mount mammary glands from transplants stained with carmine red. Cleared mammary gland with transplanted ducts (*left*) and the contralateral, untouched gland of the same mouse (*right*). The area occupied by the ducts has been outlined in white. All pictures were taken at 8X magnification on a Leica MXFL III stereo microscope. **B.** Whole mounts of one transplant pair where the $X^{tfm}Y$ contralateral showed outgrowth. The transplanted glands are shown on the left and the contralateral glands on the right. Growing ducts in the contralateral are indicated with arrows. The ductal area is outlined as in A. **C.** The individual areas of the fat pad occupied by ducts in the contralateral and transplanted glands were outlined and measured using ImageJ software and graphed. Contralateral ductal area is shown on the left and transplants on the right. Black diamonds are median values within each transplant gland type. Open shapes indicate four $X^{tfm}Y$ mice whose contralateral gland grew beyond the lymph node and the transplanted glands from the same transplant pair. **D.** Average ratio of transplanted ductal area to contralateral area for tfm ducts in a female host compared to female ducts in a female host (+ SEM). The ratio takes into account variation in contralateral ductal outgrowth.

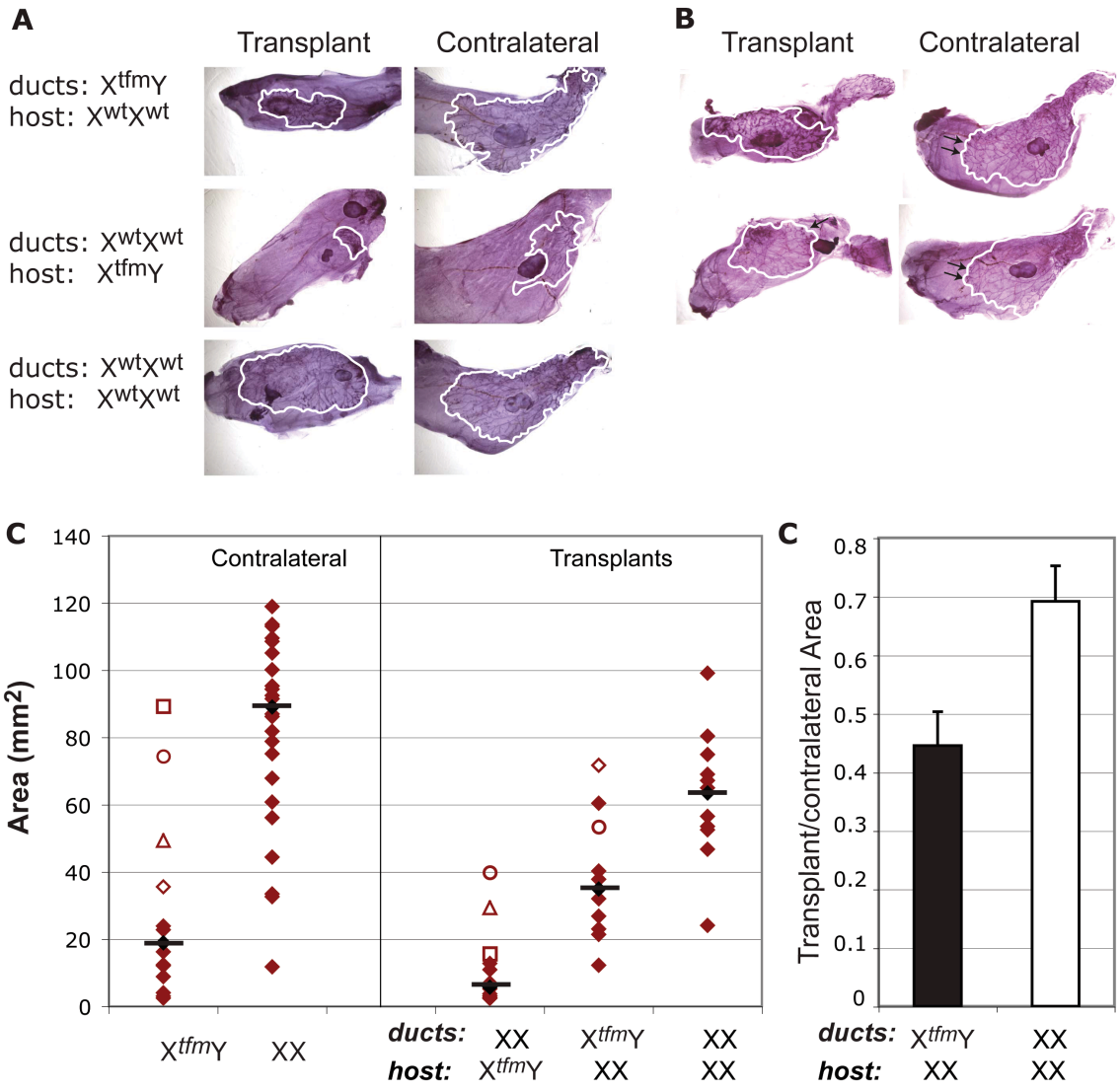

Figure 5.3. Mammary gland transplants reveal intrinsic and extrinsic effects of AR on mammary gland development.

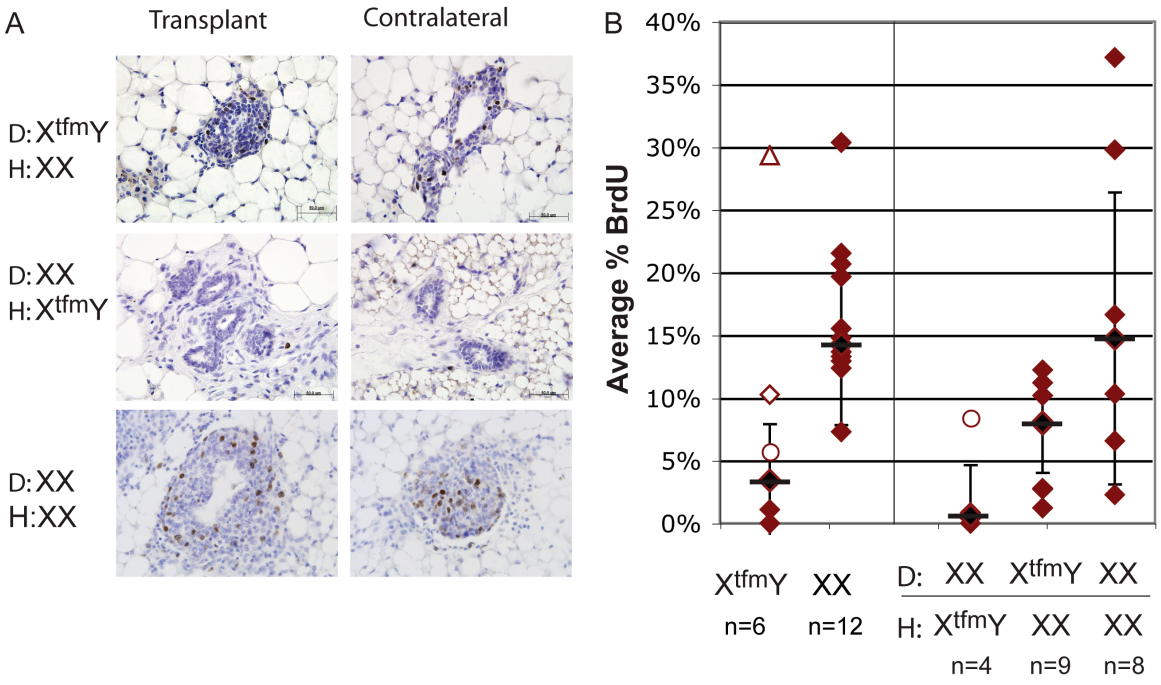

Figure 5.4. X^{tfm}Y TEBs show less proliferation than female TEBs.

A. Representative TEBs showing BrdU positive cells in transplants (*left*) and contralateral glands (*right*). Mice were injected with BrdU one hour before sacrifice to label proliferating cells. BrdU was detected in formalin-fixed, paraffin-embedded sections by immunohistochemistry (See Materials and Methods). **B.** Average percent of BrdU positive cells in TEBs. The percentage of BrdU positive cells in 5 TEBs from contralateral and transplanted glands were counted and averaged. Black diamonds represent median values. Open shapes indicate three X^{tfm}Y mice whose contralateral gland grew beyond the lymph node and the transplanted glands from the same transplant pair when available. Error bars are SEM.

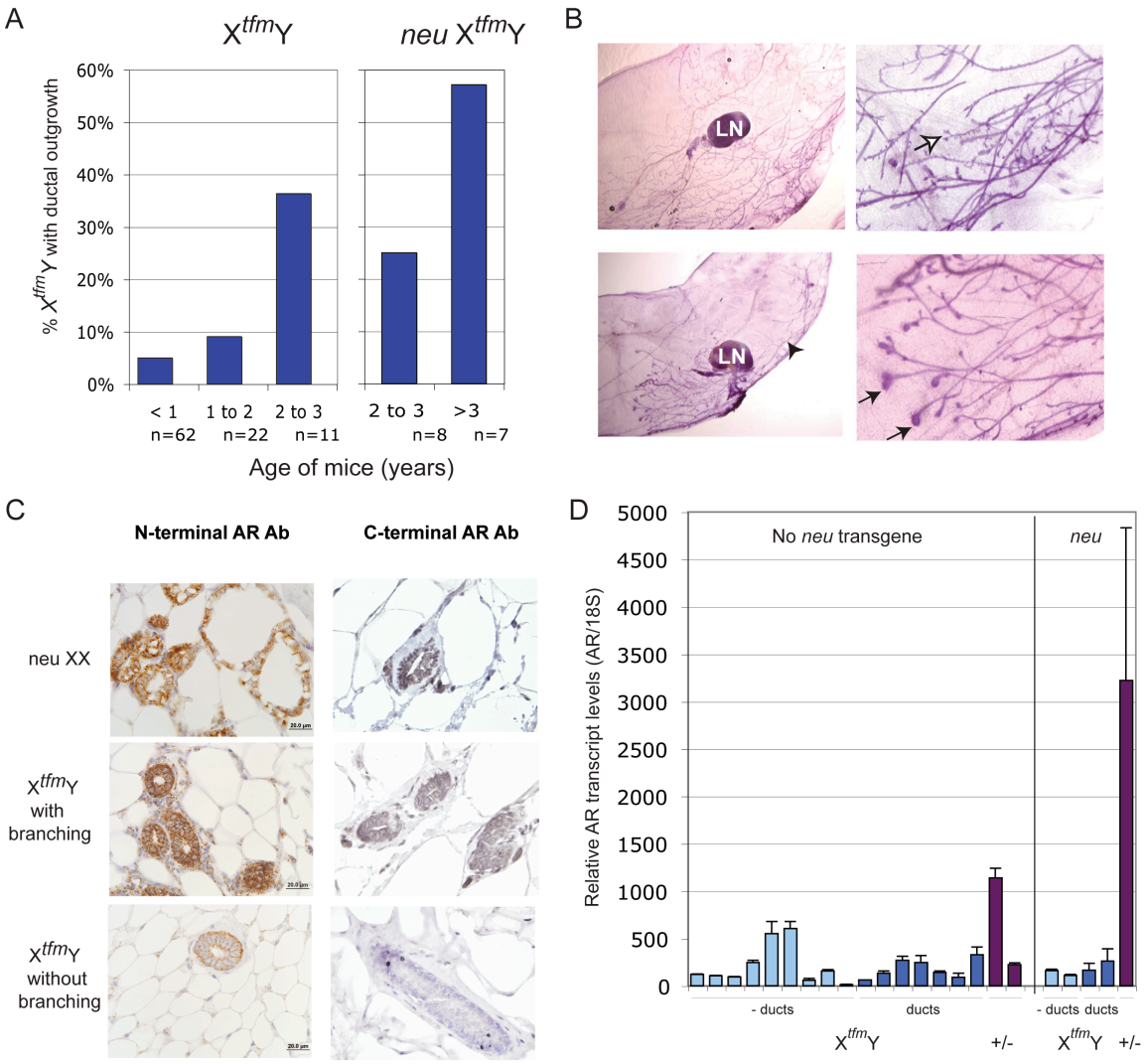

Figure 5.5. Stochastic mammary gland outgrowth in aging *neu* X^{tfm}Y mice.

A. Stochastic outgrowth in aging X^{tfm}Y mice with and without the *neu* transgene parsed by age. **B.** Whole mounts of two 3-year-old *neu* X^{tfm}Y with outgrowth. Low magnification stereoscope image (*left*, 8X) and high magnification (*right*, 32X). Note the abnormal branching (open arrows, *top right*) and prominent TEBs (arrows, *bottom right*). Ductal outgrowth (*bottom left*) appears to be clonal arising from a single duct (arrowhead). **C.** X^{tfm}Y mammary glands that show outgrowth are also positive for AR protein in the ducts using both an N-terminal (N20) and C-terminal (C19) AR antibody. An X^{tfm}Y mouse with no growth exhibits light epithelial staining with the N-terminal but not the C-terminal antibody likely due to the presence of residual truncated protein. **D.** Relative quantitative RT-PCR for AR transcripts in individual *tfm* mice with (dark blue) and without (light blue) ductal outgrowth. Female controls are shown for comparison (purple).

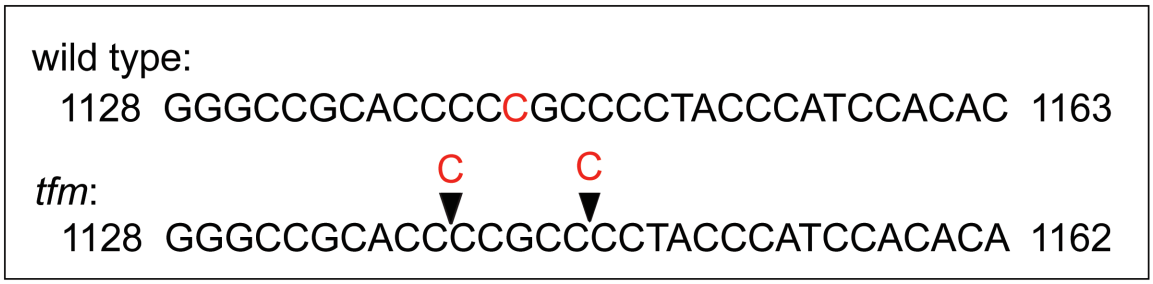

Figure 5.6. Possible reversion events by reinsertion of a single C in the *tfm* sequence.

The wild type sequence (*top*) around the site of the *tfm* mutation with the single cytosine difference in the wild type versus *tfm* sequence shown in red. The *tfm* sequence (*bottom*) with two possible reversion events that could occur (solid arrow heads) by insertion of a cytosine in one of two strings of cytosines near the *tfm* mutation site. Numbering is from the mouse *Ar* sequence (GenBank sequence accession number NM_013476).

Chapter 6

Conclusion

Somatic mutations are a hallmark of cancer and are important in tumor initiation and progression. In hormone-responsive tumors, mutations in the steroid receptor genes, *AR* in the case of prostate cancer and *ER* in the case of breast cancer, have been reported in numerous cases. However, the prevalence of these mutations and their effect on disease progression still remains unclear. In human prostate cancer, estimates of *AR* mutations, based primarily on bulk sequencing, indicate that *AR* mutations occur in between 10-30% of tumors (Linja et al. 2004). However, this does not take into account the genetic heterogeneity present in multifocal prostate tumors. By using a method that can detect rare *AR* mutations, our work reveals that all prostate tumors may harbor subsets of cells carrying mutations in *AR*. These mutant ARs may then be selected during treatment.

We have examined the possible selection of AR mutations during antiandrogen treatment in both a mouse model of prostate cancer and in patient metastases. The benefit of performing both mouse and human studies using the same methodology is that two distinct disease modalities can be juxtaposed for a greater depth of knowledge. Mouse tumors derived from a large, genetically homogeneous population can indicate the frequency of *Ar* mutations in prostate cancer and can provide insight into tumor divergence during disease progression under experimentally controlled conditions.

Although TRAMP tumors recapitulate progression from PIN to prostate cancer seen in human disease, they are artificially induced by the androgen-responsive expression of the T antigen oncogene and therefore cannot accurately represent the human disease, which may be initiated by a variety of mutation events independent of AR. Newer mouse models such as the *Nkx3.1*; *Pten* mouse (Abate-Shen et al. 2003), use loss-of-function mutations in tumor suppressor genes to induce prostate cancer thus allowing the decoupling of tumor initiation and AR activity. These models may offer new insights into the role of AR in tumor progression.

Patient samples give an indication of the importance of *AR* mutations in spontaneously arising, heterogeneous tumors treated in a clinical setting. However, genetic heterogeneity in the patient population can affect tumor initiation, rate of growth, and response to therapy thus complicating analysis. Furthermore, sample sizes are often small and individualized treatment, although beneficial to the patient, makes comparison among patients difficult. This is especially relevant in metastatic prostate cancer where patients are often switched to secondary hormone therapy once the tumor becomes refractory to the first (Small et al. 2006). In restricting analysis to patients treated with only a single antiandrogen, our numbers were limited, but we were able to compare two antiandrogen treatments.

With so many differences in disease initiation, progression and treatment between the mouse model and patient samples, the fact that similar results were derived from both data sets is striking. Both mouse and human tumors exhibited similar mutation spectra, a breakdown of the types of base pair changes. These spectra differed from the random mutations found in testis samples (Figure 6.1). Mutation spectra of a cancer type can

often indicate the mechanism of mutation. For instance, mutations in melanomas are almost entirely C to T transitions due to UV DNA damage, while breast cancers have a high percentage of C:G to G:C transversions due to an unknown mechanism (Greenman et al. 2007). Samples from mouse and human prostate cancer showed a high percentage of T:A to C:G and C:G to A:T mutations that may indicate a common mechanism.

Both studies revealed many *AR* mutations present at a low frequency in the tumor population, even in intact or hormone-naïve tumors. These mutations cannot be explained by sequencing error, since sequencing normal mouse testis yielded a much lower *Ar* mutation rate. This suggests that prostate cancer has a mutator phenotype that increases random mutation rates in tumors creating a heterogeneous tumor cell population (Bielas et al. 2006). Antiandrogen treatment can then select for AR mutations that provide a growth advantage leading to an increase in cells containing AR mutations (Figure 6.2). This was most obvious in patient metastases where more mutations were identified in more than one clone from an individual sample.

In both studies, treatment with anti-androgens increased the number of recurring mutations within a tumor sample. This would agree with selection of existing AR mutations by treatment (Figure 6.2). In this scenario, cells carrying mutations would be present at the same low rate in intact or hormone-naïve disease. Treatment would then select for growth of a subpopulation of cells carrying advantageous mutations. This would then be seen as a higher number of clones carrying the same mutation within a sample. Dominance of a single mutation was not seen in the mouse study and only occurred in one patient with metastatic disease indicating that the repopulation of a tumor by clonal expansion of cells carrying a single AR mutation is rare. However, the

presence of many mutations in both mice and patients suggests that there are numerous *AR* mutations that can help prostate cancer cells evade treatment.

AR mutants use diverse mechanisms to alter AR function

By first identifying AR mutations from androgen-independent disease, and then functionally analyzing the mutant receptors, we can use the selective pressures applied during disease progression to pinpoint important AR residues involved in resistance and identify the mechanism of action of the mutant ARs. This analysis has shown that mutant ARs utilize multiple mechanisms to evade therapy, making it very difficult to develop effective secondary treatments for resistant prostate cancer. Promoter-selective activation as seen with R753Q may favor activation of general response elements leading to increased proliferation. While this mutation is a loss of function during development, it may be a gain of function in a prostate cancer context. Similar differential transactivation was observed in the two mutant ARs from male breast cancer patients suggesting that loss of function on AR-specific AREs in combination with normal to high activation on canonical HREs may favor activation of a subset of AR targets promoting tumor growth in both prostate cancer and breast cancer.

Selection of promiscuous receptors such as V716M allows receptor activation under low androgen conditions and can even convert antiandrogens into agonists. While promiscuous receptors, including V716M, have been identified previously, we were able to examine V716M's prevalence in three separate metastases from the same patient. The presence of promiscuous receptors in androgen-independent prostate cancer is one of the strongest arguments for selection of AR mutants in cancer progression. V716M was

present in all clones sequenced from a single patient compared to other mutants that were present in one or two clones. This indicates that V716M likely contributed to treatment resistance and facilitated metastatic spread.

Treatment-specific altered splicing creating AR23 was seen in 5 of 8 antiandrogen-treated patients. Disregulation of splicing, either through altered activity of splicing factors or mutations that either destroy splice sites or create cryptic splice sites, has been identified in many cancers (Venables 2006). Some of these alternatively spliced products encode loss of function variants of tumor suppressors, or act as dominant negative antagonists of the wild type protein as in the case of alternatively spliced ERß (Sato et al. 2005). There are other instances where alternative splicing creates oncogenic splice forms such as a constitutively active Rac1 that facilitates tumor invasion. By itself, the AR23 appears to be loss of function, yet AR23 enhances transactivation of the wild type AR in co-transfections, perhaps by acting as a decoy receptor. Interestingly, another AR splice variant that lacks the second zinc finger of the DBD and is likely defective in DNA binding as well has been identified in breast tumors (Zhu et al. 1997). It was thought that this variant lacking exon 3 might act to limit AR-dependent growth inhibition. Based on the functional studies with AR23 (Chapter 3) and with the AR DBD mutants from male breast cancer (Chapter 4), it is intriguing to think that the AR splice variant expressed in breast cancer might also retain similar functions.

Finally, increased stability and androgen-independent nuclear localization as seen in AR-E255K may also lead to treatment resistance. Increased expression of AR correlated with androgen independent growth in a xenograft model (Chen et al. 2004) and expression of a hyperactive AR in LNCaP cells facilitated androgen-independent growth

(Hsieh et al. 2008). Similarly, the more stable AR-E255K may allow ligand independent activation, particularly when combined with activated growth factor pathways. Future research should examine transactivation in the presence of an activated AKT or RAF, which are known to phosphorylate AR.

AR targets in proliferation and differentiation

AR has diverse effects on target cells, encouraging proliferation in prostate stroma, while causing differentiation in prostate epithelia. Because of its opposing effects, it has been suggested that complete androgen depletion and inactivation of the AR may not be the best treatment for prostate cancer (Prehn 1999). A better outcome for prostate cancer patients is associated with PSA expression (Sterbis et al. 2008), while loss of AR in the prostate epithelia increases proliferation and reduces differentiation (Wu et al. 2007).

Mutants identified in mouse and human tumors demonstrated differential promoter response, which might promote proliferation by favoring subsets of target genes. Interestingly, AR-R753Q is unable to activate the male developmental pathway, since it leads to complete androgen insensitivity as a germline mutation. However, it is active in PC-3 cells, suggesting that developmental genes might have a promoter signature that is more sensitive to AR-R753Q. Since target promoters are composed of a unique combination of androgen response elements and other transcription factor binding sites, a subset of targets may be more sensitive to loss of function at selective response elements. Work in the SPARKI mouse, which expresses an AR that is unable to bind selective elements but can bind canonical elements, has begun to distinguish targets in

male reproductive development whose promoters are influenced by AR-selective elements versus targets that can be activated without activation of selective AREs. Differential gene expression studies in the SPARKI mouse identified the reproductive homeobox X-linked gene 5 (*Rhox5* or *Pem*) whose promoter contains a selective ARE (Barbulescu et al. 2001; Denolet et al. 2006), is expressed solely in male reproductive tissues, and is sensitive to mild AR mutations associated with male infertility (Zuccarello et al. 2008).

The identification of partial loss of function mutations in both prostate and breast cancer that exhibit reduced function on selective elements while maintaining activity on general elements suggests that this aberrant expression may encourage aspects of tumorigenesis. In the future, it would be interesting to examine these particular mutants in cancer models. If these partial loss of function mutations contribute to tumorigenesis, they would be expected to show earlier initiation or more rapid tumor growth. The SPARKI mouse might be useful for these studies since they are fully functional males, unlike the *tfm* rat that carries the R753Q mutation.

Gene fusions in prostate cancer and their potential affect on selective pressures

The apparent difference in effects of AR mutants from mouse versus human prostate cancer suggests unique factors involved in the human disease. One major difference may be the presence of AR-responsive *TMPRSS2-ETS* family fusion genes in human prostate cancer (Tomlins et al. 2005). *TMPRSS2-ETS* fusion products have been identified in both low and high-grade PIN (Clark et al. 2008) as well as prostate cancer (Tomlins et al. 2005), implicating these fusions in early disease progression. The *ERG*

gene is the most common ETS family fusion partner of TMPRSS2 in prostate cancer. ERG appears to upregulate *C-MYC* and together these proteins repress differentiation in prostate epithelia (Sun et al. 2008). ERG also upregulates the plasminogen activation pathway that encourages invasion (Tomlins et al. 2008). Upregulation of these fusion proteins may be favored early in cancer progression from normal growth to PIN, while other AR targets that increase metastatic spread may be favored late in disease.

The recent discovery of androgen-responsive *TMPRSS2-ETS* family fusion proteins in human prostate cancer further emphasizes the importance of AR in prostate cancer progression. The *TMPRSS2* fusion genes may alter selective pressures during prostate cancer progression since AR mutants that upregulate the *TMPRSS2* promoter may be selected. A single androgen response element was identified in the TMPRSS2 promoter (Lin et al. 1999), which has characteristics of an androgen-selective response element (Claessens et al. 2001). Similar to other AR-selective AREs, it has a T in the fourth position of the 5' repeat, which modeling has suggested could hinder GR binding (Verrijdt et al. 2003). Mutation of this 4th T to an A in two AR-selective response elements, *slp*-HRE2 and *sc*-ARE1.2, destroys the selectivity of the element allowing transactivation by GR (Verrijdt et al. 2003). Interestingly, the TMPRSS2 putative ARE has the same 5' half site as the selective Slp HRE2.

Therapy that may favor differentiation in *TMPRSS2-ETS* fusion-negative prostate cancer may do the opposite in fusion-positive tumors. *TMPRSS2-ERG* fusions are thought to increase proliferation through C-MYC, while at the same time downregulating the AR-dependent differentiation markers such as PSA and prostein and inhibiting differentiation (Sun et al. 2008). In the future, mutants identified in patient metastases

should be tested on the *TMPRSS2* promoter to see if they might be hyperactive. In patients, this may lead to selection of mutant receptors that upregulate transactivation on selective response elements, but not in the mouse model, which is not known to carry TMPRSS2 fusions.

Future strategies for prostate cancer treatment

The heterogeneous nature of prostate tumor cells has important implications for prostate cancer therapy. Antiandrogen therapy with flutamide or bicalutamide is initially successful when combined with luteinizing hormone-releasing hormone agonists (LHRHa) to control androgen production and AR activity. Bicalutamide is considered a superior antiandrogen to flutamide because it has fewer side effects. Also bicalutamide does not have the partial agonist activity of flutamide, so it was hoped that tumors would not be able to evade bicalutamide treatment. However, tumors do become refractory to bicalutamide, and mutations in the AR LBD that allow activation with bicalutamide have been identified in some cases of antiandrogen-resistant tumors (Haapala et al. 2001). Currently, much effort is being directed towards synthesizing new antiandrogens that may be more effective. However, the heterogeneous nature of prostate tumors and the ability of the AR LBD to accommodate even bulky ligands such as bicalutamide after single amino acid substitutions, suggests that tumor cells will likely find ways to evade these new antiandrogens as well.

Since *AR* mutations that create promiscuous receptors are often treatment-specific, it has been suggested that switching to a secondary antiandrogen after therapy resistance might be effective (Urushibara et al. 2007). Based on the *AR* heterogeneity

seen in our studies, it might be predicted that, while switching therapies may slow down progression, tumor cells will eventually evade this secondary therapy as well. The presence of many *AR* mutations, even in metastatic prostate cancer that likely derives from clonal populations, suggests that prostate tumor cells continue to accumulate novel mutations throughout disease progression. Therefore, treatment might be more effective if it were to target, not AR itself, but the interacting proteins that enable AR activity.

The mutants identified in our studies point to pathways that might be targeted. For instance, the mutant AR-E255K, exhibits increased stability and nuclear localization in the absence of ligand. Therefore, targeting interacting proteins that effect AR stability and nuclear translocation may impact tumor progression (Figure 6.3). The chaperone, Hsp90, which is important for AR folding and stability, can be targeted with antibiotics such as geldanamycin, which prevents dissociation of AR from Hsp90 thus limiting AR nuclear translocation and increasing AR degradation by the proteasome (Segnitz et al. 1997; Saporita et al. 2007). Hsp90 inhibitors are now being tested in clinical trials. AR phosphorylation can affect nuclear translocation and ligand-independent activation. Thus treatment could target the kinases responsible for AR phosphorylation such as AKT, MAPK, and Src kinase. Effective small molecule inhibitors for these pathways exist and might be used in combination with current therapy (Kung et al. 2009).

Alternatively, the dual nature of AR action could be harnessed to control tumor growth through selective activation of downstream AR targets (Figure 6.3). Completely suppressing AR activity may not be the best therapy since this limits both differentiation and proliferation signals. New therapies might try to manipulate AR activity to favor its differentiation action over proliferation. The first step is to identify AR targets that may

influence differentiation over proliferation. Surprisingly few AR targets are known to date, although recent expression analysis has made marked progress in this area (Dehm et al. 2006). Use of the mutants identified in this study that exhibit differential promoter activation might shed light on AR targets that are more relevant to disease and are either selectively activated during prostate cancer tumorigenesis, or regulatory genes that are specifically repressed in cancer. Analysis of the promoters of these targets can determine whether these targets have a promoter signature that might allow selective activation of one set over the other. Can different coactivators influence transactivation of AR targets involved in differentiation versus proliferation? Does binding to selective versus canonical AREs selectively affect one set of target genes? Do androgen levels affect target gene activation since low testosterone doses lead to more aggressive disease than normal testosterone doses in the *Nkx3.1;Pten* mouse model (Banach-Petrosky et al. 2007)?

Comparison of AR's role in prostate and breast cancer

The prostate and mammary gland have similar developmental requirements including hormone-dependent ductal proliferation and invasion of ductal epithelia into the surrounding tissue and important stromal-epithelial cross talk. These tissues share similar downstream pathways during development including inhibin/ activin expression, and a requirement for Stat5a (Hennighausen et al. 1998; Nevalainen et al. 2000; Jeruss et al. 2003) suggesting overlap between AR and ER targets in these tissues. The role of ER in prostate has begun to be addressed in mouse models and has demonstrated synergistic activity with AR (Cunha et al. 2001). In breast cancer, the classic model suggests that AR

counteracts ER-mediated proliferation. In Chapter 5, examination of mammary gland development in AR null *tfm* mice suggests a proliferative role for AR during pubertal ductal development. This raises the possibility that AR action may have a dual role in the mammary gland similar to its role in prostate (Figure 6.4). While expression of AR in the majority of breast cancers makes AR a tempting target for therapy, especially in those cases that are ER negative, it is important to first understand ARs actions in the breast.

In this thesis, identification of *AR* mutations in both mouse and human prostate cancer has provided potential mechanisms for treatment evasion. Functional analysis of these AR mutants and others identified in male breast cancer has demonstrated that mutations, which lead to deficiencies in male development when occurring in the germline, may promote proliferation in both prostate and breast cancer through activation of a subset of AR targets. Exploring the context-dependent opposing functions of AR using these mutant ARs, may identify targets for therapy in hormone-responsive cancer.

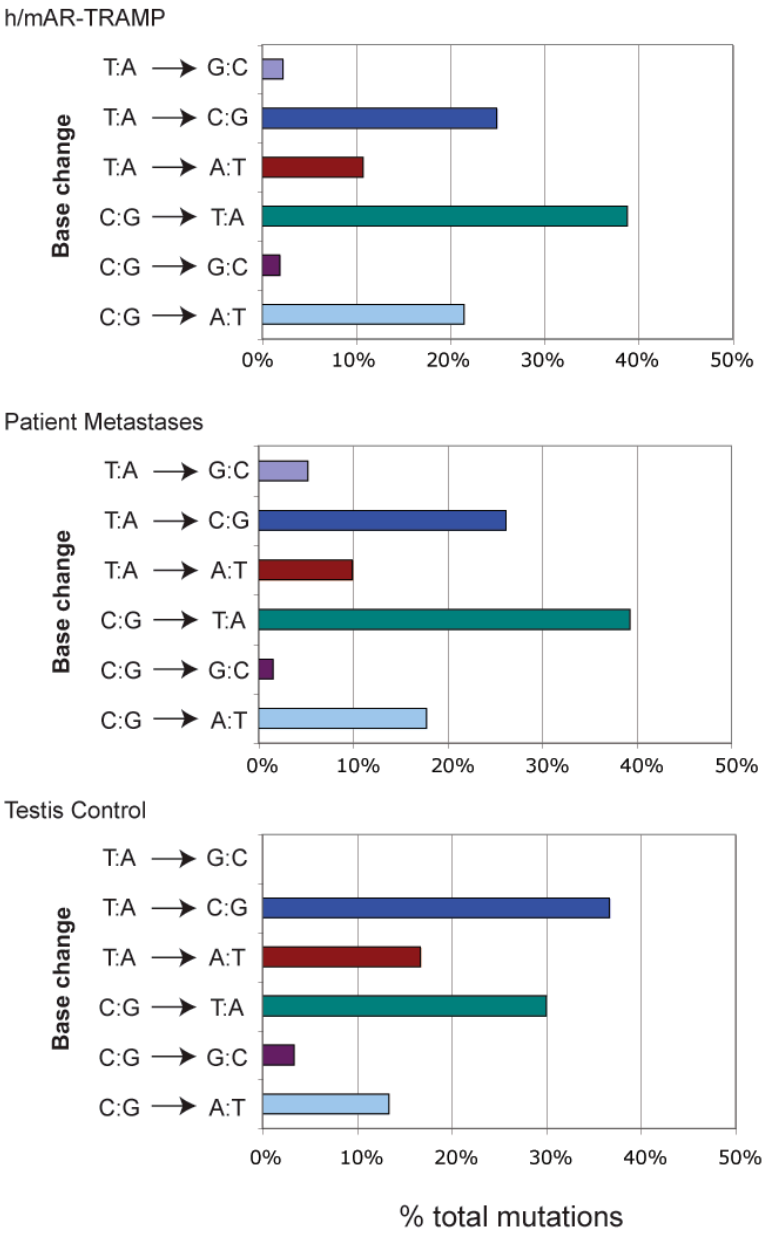

Figure 6.1. Mutation spectra of *AR* mutations identified in prostate tumors.

% of all single nucleotide mutations causing a specific base change in h/mAR mouse tumors (*top*), patient metastases (*middle*), and mouse testis controls (*bottom*). Note that the spectra of the h/mAR mouse tumors and patient metastases are very similar with many C:G to A:T and C:G to T:A base changes. . Mutations occurring in the testis control show a different mutation spectra favoring T:A to G:C transversions.

Figure 6.2. Inferred selection of *AR* mutations in prostate cancer based on our data.

A. Mutation and selection in the h/mAR TRAMP mouse model. All tumors accumulate *Ar* mutations due to an overall increased mutation rate. In hormone-dependent tumors from intact mice, these mutations may be selected against, while in tumors from antiandrogen-treated or castrated mice cells with *Ar* mutations have a growth advantage. This results in a higher frequency of *Ar* mutations in treated versus intact tumors. Cells containing *Ar* mutations are shown in different colors representing unique mutations. White cells carry wild type *Ar*. Boxed tumors indicate the tumor types that were sequenced in this study. **B.** Mutation and selection in human metastatic prostate cancer. As in the mouse model, primary tumors may accumulate *AR* mutations, but cells containing wild type *AR* should have a growth advantage in hormone-naïve (untreated) metastases. Dashed arrows indicate possible metastasis of tumor cells carrying wild type *AR,* based on the presence of wild type *AR* transcripts in hormone-naïve and antiandrogen-treated metastases. When metastatic disease is then treated with antiandrogens, selection of existing *AR* mutations that allow growth under these new conditions may occur. Occasionally an *AR* mutation, such as V716M, will dominate the metastases such that all tumor cells will carry the mutation (*top branch*). Some metastases may not carry mutations that allow survival and may regress (*middle branch*). Otherwise, there may be multiple *AR* mutations that allow proliferation during treatment (*bottom branch*). The tumor will therefore consist of a heterogeneous population of cells either containing *AR* mutations or that have a wild type *AR* but may have acquired mutations in other genes that provide a growth advantage. Cells containing *AR* mutations are colored as in A. Boxes indicate tumor types that were sequenced in this study.

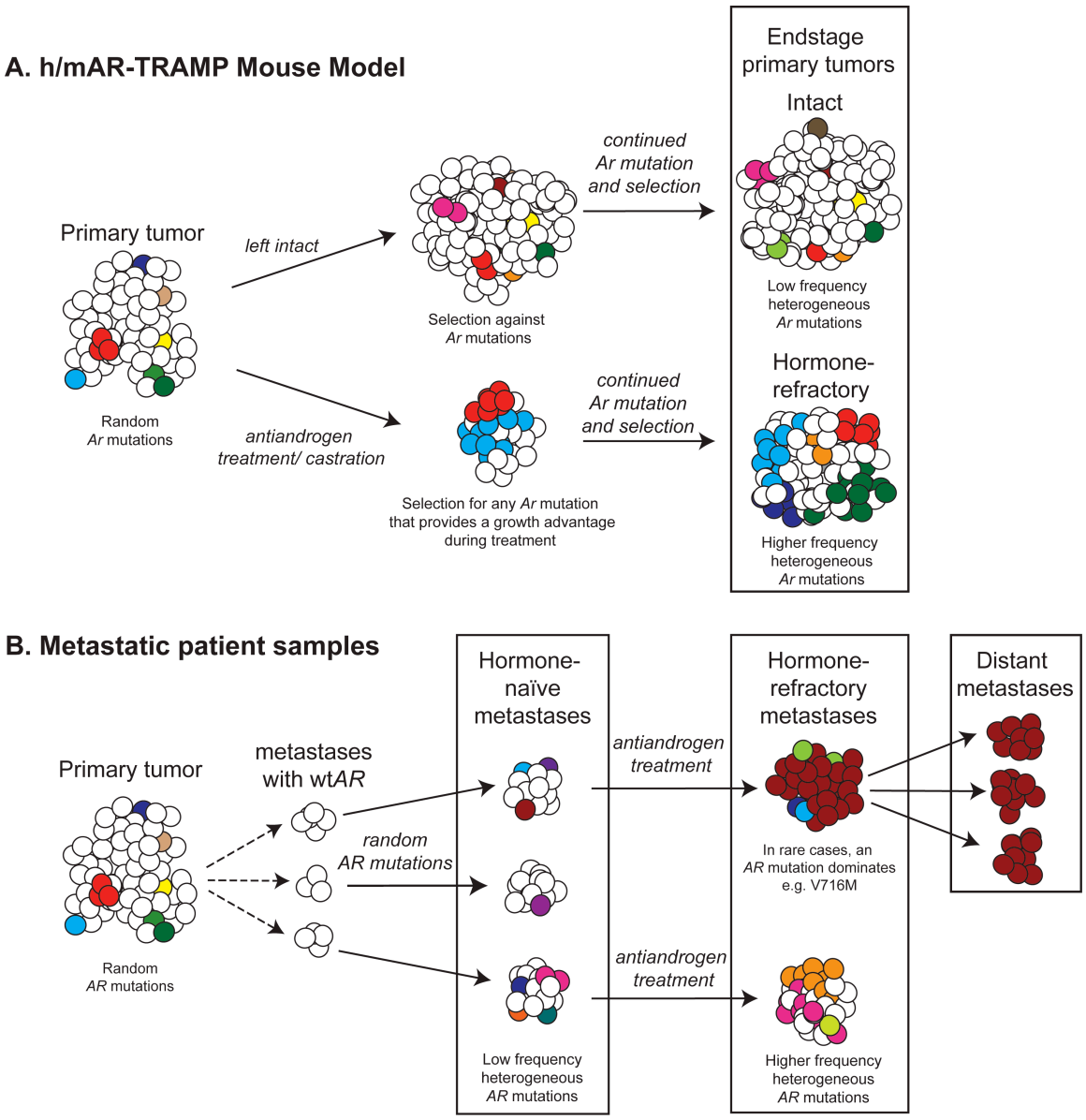

Figure 6.2. Inferred selection of *AR* mutations in prostate cancer based on our data.

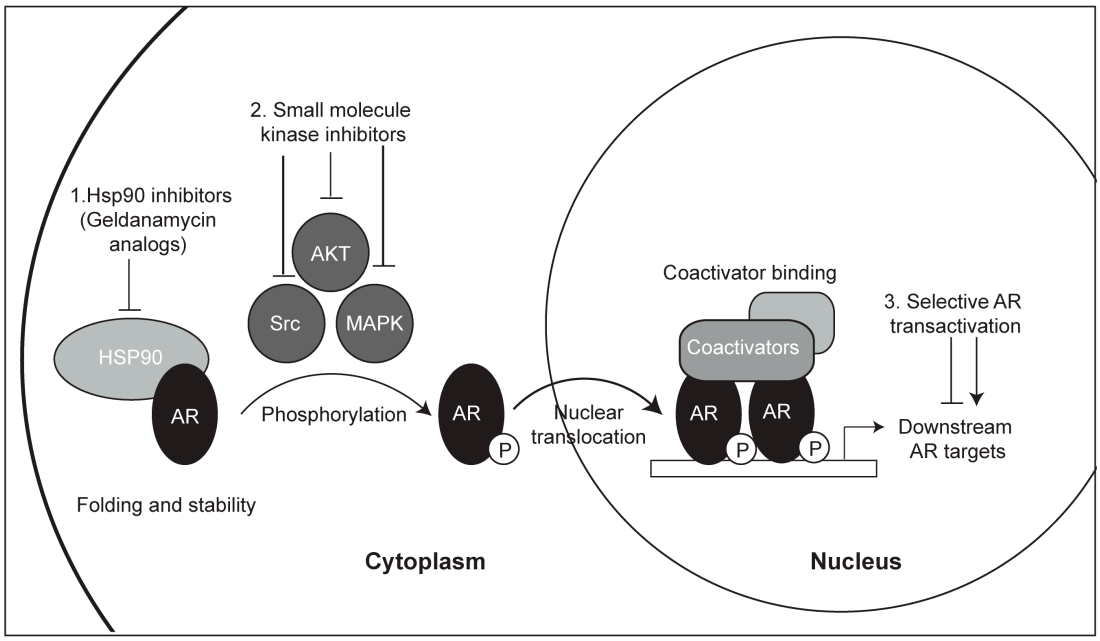

Figure 6.3. Targeting the AR pathway in prostate cancer

The variety of *AR* mutations identified in prostate cancer indicates that future therapy might be more effective by targeting AR interacting proteins. Therapies might target Hsp90, a chaperone that binds AR in the cytoplasm and is involved in AR protein folding and stability. Hsp90 inhibitors (1) are being tested currently in clinical trials. Substances such as geldanamycin can bind to Hsp90 and prevent the release and nuclear translocation of AR. Phosphorylation by a variety of kinases can trigger ligand-independent activation of AR. Small molecule kinase inhibitors (2) could be used to reduce AR ligand-independent activity. Finally, identification of AR targets involved in cancer progression might allow selective activation of a subset of target genes that favor differentiation over proliferation.

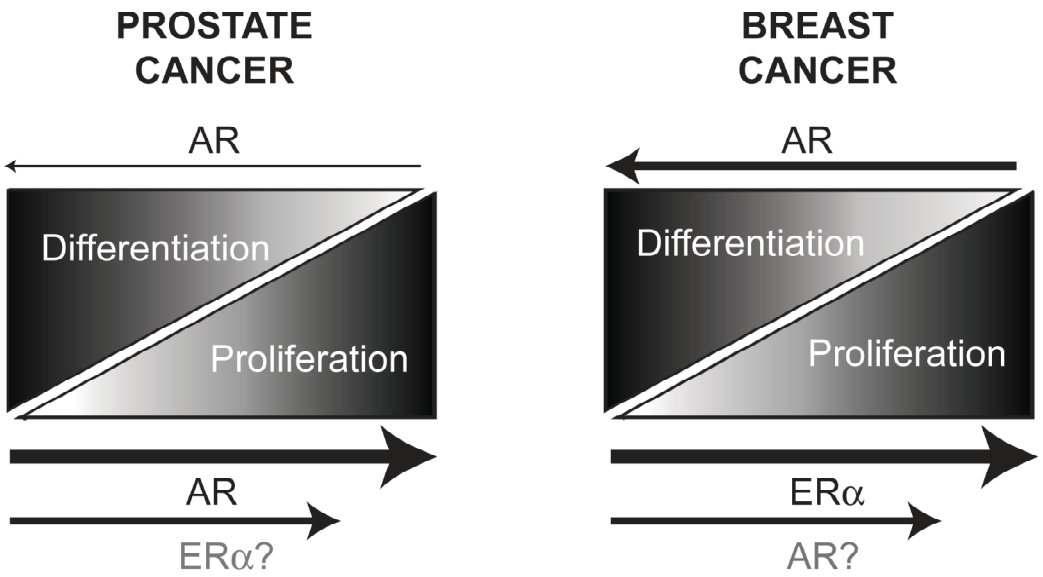

Figure 6.4. A model of AR and ERα activity in prostate and breast cancer.

AR can activate target genes involved in both differentiation and proliferation. In prostate cancer, AR's role in proliferation is favored (*left*). In breast cancer, ERα is the main driver of proliferation (*right*). Classically AR and ERα are thought to oppose each other's actions. However, recent studies in both prostate and breast suggest that these two receptor pathways may work synergistically in hormone-responsive cancers.

References

Aarnisalo, P., Santti, H., et al. (1999). Transcription activating and repressing functions of the androgen receptor are differentially influenced by mutations in the deoxyribonucleic acid-binding domain. Endocrinology **140**(7): 3097-105.

Abate-Shen, C., Banach-Petrosky, W. A., et al. (2003). Nkx3.1; pten mutant mice develop invasive prostate adenocarcinoma and lymph node metastases. Cancer Res **63**(14): 3886-90.

Agoff, S. N., Swanson, P. E., et al. (2003). Androgen receptor expression in estrogen receptor-negative breast cancer. Immunohistochemical, clinical, and prognostic associations. Am J Clin Pathol **120**(5): 725-31.

Agoulnik, I. U., Vaid, A., et al. (2005). Role of src-1 in the promotion of prostate cancer cell growth and tumor progression. Cancer Res **65**(17): 7959-7967.

Albertelli, M. A., O'Mahony, O. A., et al. (2008). Glutamine tract length of human androgen receptors affects hormone-dependent and -independent prostate cancer in mice. Hum Mol Genet **17**(1): 98-110.

Albertelli, M. A., Scheller, A., et al. (2006). Replacing the mouse androgen receptor with human alleles demonstrates glutamine tract length-dependent effects on physiology and tumorigenesis in mice. Mol Endocrinol **20**(6): 1248-60.

Alvarado, C., Beitel, L. K., et al. (2005). Somatic mosaicism and cancer: A micro-genetic examination into the role of the androgen receptor gene in prostate cancer. Cancer Res **65**(18): 8514-8.

Amador, A., Parkening, T., et al. (1986). Testicular lh receptors and circulating hormone levels in three mouse models for inherited diseases (tfm/y, lit/lit and hyt/hyt). Endocrinol Exp. **20**(4): 349-358.

Arezi, B. and Hogrefe, H. H. (2007). Escherichia coli DNA polymerase iii epsilon subunit increases moloney murine leukemia virus reverse transcriptase fidelity and accuracy of rt-pcr procedures. Anal Biochem **360**(1): 84-91.

Arnold, K., Bordoli, L., et al. (2006). The swiss-model workspace: A web-based environment for protein structure homology modeling. Bioinformatics **22**(2): 195-201.

Aspinall, S. R., Stamp, S., et al. (2004). The proliferative effects of 5-androstene-3[beta],17[beta]-diol and 5[alpha]-dihydrotestosterone on cell cycle analysis and cell proliferation in mcf7, t47d and mdamb231 breast cancer cell lines. J Steroid Biochem Mol Biol **88**(1): 37-51.

Balk, S. P. (2002). Androgen receptor as a target in androgen-independent prostate cancer. Urology **60**(3 Suppl 1): 132-8; discussion 138-9.

Banach-Petrosky, W., Jessen, W. J., et al. (2007). Prolonged exposure to reduced levels of androgen accelerates prostate cancer progression in nkx3.1; pten mutant mice. Cancer Res **67**(19): 9089-96.

Barbulescu, K., Geserick, C., et al. (2001). New androgen response elements in the murine pem promoter mediate selective transactivation. Mol Endocrinol **15**(10): 1803-16.

Batch, J. A., Williams, D. M., et al. (1992). Androgen receptor gene mutations identified by sscp in fourteen subjects with androgen insensitivity syndrome. Hum Mol Genet **1**(7): 497-503.

Bentel, J. M. and Tilley, W. D. (1996). Androgen receptors in prostate cancer. J Endocrinol **151**(1): 1-11.

Bevan, C. L., Brown, B. B., et al. (1996). Functional analysis of six androgen receptor mutations identified in patients with partial androgen insensitivity syndrome. Hum Mol Genet **5**(2): 265-73.

Bielas, J. H., Loeb, K. R., et al. (2006). Human cancers express a mutator phenotype. Proc Natl Acad Sci **103**(48): 18238-18242.

Birrell, S. N., Bentel, J. M., et al. (1995). Androgens induce divergent proliferative responses in human breast cancer cell lines. J Steroid Biochem Mol Biol **52**(5): 459-67.

Birrell, S. N., Hall, R. E., et al. (1998). Role of the androgen receptor in human breast cancer. J Mammary Gland Biol Neoplasia **3**(1): 95-103.

Bohl, C. E., Miller, D. D., et al. (2005). Structural basis for accommodation of nonsteroidal ligands in the androgen receptor. J. Biol. Chem. **280**(45): 37747-37754.

Bonagura, T. W., Deng, M., et al. (2007). A naturally occurring mutation in the human androgen receptor of a subject with complete androgen insensitivity confers binding and transactivation by estradiol. Mol Cell Endocrinol **263**(1-2): 79-89.

Brockschmidt, F. F., Nothen, M. M., et al. (2007). The two most common alleles of the coding ggn repeat in the androgen receptor gene cause differences in protein function. J Mol Endocrinol **39**(1): 1-8.

Bruggenwirth, H. T., Boehmer, A. L., et al. (1997). Molecular analysis of the androgen-receptor gene in a family with receptor-positive partial androgen insensitivity: An unusual type of intronic mutation. Am J Hum Genet **61**(5): 1067-77.

Buchanan, G., Birrell, S. N., et al. (2005). Decreased androgen receptor levels and receptor function in breast cancer contribute to the failure of response to medroxyprogesterone acetate. Cancer Res **65**(18): 8487-96.

Buchanan, G., Greenberg, N. M., et al. (2001). Collocation of androgen receptor gene mutations in prostate cancer. Clin Cancer Res **7**(5): 1273-1281.

Buchanan, G., Irvine, R. A., et al. (2001). Contribution of the androgen receptor to prostate cancer predisposition and progression. Cancer Metastasis Rev **20**(3-4): 207-23.

Buchanan, G., Ricciardelli, C., et al. (2007). Control of androgen receptor signaling in prostate cancer by the cochaperone small glutamine rich tetratricopeptide repeat containing protein α. Cancer Res **67**(20): 10087-10096.

Buchanan, G., Yang, M., et al. (2004). Structural and functional consequences of glutamine tract variation in the androgen receptor. Hum Mol Genet **13**(16): 1677-92.

Callewaert, L., Verrijdt, G., et al. (2004). Differential effect of small ubiquitin-like modifier (sumo)-ylation of the androgen receptor in the control of cooperativity on selective versus canonical response elements. Mol Endocrinol **18**(6): 1438-49.

Ceraline, J., Cruchant, M. D., et al. (2004). Constitutive activation of the androgen receptor by a point mutation in the hinge region: A new mechanism for androgen-independent growth in prostate cancer. Int J Cancer **108**(1): 152-7.

Chamberlain, N. L., Driver, E. D., et al. (1994). The length and location of cag trinucleotide repeats in the androgen receptor n-terminal domain affect transactivation function. Nucleic Acids Res **22**(15): 3181-6.

Chandra, S., Shao, J., et al. (2008). A common motif targets huntingtin and the androgen receptor to the proteasome. J Biol Chem.

Chang, C. Y. and McDonnell, D. P. (2002). Evaluation of ligand-dependent changes in ar structure using peptide probes. Mol Endocrinol **16**(4): 647-60.

Charest, N. J., Zhou, Z. X., et al. (1991). A frameshift mutation destabilizes androgen receptor messenger rna in the tfm mouse. Mol Endocrinol **5**(4): 573-81.

Chen, C. D., Welsbie, D. S., et al. (2004). Molecular determinants of resistance to antiandrogen therapy. Nat Med **10**(1): 33-9.

Chen, G., Wang, X., et al. (2005). Androgen receptor mutants detected in recurrent prostate cancer exhibit diverse functional characteristics. Prostate **63**(4): 395-406.

Claessens, F., Verrijdt, G., et al. (2001). Selective DNA binding by the androgen receptor as a mechanism for hormone-specific gene regulation. J Steroid Biochem Mol Biol **76**(1-5): 23-30.

Clark, J., Attard, G., et al. (2008). Complex patterns of ets gene alteration arise during cancer development in the human prostate. Oncogene **27**(14): 1993-2003.

Cox, D., Blanche, H., et al. (2006). A comprehensive analysis of the androgen receptor gene and risk of breast cancer: Results from the national cancer institute breast and prostate cancer cohort consortium (bpc3). Breast Cancer Research **8**(5): R54.

Culig, Z., Hobisch, A., et al. (1993). Mutant androgen receptor detected in an advanced-stage prostatic carcinoma is activated by adrenal androgens and progesterone. Mol Endocrinol **7**(12): 1541-1550.

Culig, Z., Hobisch, A., et al. (1994). Androgen receptor activation in prostatic tumor cell lines by insulin-like growth factor-i, keratinocyte growth factor, and epidermal growth factor. Cancer Res **54**(20): 5474-8.

Culig, Z., Hobisch, A., et al. (1998). Expression, structure, and function of androgen receptor in advanced prostatic carcinoma. Prostate **35**(1): 63-70.

Culig, Z., Hoffmann, J., et al. (1999). Switch from antagonist to agonist of the androgen receptor bicalutamide is associated with prostate tumour progression in a new model system. Br J Cancer. **81**(2): 242-251.

Culig, Z., Stober, J., et al. (1996). Activation of two mutant androgen receptors from human prostatic carcinoma by adrenal androgens and metabolic derivatives of testosterone. Cancer Detect Prev **20**(1): 68-75.

Cunha, G. R., Wang, Y. Z., et al. (2001). Estrogenic effects on prostatic differentiation and carcinogenesis. Reprod Fertil Dev **13**(4): 285-96.

Darne, C. H., Morel, L., et al. (1997). Ubiquitous transcription factors nf1 and sp1 are involved in the androgen activation of the mouse vas deferens protein promoter. Mol Cell Endocrinol **132**(1-2): 13-23.

Dehm, S. M., Regan, K. M., et al. (2007). Selective role of an nh2-terminal wxxlf motif for aberrant androgen receptor activation in androgen depletion independent prostate cancer cells. Cancer Res **67**(20): 10067-77.

Dehm, S. M. and Tindall, D. J. (2006). Ligand-independent androgen receptor activity is activation function-2-independent and resistant to antiandrogens in androgen refractory prostate cancer cells. J Biol Chem **281**(38): 27882-93.

Dehm, S. M. and Tindall, D. J. (2006). Molecular regulation of androgen action in prostate cancer. J Cell Biochem **99**(2): 333-44.

Denolet, E., Gendt, K. D., et al. (2006). Transfection with steroid-responsive reporter constructs shows glucocorticoid rather than androgen responsiveness in cultured sertoli cells. J Steroid Biochem Mol Biol **98**(2-3): 164-73.

Dickson, R. B., Bates, S. E., et al. (1986). Characterization of estrogen responsive transforming activity in human breast cancer cell lines. Cancer Res **46**(4 Pt 1): 1707-13.

Dimitrakakis, C., Zhou, J., et al. (2003). A physiologic role for testosterone in limiting estrogenic stimulation of the breast. Menopause **10**(4): 292-298.

Doane, A. S., Danso, M., et al. (2006). An estrogen receptor-negative breast cancer subset characterized by a hormonally regulated transcriptional program and response to androgen. **25**(28): 3994-4008.

Ellem, S. J. and Risbridger, G. P. (2007). Treating prostate cancer: A rationale for targeting local oestrogens. Nat Rev Cancer **7**(8): 621-7.

Estebanez-Perpina, E., Moore, J. M. R., et al. (2005). The molecular mechanisms of coactivator utilization in ligand-dependent transactivation by the androgen receptor. J. Biol. Chem. **280**(9): 8060-8068.

Evans, B. A., Harper, M. E., et al. (1996). Low incidence of androgen receptor gene mutations in human prostatic tumors using single strand conformation polymorphism analysis. Prostate **28**(3): 162-71.

Evans, R. M. (1988). The steroid and thyroid hormone receptor superfamily. Science **240**(4854): 889-95.

Fabre, S., Manin, M., et al. (1994). Identification of a functional androgen response element in the promoter of the gene for the androgen-regulated aldose reductase-like protein specific to the mouse vas deferens. Journal of Biological Chemistry **269**(8): 5857-5864.

Fang, Y., Fliss, A. E., et al. (1996). Hsp90 regulates androgen receptor hormone binding affinity in vivo. J Biol Chem **271**(45): 28697-702.

Farabaugh, P. J. (2000). Translational frameshifting: Implications for the mechanism of translational frame maintenance. Prog Nucleic Acid Res Mol Biol **64**: 131-70.

Faus, H. and Haendler, B. (2007). Androgen receptor acetylation sites differentially regulate gene control. J Cell Biochem.

Feldman, B. J. and Feldman, D. (2001). The development of androgen-independent prostate cancer. Nat Rev Cancer **1**(1): 34-45.

Feldman, S. R. (1992). Androgen insensitivity syndrome (testicular feminization): A model for understanding steroid hormone receptors. J Am Acad Dermatol **27**(4): 615-9.

Fenton, M., Shuster, T., et al. (1997). Functional characterization of mutant androgen receptors from androgen-independent prostate cancer. Clin Cancer Res **3**(8): 1383-1388.

Freedman, L. P. (1992). Anatomy of the steroid receptor zinc finger region. Endocr Rev **13**(2): 129-45.

Fu, M., Rao, M., et al. (2003). Acetylation of androgen receptor enhances coactivator binding and promotes prostate cancer cell growth. Mol Cell Biol **23**(23): 8563-75.

Funderburk, S. F., Shatkina, L., et al. (2008). Specific n-terminal mutations in the human androgen receptor induce cytotoxicity. Neurobiol Aging.

Fuqua, S. A., Chamness, G. C., et al. (1993). Estrogen receptor mutations in breast cancer. J Cell Biochem **51**(2): 135-9.

Gaddipati, J. P., McLeod, D. G., et al. (1994). Frequent detection of codon 877 mutation in the androgen receptor gene in advanced prostate cancers. Cancer Res **54**(11): 2861-4.

Gao, H., Ouyang, X., et al. (2006). Combinatorial activities of akt and b-raf/erk signaling in a mouse model of androgen-independent prostate cancer. Proc Natl Acad Sci **103**(39): 14477-82.

Gao, T., Marcelli, M., et al. (1996). Transcriptional activation and transient expression of the human androgen receptor. J Steroid Biochem Mol Biol **59**(1): 9-20.

Gaspar, M. L., Meo, T., et al. (1991). A single base deletion in the tfm androgen receptor gene creates a short-lived messenger rna that directs internal translation initiation. Proc Natl Acad Sci U S A **88**(19): 8606-10.

Gaspar, M. L., Meo, T., et al. (1990). Structure and size distribution of the androgen receptor mrna in wild-type and tfm/y mutant mice. Mol Endocrinol **4**(10): 1600-10.

Gelmann, E. P. (2002). Molecular biology of the androgen receptor. J Clin Oncol **20**(13): 3001-15.

Gingrich, J. R., Barrios, R. J., et al. (1996). Metastatic prostate cancer in a transgenic mouse. Cancer Res **56**(18): 4096-102.

Gioeli, D., Ficarro, S. B., et al. (2002). Androgen receptor phosphorylation. Regulation and identification of the phosphorylation sites. J. Biol. Chem. **277**(32): 29304-29314.

Giordano, S. H., Cohen, D. S., et al. (2004). Breast carcinoma in men: A population-based study. Cancer **101**(1): 51-7.

Gonzalez, M. I. and Robins, D. M. (2001). Oct-1 preferentially interacts with androgen receptor in a DNA-dependent manner that facilitates recruitment of src-1. J Biol Chem **276**(9): 6420-8.

Gottlieb, B., Beitel, L. K., et al. (2004). The androgen receptor gene mutations database (ardb): 2004 update. Hum Mutat **23**(6): 527-33.

Greenberg, N. M., DeMayo, F., et al. (1995). Prostate cancer in a transgenic mouse. Proc Natl Acad Sci U S A **92**(8): 3439-43.

Greenman, C., Stephens, P., et al. (2007). Patterns of somatic mutation in human cancer genomes. Nature **446**(7132): 153-8.

Gregory, C. W., He, B., et al. (2001). A mechanism for androgen receptor-mediated prostate cancer recurrence after androgen deprivation therapy. Cancer Res **61**(11): 4315-9.

Guy, C., Webster, M., et al. (1992). Expression of the neu protooncogene in the mammary epithelium of transgenic mice induces metastatic disease. Proc Natl Acad Sci **89**(22): 10578-10582.

Haapala, K., Hyytinen, E. R., et al. (2001). Androgen receptor alterations in prostate cancer relapsed during a combined androgen blockade by orchiectomy and bicalutamide. Lab Invest **81**(12): 1647-51.

Haapala, K., Kuukasjarvi, T., et al. (2007). Androgen receptor amplification is associated with increased cell proliferation in prostate cancer. Hum Pathol **38**(3): 474-8.

Haelens, A., Tanner, T., et al. (2007). The hinge region regulates DNA binding, nuclear translocation, and transactivation of the androgen receptor. Cancer Res **67**(9): 4514-23.

Han, G., Buchanan, G., et al. (2005). Mutation of the androgen receptor causes oncogenic transformation of the prostate. Proc Natl Acad Sci U S A **102**(4): 1151-6.

Han, G., Foster, B. A., et al. (2001). Hormone status selects for spontaneous somatic androgen receptor variants that demonstrate specific ligand and cofactor dependent activities in autochthonous prostate cancer. J Biol Chem **276**(14): 11204-13.

Hara, T., Kouno, J., et al. (2005). Possible role of adaptive mutation in resistance to antiandrogen in prostate cancer cells. Prostate **65**(3): 268-75.

Hara, T., Miyazaki, J., et al. (2003). Novel mutations of androgen receptor: A possible mechanism of bicalutamide withdrawal syndrome. Cancer Res **63**(1): 149-53.

Hara, T., Nakamura, K., et al. (2003). Enhanced androgen receptor signaling correlates with the androgen-refractory growth in a newly established mda pca 2b-hr human prostate cancer cell subline. Cancer Res **63**(17): 5622-8.

He, B., Bai, S., et al. (2004). An androgen receptor nh2-terminal conserved motif interacts with the cooh terminus of the hsp70-interacting protein (chip). J Biol Chem **279**(29): 30643-53.

He, B., Gampe, R. T., Jr., et al. (2006). Probing the functional link between androgen receptor coactivator and ligand-binding sites in prostate cancer and androgen insensitivity. J Biol Chem **281**(10): 6648-63.

He, B., Gampe, R. T., Jr., et al. (2004). Structural basis for androgen receptor interdomain and coactivator interactions suggests a transition in nuclear receptor activation function dominance. Mol Cell **16**(3): 425-38.

He, B., Kemppainen, J. A., et al. (2000). Fxxlf and wxxlf sequences mediate the nh2-terminal interaction with the ligand binding domain of the androgen receptor. J Biol Chem **275**(30): 22986-94.

He, B., Lee, L. W., et al. (2002). Dependence of selective gene activation on the androgen receptor nh2- and cooh-terminal interaction. J Biol Chem **277**(28): 25631-9.

He, W., Kumar, M., et al. (1991). A frame-shift mutation in the androgen receptor gene causes complete androgen insensitivity in the testicular-feminized mouse. Nucleic Acids Res. **19**: 2373-2378.

Henderson, B. E. and Feigelson, H. S. (2000). Hormonal carcinogenesis. Carcinogenesis **21**(3): 427-33.

Hennighausen, L. and Robinson, G. W. (1998). Think globally, act locally: The making of a mouse mammary gland. Genes Dev **12**(4): 449-55.

Hofer, M. D., Kuefer, R., et al. (2006). Prognostic factors in lymph node-positive prostate cancer. Urology **67**(5): 1016-21.

Holst, F., Stahl, P. R., et al. (2007). Estrogen receptor alpha (esr1) gene amplification is frequent in breast cancer. Nat Genet **39**(5): 655-60.

Hsieh, C. L., Cai, C., et al. (2008). Expression of a hyperactive androgen receptor leads to androgen-independent growth of prostate cancer cells. J Mol Endocrinol **41**(1): 13-23.

Huggins, C. and Hodges, C. (1941). The effect of castration, of estrogen and of androgen injection on serum phosphatases in metastatic carcinoma of the prostate. Cancer Res **1**: 293-297.

Hultborn, R., Hanson, C., et al. (1997). Prevalence of klinefelter's syndrome in male breast cancer patients. Anticancer Res **17**(6D): 4293-7.

Hur, E., Pfaff, S. J., et al. (2004). Recognition and accommodation at the androgen receptor coactivator binding interface. PLoS Biol **2**(9): E274.

Hyytinen, E. R., Haapala, K., et al. (2002). Pattern of somatic androgen receptor gene mutations in patients with hormone-refractory prostate cancer. Lab Invest **82**(11): 1591-8.

Ingle, J. N., Twito, D. I., et al. (1991). Combination hormonal therapy with tamoxifen plus fluoxymesterone versus tamoxifen alone in postmenopausal women with metastatic breast cancer. An updated analysis. Cancer **67**(4): 886-91.

Irvine, R. A., Ma, H., et al. (2000). Inhibition of p160-mediated coactivation with increasing androgen receptor polyglutamine length. Hum Mol Genet **9**(2): 267-74.

Isaacs, J. T., Isaacs, W. B., et al. (1992). Comparative aspects of multistep prostatic carcinogenesis in humans and rodents. Prog. Clin. Biol. Res. **376**: 261-288.

Jagla, M., Feve, M., et al. (2007). A splicing variant of the androgen receptor detected in a metastatic prostate cancer exhibits exclusively cytoplasmic actions. Endocrinology **148**(9): 4334-4343.

James, A. J., Agoulnik, I. U., et al. (2002). A novel androgen receptor mutant, a748t, exhibits hormone concentration-dependent defects in nuclear accumulation and activity despite normal hormone-binding affinity. Mol Endocrinol **16**(12): 2692-705.

Jaworski, T. (2006). Degradation and beyond: Control of androgen receptor activity by the proteasome system. Cell Mol Biol Lett **11**(1): 109-31.

Jemal, A., Siegel, R., et al. (2008). Cancer statistics, 2008. CA Cancer J Clin **58**(2): 71-96.

Jenster, G., van der Korput, H. A., et al. (1995). Identification of two transcription activation units in the n-terminal domain of the human androgen receptor. J Biol Chem **270**(13): 7341-6.

Jeruss, J. S., Santiago, J. Y., et al. (2003). Localization of activin and inhibin subunits, receptors and smads in the mouse mammary gland. Mol Cell Endocrinol **203**(1-2): 185-96.

Johnson, M. A., Iversen, P., et al. (2005). Castration triggers growth of previously static androgen-independent lesions in the transgenic adenocarcinoma of the mouse prostate (tramp) model. Prostate **62**(4): 322-38.

Katsumata, N., Horikawa, R., et al. (2008). Novel missense mutation in the p-box of androgen receptor in a patient with androgen insensitivity syndrome. Endocr J **55**(1): 225-8.

Kesler, C. T., Gioeli, D., et al. (2007). Subcellular localization modulates activation function 1 domain phosphorylation in the androgen receptor. Mol Endocrinol **21**(9): 2071-84.

Kijas, J. M., Moller, M., et al. (2001). A frameshift mutation in mc1r and a high frequency of somatic reversions cause black spotting in pigs. Genetics **158**(2): 779-85.

Korach, K., Couse, J., et al. (1996). Estrogen receptor gene disruption: Molecular characterization and experimental and clinical phenotypes. Recent Prog Horm Res(51): 159-86.

Kratochwil, K. (1977). Development and loss of androgen responsiveness in the embryonic rudiment of the mouse mammary gland. Dev Biol **61**(2): 358-65.

Kratochwil, K. and Schwartz, P. (1976). Tissue interaction in androgen response of embryonic mammary rudiment of mouse: Identification of target tissue for testosterone. Proc Natl Acad Sci U S A. **73**(11): 4041-4044.

Kraus, S., Gioeli, D., et al. (2006). Receptor for activated c kinase 1 (rack1) and src regulate the tyrosine phosphorylation and function of the androgen receptor. Cancer Res **66**(22): 11047-54.

Krishnan, A. V., Zhao, X. Y., et al. (2002). A glucocorticoid-responsive mutant androgen receptor exhibits unique ligand specificity: Therapeutic implications for androgen-independent prostate cancer. Endocrinology **143**(5): 1889-900.

Krongrad, A., Wilson, C. M., et al. (1991). Androgen increases androgen receptor protein while decreasing receptor mrna in lncap cells. Mol Cell Endocrinol **76**(1-3): 79-88.

Kumar-Sinha, C., Tomlins, S. A., et al. (2008). Recurrent gene fusions in prostate cancer. Nat Rev Cancer **8**(7): 497-511.

Kung, H. J. and Evans, C. P. (2009). Oncogenic activation of androgen receptor. Urol Oncol **27**(1): 48-52.

La Spada, A. R., Wilson, E. M., et al. (1991). Androgen receptor gene mutations in x-linked spinal and bulbar muscular atrophy. Nature **352**(6330): 77-9.

Labrie, F. (2006). Dehydroepiandrosterone, androgens and the mammary gland. Gynecol Endocrinol **22**(3): 118-30.

Labrie, F., Dupont, A., et al. (1983). New approach in the treatment of prostate cancer: Complete instead of partial withdrawal of androgens. Prostate **4**(6): 579-94.

Labrie, F., Luu-The, V., et al. (2003). Endocrine and intracrine sources of androgens in women: Inhibition of breast cancer and other roles of androgens and their precursor dehydroepiandrosterone. Endocr Rev **24**(2): 152-82.

Lamb, D. J., Puxeddu, E., et al. (2003). Molecular analysis of the androgen receptor in ten prostate cancer specimens obtained before and after androgen ablation. J Androl **24**(2): 215-25.

Langley, E., Kemppainen, J. A., et al. (1998). Intermolecular nh2-/carboxyl-terminal interactions in androgen receptor dimerization revealed by mutations that cause androgen insensitivity. J Biol Chem **273**(1): 92-101.

Lapointe, J., Fournier, A., et al. (1999). Androgens down-regulate bcl-2 protooncogene expression in zr-75-1 human breast cancer cells. Endocrinology **140**(1): 416-21.

Lapouge, G., Erdmann, E., et al. (2007). Unexpected paracrine action of prostate cancer cells harboring a new class of androgen receptor mutation--a new paradigm for cooperation among prostate tumor cells. Int J Cancer **121**(6): 1238-44.

Li, H., Xu, L. L., et al. (2008). A feedback loop between the androgen receptor and a nedd4 binding protein, pmepa1 in prostate cancer cells. J Biol Chem.

Liao, D., Pantazis, C., et al. (1998). Promotion of estrogen-induced mammary gland carcinogenesis by androgen in the male noble rat: Probable mediation by steroid receptors. Carcinogenesis **19**(12): 2173-2180.

Liden, J., Delaunay, F., et al. (1997). A new function for the c-terminal zinc finger of the glucocorticoid receptor. Repression of rela transactivation. J Biol Chem **272**(34): 21467-72.

Lin, B., Ferguson, C., et al. (1999). Prostate-localized and androgen-regulated expression of the membrane-bound serine protease tmprss2. Cancer Res **59**(17): 4180-4.

Lin, H. K., Altuwaijri, S., et al. (2002). Proteasome activity is required for androgen receptor transcriptional activity via regulation of androgen receptor nuclear translocation and interaction with coregulators in prostate cancer cells. J Biol Chem **277**(39): 36570-6.

Lin, H. K., Wang, L., et al. (2002). Phosphorylation-dependent ubiquitylation and degradation of androgen receptor by akt require mdm2 e3 ligase. Embo J **21**(15): 4037-48.

Linja, M. J. and Visakorpi, T. (2004). Alterations of androgen receptor in prostate cancer. J Steroid Biochem Mol Biol **92**(4): 255-64.

Lobaccaro, J., Lumbroso, S., et al. (1993). Androgen receptor gene mutation in male breast cancer. Hum Mol Genet. **2**(11): 1799-1802.

Loeb, L. A., Bielas, J. H., et al. (2008). Cancers exhibit a mutator phenotype: Clinical implications. Cancer Res **68**(10): 3551-7; discussion 3557.

Luisi, B. F., Xu, W. X., et al. (1991). Crystallographic analysis of the interaction of the glucocorticoid receptor with DNA. Nature **352**(6335): 497-505.

Lyon, M. F. and Glenister, P. H. (1980). Reduced reproductive performance in androgen-resistant tfm/tfm female mice. Proc R Soc Lond B Biol Sci **208**(1170): 1-12.

Lyon, M. F. and Hawkes, S. G. (1970). X-linked gene for testicular feminization in the mouse. Nature **227**(5264): 1217-9.

Macedo, L. F., Guo, Z., et al. (2006). Role of androgens on mcf-7 breast cancer cell growth and on the inhibitory effect of letrozole. Cancer Res **66**(15): 7775-82.

Maclean, H. E., Brown, R. W., et al. (2004). Increased frequency of long androgen receptor cag repeats in male breast cancers. Breast Cancer Res Treat **88**(3): 239-246.

Marcelli, M., Ittmann, M., et al. (2000). Androgen receptor mutations in prostate cancer. Cancer Res **60**(4): 944-9.

Marcelli, M., Stenoien, D. L., et al. (2006). Quantifying effects of ligands on androgen receptor nuclear translocation, intranuclear dynamics, and solubility. J Cell Biochem **98**(4): 770-88.

Martz, E. (2002). Protein explorer: Easy yet powerful macromolecular visualization. Trends Biochem Sci **27**(2): 107-9.

Matias, P. M., Donner, P., et al. (2000). Structural evidence for ligand specificity in the binding domain of the human androgen receptor. Implications for pathogenic gene mutations. J Biol Chem **275**(34): 26164-71.

McCall, P., Gemmell, L. K., et al. (2008). Phosphorylation of the androgen receptor is associated with reduced survival in hormone-refractory prostate cancer patients. Br J Cancer **98**(6): 1094-101.

McGuire, W. L., Chamness, G. C., et al. (1992). Abnormal estrogen receptor in clinical breast cancer. J Steroid Biochem Mol Biol **43**(1-3): 243-7.

Micheli, A., Meneghini, E., et al. (2007). Plasma testosterone and prognosis of postmenopausal breast cancer patients. J Clin Oncol **25**(19): 2685-90.

Miller, S. A., Dykes, D. D., et al. (1988). A simple salting out procedure for extracting DNA from human nucleated cells. Nucleic Acids Res **16**(3): 1215.

Monge, A., Jagla, M., et al. (2006). Unfaithfulness and promiscuity of a mutant androgen receptor in a hormone-refractory prostate cancer. Cell Mol Life Sci **63**(4): 487-497.

Moras, D. and Gronemeyer, H. (1998). The nuclear receptor ligand-binding domain: Structure and function. Curr Opin Cell Biol **10**(3): 384-91.

Murphy, L. and O'Shaughnessy, P. (1991). Testicular steroidogenesis in the testicular feminized (tfm) mouse: Loss of 17 alpha-hydroxylase activity. J Endocrinol. **131**(3): 443-449.

Naderi, A. and Hughes-Davies, L. (2008). A functionally significant cross-talk between androgen receptor and erbb2 pathways in estrogen receptor negative breast cancer. Neoplasia **10**(6): 542-8.

Nagaya, T., Kopp, P., et al. (1996). Second zinc finger mutants of thyroid hormone receptor selectively preserve DNA binding and heterodimerization but eliminate transcriptional activation. Biochem Biophys Res Commun **222**(2): 524-30.

Nelius, T., Filleur, S., et al. (2007). Androgen receptor targets nfkappab and tsp1 to suppress prostate tumor growth in vivo. Int J Cancer **121**(5): 999-1008.

Nevalainen, M. T., Ahonen, T. J., et al. (2000). Epithelial defect in prostates of stat5a-null mice. Lab Invest **80**(7): 993-1006.

Newmark, J. R., Hardy, D. O., et al. (1992). Androgen receptor gene mutations in human prostate cancer. Proc Natl Acad Sci U S A **89**(14): 6319-23.

Nguyen, D., Steinberg, S. V., et al. (2001). A g577r mutation in the human ar p box results in selective decreases in DNA binding and in partial androgen insensitivity syndrome. Mol Endocrinol **15**(10): 1790-802.

Ning, Y. M. and Robins, D. M. (1999). Aml3/cbfalpha1 is required for androgen-specific activation of the enhancer of the mouse sex-limited protein (slp) gene. J Biol Chem **274**(43): 30624-30.

O'Mahony, O. A., Steinkamp, M. P., et al. (2008). Profiling human androgen receptor mutations reveals treatment effects in a mouse model of prostate cancer. Mol Cancer Res **6** (11)1691-1701.

Onland-Moret, N. C., Kaaks, R., et al. (2003). Urinary endogenous sex hormone levels and the risk of postmenopausal breast cancer. Br J Cancer **88**(9): 1394-9.

Palvimo, J. J., Reinikainen, P., et al. (1996). Mutual transcriptional interference between rela and androgen receptor. J. Biol. Chem. **271**(39): 24151-24156.

Perez-Stable, C. M., Pozas, A., et al. (2000). A role for gata transcription factors in the androgen regulation of the prostate-specific antigen gene enhancer. Mol Cell Endocrinol **167**(1-2): 43-53.

Pichon, M. F., Broet, P., et al. (1996). Prognostic value of steroid receptors after long-term follow-up of 2257 operable breast cancers. Br J Cancer **73**(12): 1545-51.

Pienta, K. J. and Bradley, D. (2006). Mechanisms underlying the development of androgen-independent prostate cancer. Clin Cancer Res **12**(6): 1665-71.

Ponguta, L. A., Gregory, C. W., et al. (2008). Site-specific androgen receptor serine phosphorylation linked to epidermal growth factor-dependent growth of castration-recurrent prostate cancer. J Biol Chem **283**(30): 20989-1001.

Popov, V. M., Wang, C., et al. (2007). The functional significance of nuclear receptor acetylation. Steroids **72**(2): 221-30.

Poujol, N., Lobaccaro, J., et al. (1997). Functional and structural analysis of r607q and r608k androgen receptor substitutions associated with male breast cancer. Mol Cell Endocrinol. **130**(1-2): 43-51.

Poukka, H., Karvonen, U., et al. (2000). Covalent modification of the androgen receptor by small ubiquitin-like modifier 1 (sumo-1). Proc Natl Acad Sci U S A **97**(26): 14145-50.

Prehn, R. T. (1999). On the prevention and therapy of prostate cancer by androgen administration. Cancer Res **59**(17): 4161-4.

Rees, I., Lee, S., et al. (2006). The e3 ubiquitin ligase chip binds the androgen receptor in a phosphorylation-dependent manner. Biochim Biophys Acta **1764**(6): 1073-9.

Riva, A. and Kohane, I. (2004). A snp-centric database for the investigation of the human genome. BMC Bioinformatics **5**(1): 33.

Robins, D. M. (2004). Multiple mechanisms of male-specific gene expression: Lessons from the mouse sex-limited protein (slp) gene. Prog Nucleic Acid Res Mol Biol **78**: 1-36.

Robins, D. M. (2005). Androgen receptor and molecular mechanisms of male-specific gene expression. Novartis Found Symp **268**: 42-52; discussion 53-6, 96-9.

Rosenberg, S. M. (2001). Evolving responsively: Adaptive mutation. Nat Rev Genet **2**(7): 504-15.

Ruizeveld de Winter, J. A., Trapman, J., et al. (1991). Androgen receptor expression in human tissues: An immunohistochemical study. J Histochem Cytochem **39**(7): 927-36.

Saporita, A. J., Ai, J., et al. (2007). The hsp90 inhibitor, 17-aag, prevents the ligand-independent nuclear localization of androgen receptor in refractory prostate cancer cells. Prostate **67**(5): 509-20.

Saporita, A. J., Zhang, Q., et al. (2003). Identification and characterization of a ligand-regulated nuclear export signal in androgen receptorJ. Biol. Chem. **278**(43): 41998-42005.

Sato, S., Idogawa, M., et al. (2005). Beta-catenin interacts with the fus proto-oncogene product and regulates pre-mrna splicing. Gastroenterology **129**(4): 1225-36.

Schauwaers, K., De Gendt, K., et al. (2007). Loss of androgen receptor binding to selective androgen response elements causes a reproductive phenotype in a knockin mouse model. Proc Natl Acad Sci U S A **104**(12): 4961-6.

Scheller, A., Hughes, E., et al. (1998). Multiple receptor domains interact to permit, or restrict, androgen-specific gene activation. J Biol Chem **273**(37): 24216-22.

Scheller, A., Scheinman, R. I., et al. (1996). Contextual dependence of steroid receptor function on an androgen-responsive enhancer. Mol Cell Endocrinol **121**(1): 75-86.

Schena, M., Freedman, L., et al. (1989). Mutations in the glucocorticoid receptor zinc finger region that distinguish interdigitated DNA binding and transcriptional enhancement activities. Genes Dev. **3**(10): 1590-1601.

Scher, H. I., Buchanan, G., et al. (2004). Targeting the androgen receptor: Improving outcomes for castration-resistant prostate cancer. Endocr Relat Cancer **11**(3): 459-76.

Scher, H. I. and Kelly, W. K. (1993). Flutamide withdrawal syndrome: Its impact on clinical trials in hormone-refractory prostate cancer. J Clin Oncol **11**(8): 1566-72.

Scher, H. I. and Kolvenbag, G. J. (1997). The antiandrogen withdrawal syndrome in relapsed prostate cancer. Eur Urol **31 Suppl 2**: 3-7; discussion 24-7.

Schoenberg, M. P., Hakimi, J. M., et al. (1994). Microsatellite mutation (cag24-->18) in the androgen receptor gene in human prostate cancer. Biochem Biophys Res Commun **198**(1): 74-80.

Schoenemakers, E., Alen, P., et al. (1999). Differential DNA binding by the androgen and glucocorticoid receptors involves the second zn-finger and a c-terminal extension of the DNA-binding domains. Biochem. J. **341**(Pt 3): 515-521.

Schoenmakers, E., Verrijdt, G., et al. (2000). Differences in DNA binding characteristics of the androgen and glucocorticoid receptors can determine hormone-specific responses. J Biol Chem **275**(16): 12290-7.

Schweizer, L., Rizzo, C. A., et al. (2008). The androgen receptor can signal through wnt/beta-catenin in prostate cancer cells as an adaptation mechanism to castration levels of androgens. BMC Cell Biol **9**: 4.

Segnitz, B. and Gehring, U. (1997). The function of steroid hormone receptors is inhibited by the hsp90-specific compound geldanamycin. J Biol Chem **272**(30): 18694-701.

Seralini, G. and Moslemi, S. (2001). Aromatase inhibitors: Past, present and future. Mol Cell Endocrinol **178**(1-2): 117-31.

Shaffer, P. L., Jivan, A., et al. (2004). Structural basis of androgen receptor binding to selective androgen response elements. Proc Natl Acad Sci U S A **101**(14): 4758-63.

Shah, R. B., Mehra, R., et al. (2004). Androgen-independent prostate cancer is a heterogeneous group of diseases: Lessons from a rapid autopsy program. Cancer Res **64**(24): 9209-16.

Shang, Y., Myers, M., et al. (2002). Formation of the androgen receptor transcription complex. Mol Cell **9**(3): 601-10.

Shen, H. C. and Coetzee, G. A. (2005). The androgen receptor: Unlocking the secrets of its unique transactivation domain. Vitam Horm **71**: 301-19.

Shi, X. B., Ma, A. H., et al. (2002). Functional analysis of 44 mutant androgen receptors from human prostate cancer. Cancer Res **62**(5): 1496-502.

Small, E. J. and Ryan, C. J. (2006). The case for secondary hormonal therapies in the chemotherapy age. J Urol **176**(6 Pt 2): S66-71.

Soule, H. D., Maloney, T. M., et al. (1990). Isolation and characterization of a spontaneously immortalized human breast epithelial cell line, mcf-10. Cancer Res **50**(18): 6075-86.

Sterbis, J. R., Gao, C., et al. (2008). Higher expression of the androgen-regulated gene psa/hk3 mrna in prostate cancer tissues predicts biochemical recurrence-free survival. Clin Cancer Res **14**(3): 758-63.

Sun, C., Dobi, A., et al. (2008). Tmprss2-erg fusion, a common genomic alteration in prostate cancer activates c-myc and abrogates prostate epithelial differentiation. Oncogene **27**(40): 5348-53.

Sun, C., Dobi, A., et al. (2008). Tmprss2-erg fusion, a common genomic alteration in prostate cancer activates c-myc and abrogates prostate epithelial differentiation. Oncogene **27**(40): 5348-5353.

Suzuki, H., Akakura, K., et al. (1996). Codon 877 mutation in the androgen receptor gene in advanced prostate cancer: Relation to antiandrogen withdrawal syndrome. Prostate **29**(3): 153-8.

Suzuki, H., Okihara, K., et al. (2008). Alternative nonsteroidal antiandrogen therapy for advanced prostate cancer that relapsed after initial maximum androgen blockade. J Urol **180**(3): 921-7.

Swerdlow, A. J., Schoemaker, M. J., et al. (2005). Cancer incidence and mortality in men with klinefelter syndrome: A cohort study. J Natl Cancer Inst **97**(16): 1204-10.

Tanner, T., Claessens, F., et al. (2004). The hinge region of the androgen receptor plays a role in proteasome-mediated transcriptional activation. Ann N Y Acad Sci **1030**: 587-92.

Taplin, M. E., Bubley, G. J., et al. (1999). Selection for androgen receptor mutations in prostate cancers treated with androgen antagonist. Cancer Res **59**(11): 2511-5.

Taplin, M. E., Bubley, G. J., et al. (1995). Mutation of the androgen-receptor gene in metastatic androgen-independent prostate cancer. N Engl J Med **332**(21): 1393-8.

Tarraga, J., Medina, I., et al. (2007). Phylemon: A suite of web tools for molecular evolution, phylogenetics and phylogenomics. Nucleic Acids Res **35**(Web Server issue): W38-42.

Thijssen, J. H. (2004). Local biosynthesis and metabolism of oestrogens in the human breast. Maturitas **49**(1): 25-33.

Thompson, J., Saatcioglu, F., et al. (2001). Disrupted amino- and carboxyl-terminal interactions of the androgen receptor are linked to androgen insensitivity. Mol Endocrinol **15**(6): 923-35.

Tilley, W. D., Buchanan, G., et al. (1996). Mutations in the androgen receptor gene are associated with progression of human prostate cancer to androgen independence. Clin Cancer Res **2**(2): 277-85.

Titus, M. A., Schell, M. J., et al. (2005). Testosterone and dihydrotestosterone tissue levels in recurrent prostate cancer. Clin Cancer Res **11**(13): 4653-7.

Tomlins, S. A., Laxman, B., et al. (2007). Distinct classes of chromosomal rearrangements create oncogenic ets gene fusions in prostate cancer. Nature **448**(7153): 595-9.

Tomlins, S. A., Laxman, B., et al. (2008). Role of the tmprss2-erg gene fusion in prostate cancer. Neoplasia **10**(2): 177-88.

Tomlins, S. A., Rhodes, D. R., et al. (2005). Recurrent fusion of tmprss2 and ets transcription factor genes in prostate cancer. Science **310**(5748): 644-8.

Tormey, D. C., Lippman, M. E., et al. (1983). Evaluation of tamoxifen doses with and without fluoxymesterone in advanced breast cancer. Ann Intern Med **98**(2): 139-44.

Toumazou, C., Li, J., et al. (2007). Cofactor restriction by androgen receptor n-terminal and c-terminal interaction. Mol Endocrinol: me.2006-0228.

Truss, M. and Beato, M. (1993). Steroid hormone receptors: Interaction with deoxyribonucleic acid and transcription factors. Endocr Rev **14**(4): 459-79.

Urushibara, M., Ishioka, J., et al. (2007). Effects of steroidal and non-steroidal antiandrogens on wild-type and mutant androgen receptors. Prostate **67**(8): 799-807.

Veldscholte, J., Ris-Stalpers, C., et al. (1990). A mutation in the ligand binding domain of the androgen receptor of human lncap cells affects steroid binding characteristics and response to anti-androgens. Biochem Biophys Res Commun **173**(2): 534-40.

Venables, J. P. (2006). Unbalanced alternative splicing and its significance in cancer. Bioessays **28**(4): 378-86.

Verrijdt, G., Haelens, A., et al. (2003). Selective DNA recognition by the androgen receptor as a mechanism for hormone-specific regulation of gene expression. Mol Genet Metab **78**(3): 175-185.

Verrijdt, G., Tanner, T., et al. (2006). The androgen receptor DNA-binding domain determines androgen selectivity of transcriptional response. Biochem Soc Trans **34**(Pt 6): 1089-94.

Wang, L. G., Liu, X. M., et al. (1999). Phosphorylation/dephosphorylation of androgen receptor as a determinant of androgen agonistic or antagonistic activity. Biochem Biophys Res Commun **259**(1): 21-8.

Watson, C. J. and Khaled, W. T. (2008). Mammary development in the embryo and adult: A journey of morphogenesis and commitment. Development **135**(6): 995-1003.

Wen, Y., Hu, M. C., et al. (2000). Her-2/neu promotes androgen-independent survival and growth of prostate cancer cells through the akt pathway. Cancer Res **60**(24): 6841-5.

Wooster, R., Mangion, J., et al. (1992). A germline mutation in the androgen receptor gene in two brothers with breast cancer and reifenstein syndrome. Nature Genetics **2**(2): 132-134.

Wu, C. T., Altuwaijri, S., et al. (2007). Increased prostate cell proliferation and loss of cell differentiation in mice lacking prostate epithelial androgen receptor. Proc Natl Acad Sci U S A **104**(31): 12679-84.

Xie, B., Tsao, S. W., et al. (1999). Sex hormone-induced mammary carcinogenesis in female noble rats: The role of androgens. Carcinogenesis **20**(8): 1597-606.

Yager, J. D. and Davidson, N. E. (2006). Estrogen carcinogenesis in breast cancer. N Engl J Med **354**(3): 270-82.

Yarbrough, W. G., Quarmby, V. E., et al. (1990). A single base mutation in the androgen receptor gene causes androgen insensitivity in the testicular feminized rat. J Biol Chem **265**(15): 8893-900.

Yeh, S., Hu, Y.-C., et al. (2003). Abnormal mammary gland development and growth retardation in female mice and mcf7 breast cancer cells lacking androgen receptor. J Exp Med **198**(12): 1899-1908.

Yeh, S., Lin, H. K., et al. (1999). From her2/neu signal cascade to androgen receptor and its coactivators: A novel pathway by induction of androgen target genes through map kinase in prostate cancer cells. Proc. Natl. Acad. Sci. USA **96**: 5458-5463.

Yong, E. L., Tut, T. G., et al. (1998). Partial androgen insensitivity and correlations with the predicted three dimensional structure of the androgen receptor ligand-binding domain. Mol Cell Endocrinol **137**(1): 41-50.

Yoshida, T., Kinoshita, H., et al. (2005). Antiandrogen bicalutamide promotes tumor growth in a novel androgen-dependent prostate cancer xenograft model derived from a bicalutamide-treated patient. Cancer Res **65**(21): 9611-6.

Young, I. E., Kurian, K. M., et al. (2000). The cag repeat within the androgen receptor gene in male breast cancer patients. J Med Genet **37**(2): 139-40.

Young, L. (2000). The cleared mammary fat pad and the transportation of mammary gland morphological structures and cells. Methods in mammary gland biology and breast cancer research. M. Ip and B. Asch. New York, Kluwer Academic/Plenum Publishers**:** 67-74.

Yousef, G. M., Scorilas, A., et al. (2002). The androgen-regulated gene human kallikrein 15 (klk15) is an independent and favourable prognostic marker for breast cancer. Br J Cancer **87**(11): 1294-300.

Yu, H., Giai, M., et al. (1995). Prostate-specific antigen is a new favorable prognostic indicator for women with breast cancer. Cancer Res **55**(10): 2104-2110.

Zhang, J., Sun, Y., et al. (2004). Synergistic effects of androgen and estrogen on the mouse uterus and mammary gland. Oncol Rep **12**(4): 709-16.

Zhao, X. Y., Malloy, P. J., et al. (2000). Glucocorticoids can promote androgen-independent growth of prostate cancer cells through a mutated androgen receptor. Nat Med **6**(6): 703-6.

Zhou, J., Ng, S., et al. (2000). Testosterone inhibits estrogen-induced mammary epithelial proliferation and suppresses estrogen receptor expression. The FASEB Journal **14**(12): 1725-1730.

Zhou, Z. X., Kemppainen, J. A., et al. (1995). Identification of three proline-directed phosphorylation sites in the human androgen receptor. Mol Endocrinol **9**(5): 605-15.

Zhu, X., Daffada, A. A., et al. (1997). Identification of an exon 3 deletion splice variant androgen receptor mrna in human breast cancer. Int J Cancer **72**(4): 574-80.

Zuccarello, D., Ferlin, A., et al. (2008). Detailed functional studies on androgen receptor mild mutations demonstrate their association with male infertility. Clin Endocrinol (Oxf) **68**(4): 580-8.